N95- 27074

8

TYPICAL EXAMPLES OF CLASSICAL NOVAE

M. Hack, P. L. Selvelli, A. Bianchini, H. Duerbeck

I. INTRODUCTION

Because of the very complicated individualistic behavior of each nova, we think it necessary to review the observations of a few well-observed individuals. We have selected a few objects of different speed classes, which have been extensively observed.

They are:

V1500 Cygni 1975, very fast nova. t_3 = 3.6 d.
Range of the light curve Δm = 2.2 B-21.5p; light curve of Duerbeck type A (smooth, fast decline without major disturbances).
Quiescence: It presents short period variations.
Characteristics: Large outburst amplitude.

V603 Aql 1918, fast nova. t_3 = 8 d.
Δm = −1.1V-12.0V; light curve type Ao (smooth, fast decline without major disturbances, oscillations in the transition stage).
Spectroscopic binary P = 0.13854 d; eclipsing binary?

CP Pup 1942, fast nova. t_3 = 8 d.
Δm = 0.5V-15.0V; light curve type A.
Spectroscopic binary with P=0.061429 d; light variations with P = 0.06196 d.
Characteristics: It has the shortest binary period among novae; slightly different spectroscopic and photometric periods.

GK Per 1901, fast nova. t_3 = 13d.
Δm = 0.2V-11.8...14.0V; light curve type Ao.
Spectroscopic binary, P =1.996803 d.
Characteristics: Many unusual characteristics; minor outbursts at quiescence; it has the longest orbital period among novae.

V 1668 Cyg 1978, moderately fast nova. t_3 = 23 d.
Δm = 6.7p- 20.0p; light curve type Ba (decline with standstills or other minor fluctuations).
Quiescence: It shows short period variations.

FH Ser 1970, slow nova. t_3 = 62 d.
Δm = 4.5V- 16.2p; light curve type Cb (strong brightness decline before the onset of the transition minimum).
Characteristics: Dust formation; the bolometric magnitude remains constant for a period much longer than the optical one.

DQ Her 1934, slow nova. t_3 =94 d.
Δm = 1.3V -14.5V (var); light curve type Ca (small variation of visual brightness at maximum).
Spectroscopic and eclipsing binary with P = 0.193621 d
Characteristics: Pronounced dust formation; unusual occurrence of molecular lines in premaximum spectrum.

T Aur 1891, slow nova.t_3 = 100 d.
Δm 4.2p-15.2p; light curve type Ca.
Characteristics: Great similarity with DQ Her.

RR Pic 1925, slow nova. t_3 = 150 d.
Δm = 1.0V-11.9p; light curve type D (slow development, extended premaximum, maximum often with several brightness peaks).
Characteristics: Spectroscopic binary, P = 0.1450255d.
Light variations with the same period; eclipses shallow or absent.

HR Del 1967, very slow nova. t_3 = 230 d.
Δm = 3.5 V-12.0 V; light curve type D.
Spectroscopic binary, P = 0.2141674.
Characteristics: Extremely slow nova, with no appreciable formation of dust.

A catalogue of all observed novae, from the two oldest ones, CK Vul 1670 and WY Sge 1783 to Nova Cyg 1986, has been prepared by Duerbeck (1987c). For most objects, brightness ranges, accurate positions, finding charts, and bibliographies on light curves, spectroscopy, UV, IR, radio observations, nebular shells variability in quiescence and evidences for duplicity are given.

II. V1500 CYGNI 1975: A VERY FAST NOVA

(written by Hack)

It was discovered on August 29, 1975, and it is one of the most extensively observed novae. A large number of spectroscopic and photometric observations are collected in the issue of the Astron. Zh.54, May-June 1977 (Sov. Astron. 21, No.3). At maximum brightness, reached on August 30, V was equal to 1.7. Nova Cyg 1975 is peculiar for several reasons: a) It is an extremely fast nova, with t_3 = 3.9 days, t_7 = 45 days (Figure 8.1). b) It presented a very large light amplitude, V = 19 mag, with an absolute visual magnitude at maximum of about -10 (as derived by Becker and Duerbeck, 1980, from its nebular expansion parallax), which makes it the brightest of all galactic and extragalactic novae ever observed, with the

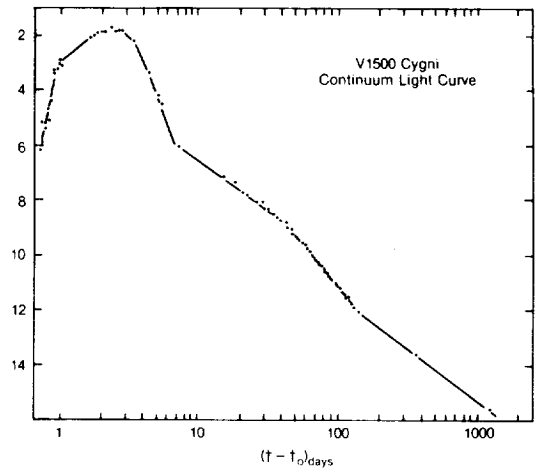

Figure 8-1. V 1500 Cygni: continuum light curve. (from Ferland et al., 1986)

exception of CP Pup, which reached M_v = -11.5 (Duerbeck and Seitter, 1979). Generally, novae at maximum are less bright than M_V = -8.5. The amplitudes of the outburst of both V1500 Cyg and CP Pup are more typical of supernovae than novae; however, their expansional velocities have the typical values of very fast novae. c) The absolute magnitude of V1500 Cyg at minimum before outburst was about +9 or fainter, which makes it similar to the U Gem stars, while the majority of novae are about 5 mag brighter. This value of M_V at minimum was deduced from the fact that superposition of the blue Palomar survey with the field of V1500 Cyg (Beardsley et al., 1975) indicates no star brighter than mag 21 on the print. However, the outburst started when the star was 5 mag brighter than the normal prenova luminosity. This increase in luminosity was observed on August 5, 1975. The color, during the pre outburst phase was B-V = 1.3 and V-R = 2.5, suggesting a color temperature of about 4,000 K, i.e., a K- or M-type star. d) At maximum, the spectral type was B2 Ia, the earliest spectral type ever observed for novae. e) The absorption spectrum shows broad diffuse bands; the two systems, diffuse-enhanced and orion, were not evident.

In fact, the diffuse-enhanced spectrum appeared at 0.3 days after optical maximum with an expansion velocity of -3,850 km/s; it

reached its greatest strength 0.9 days later and lasted slightly more than 1 day as an absorption feature. For this reason, many observers have not detected it (Ferland, 1977a). Also, the high value of the Doppler broadening can make the detection of the various components difficult, blending them together.

The penetration of the principal shell by the diffuse—enhanced occurred without any noticeable interaction, because the principal spectrum did not show any appreciable variation. The interpretation may be that the great majority of the material was expelled in one explosive event almost instantaneously. f) The expansional velocity of the principal spectrum was very high, much higher than in normal novae (Boyarchuk et al., 1977), as indicated below:

August 29: absorption expansional velocity V = -1300 km/s,
Total (Emission + Absorption) Doppler broadening ΔV =2200 km/s
August 30: V = -1700 km/s, ΔV = 4000 km/s.
August 31: V = -2200 km/s, ΔV =6100 km/s.

II.A. MASS LOST IN THE OUTBURST

A lower limit of the mass ejected in the outburst has been computed by Wolf (1977). From the equivalent widths of the Balmer absorption lines, the column density $n_{02}\ \Delta r$ (*) is computed, and from the observed temperature at maximum, by assuming a plausible value of the electron density, one gets $n_1\ \Delta r = 4.2 \times 10^{23}$ cm^{-2} using the Boltzmann and Saha equations.

From $n_1\ \Delta r$ and $N_e \approx n_1$, a value of $\Delta r = 4.2 \times 10^{13}$ cm = 600 solar radii is derived. Hence, the mass lost in the outburst is given by $\Delta m = 4\pi(\Delta r)^2 \Delta r n_1 m_H = 1.5 \times 10^{28}$ g $= 10^{-5}\ m_\odot$. As we shall see later, infrared observations by Gallagher and Ney (1976) and by Ennis et al. (1977) estimate $10^{-5}\ m_\odot < \Delta m < 10^{-3}\ m_\odot$. From this value of the mass lost in the outburst and the expansional velocity, it follows that the kinetic energy liberated in the explosion is $E_{kin} \geq 10^{28}$ g x $(2 \times 10^8$ cm/s$)^2 = 4 \times 10^{44}$ erg comparable to the energy radiated away, $E_{rad} \approx 10^{45}$ erg.

(*) $W\lambda = \frac{\lambda \pi e^2}{mc^2} f n_{02} \Delta r$ valid for an optically thin layer (Doppler branch of the curve of growth).

II.B. SPECTRAL VARIATIONS

The spectral variations were as follows: August 29 B2Ia+, T (pseudo-photosphere = T continuum) $\simeq$ 30,000 K,T(envelope) $\simeq$ 20,000 K. August 30-31 A2Ia+. The lines show P Cyg profiles with faint emission wings; the latter increase fast in intensity.

September 1, almost all the absorption features have disappeared. From September 1 to September 10, metallic emission lines appear first and He I, He II, N III, plus several forbidden lines later on. The nebular stage was reached 9 days after maximum (Figure 8-2). From September 2, 1975, to January 5, 1976, the Balmer emission lines present several peaks at almost constant velocity: -1050, -580, +150 + 600 km/s. A similar behavior is shown also by the O I 8446 A permitted line and 6300 A forbidden line. The four peaks have a different relative intensity and they are not all observable in the high excitation lines of [Fe X], Fe XI], and [S VIII] (Figure 8-3, 8-4, and 8-5). High dispersion spectra of the photographic range have been obtained from September 2 to October 2 by Sanyal and Willson (1980). Rush and Thompson (1977) have made spectrophotometric observations with time resolution of 3-15 minutes. All the hydrogen lines observed from September 7 to 11 show that the relative intensity of the four peaks change simultaneously in each Balmer line on a time scale of 5 minutes. Following a model suggested by Weaver (1974) for V603 Aql, they assume that four blobs of matter were ejected simultaneously in two opposite directions, two at higher velocities and two at lower velocities. Since each peak is produced in a separate blob, a sudden change in the radiation from the stellar pseudophotosphere will produce a change in the ionization of the hydrogen in the blob.

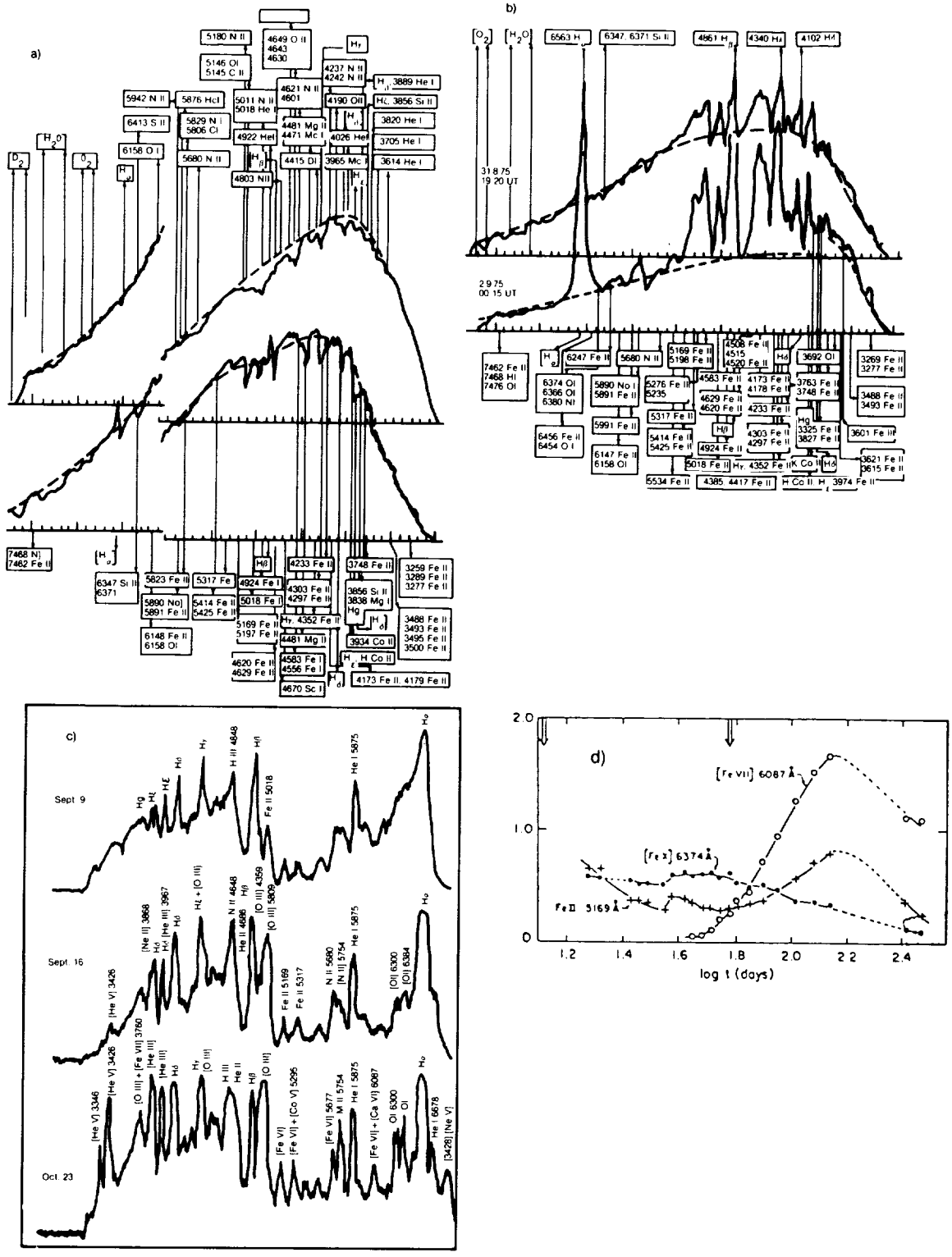

Figure 8-2. The spectrum of V 1500 Cyg: a) August 29 and 30: the absorption lines dominate the spectrum. P Cyg profiles appear on August 30; b) August 31 and September 2: the emission lines dominate the spectrum (from Voloshina and Doroshenko, 1977); c) The spectrum from the beginning of September to the end of October (from Rosino and Tempesti, 1977); d) Line intensity variation with time after maximum light (from Ferland et al., 1977).

However, the assumption that all the blobs are ejected toward and away from the observer in the direction of the line of sight seems not very plausible. It seems more plausible to assume that the blobs are ejected in several directions at about the same velocity and that the observed differences in radial velocity are rather due to projection effects.

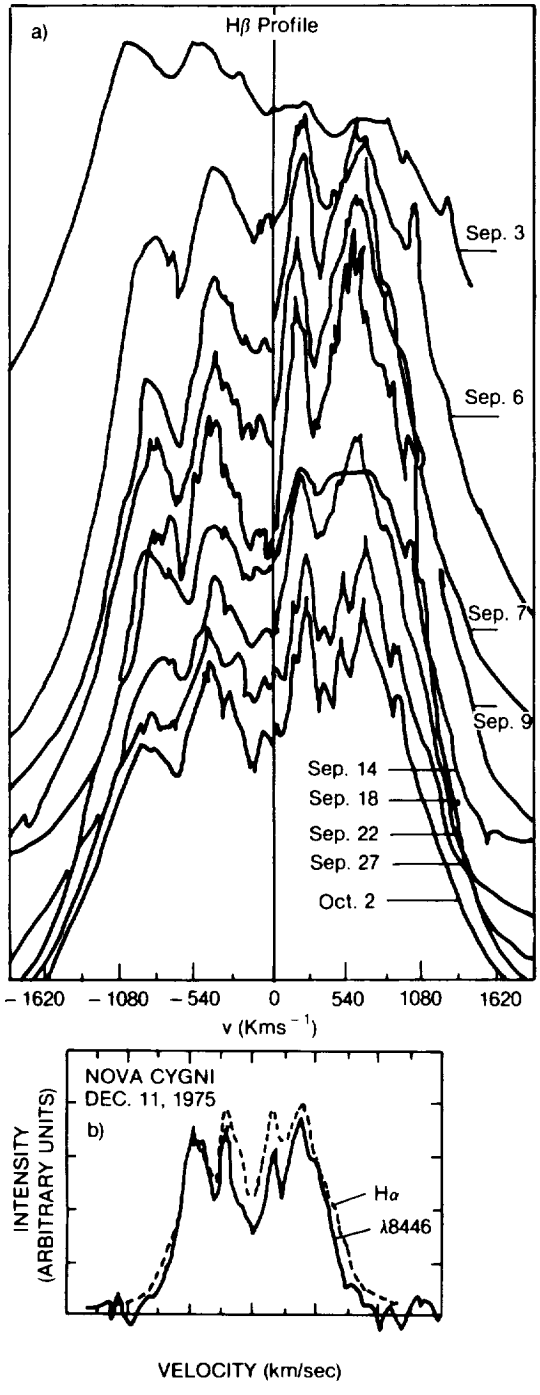

Figure 8-3a. Line profiles of Hβ at different epochs (from Sanyal and Willson, 1980). b) Line profiles of Hα and 0 1 8446 (from Strittmatter et al., 1977).

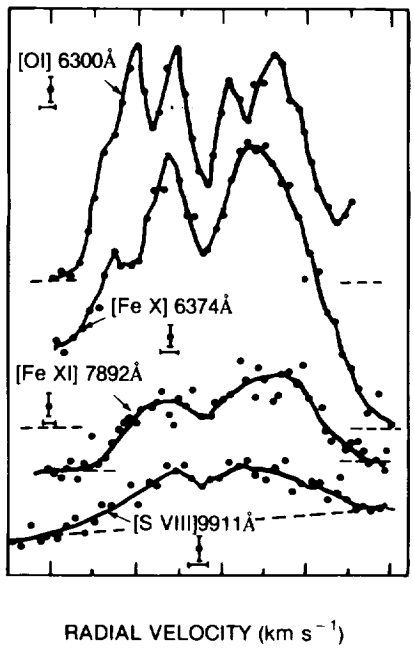

Figure 8-4. Line profiles for [OI] 6300 (Oct. 9), [Fe X] (Oct. 5 and 9), [Fe XI] 7892 (Oct. 2, 5 and 9), [S VIII] 9911 (Oct. 5, 9, 12, 15, 19, 27 and Nov. 7) (from Ferland et al. 1977).

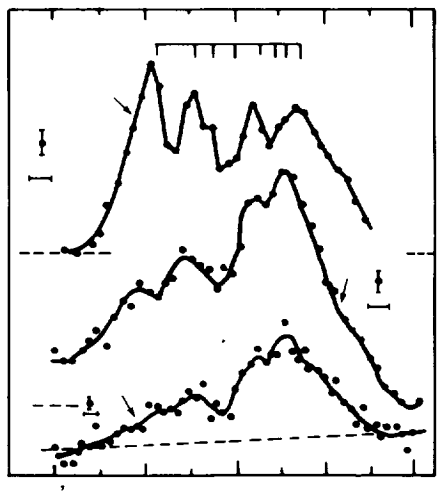

Figure 8-5. Line profiles for [OI] 6300 (Oct. 9), [FeX] (Oct. 5, 19, 23, and 27), [Fe XI] (Oct. 15, 19, 23 and 27) (from Ferland et al. 1977).

II.C. PERIODIC LIGHT AND RADIAL VELOCITY VARIABILITY

V1500 Cyg has shown periodic light variability with a period of 3.3 hours since early postmaximum (Hutchings, 1979b). The amplitude has remained in the range 0.15-0.5 mag, while the mean brightness was changing by a factor of 60,000 (about 12 mag). As we have seen in Chapter 6, the period decreased by 2% during the first year from outburst and then increased slightly and then stabilized. Flickering with time scale of 100 s was observed, i.e., a behavior typical of cataclysmic variables (Figure 8-6). Ultraviolet observations made with the photometric Astronomical Netherland Satellite (ANS) confirm the light variability with P = 0.14 days (Wu and Kester, 1977).

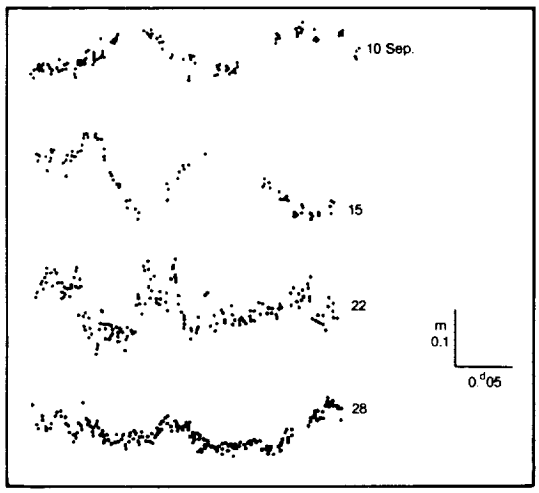

Figure 8-6. Blue light curves of V 1500 Cyg observed in Sep. 1975. The light curves are not aligned by time or by phase.
(from Ambruster et al. 1977).

Spectra taken in 1977 (Hutchings, 1979b) show the characteristic nebular emisssion lines of [O III] 4959 + 5007 and 4363, [Ne III] at 3868 and 3967 and, in addition, several permitted emissions of H I, He II, N III. The permitted lines, and especially 4686 He II, present radial velocity variations with a period of 3.3 hours like the photometric period and semiamplitude K of 350 km/s. Such a large value of K in a simple binary model would imply a large value of the mass function, and therefore—for reasonable values of the mass ratio—of the masses, which is not in agreement with the typical low masses of novae. Moreover, the Balmer lines present a different radial velocity variation than 4686 He II. These observations, therefore, suggest that they do not represent an orbital motion only, but rather stream motions or a combination of the two. A mass function consistent with the expected masses would give K = 150 km/s. Hence, the line emissions appear to originate in fast-moving streams and confirm the binary nature of the object but do not reveal anything about the orbital parameters. This is a problem common to several classes of close binaries, where streams, accretion disk, and envelopes surrounding the whole system, produce their own spectra with their own peculiar motions superposed on the orbital motions.

The system appears to have a mean radial velocity about 400 km/s more positive than the mean velocity of the nebular lines, which, therefore, indicate that the region where they are formed is an expanding envelope.

A model for explaining the behavior of the binary V1500 Cyg has been proposed by Hutchings (1979b). He suggests that the light variations can be linked to the disk, which is probably the most luminous element of the system, and the period changes may be linked to a precession of the bright and dark side of the accretion disk, partly due to nonsynchronous rotation of the white dwarf after the nova outburst. In fact, the irregularity of the light curve suggests that an eclipse of the white dwarf from the companion is not the most plausible hypothesis.

II.D. ULTRAVIOLET OBSERVATIONS

As we have seen in Chapter 6, V1500 Cyg was observed with the ultraviolet satellites ANS and Copernicus. The channels at 1800, 2200, and 2500 A of ANS are free from strong emissions, and the continuum radiation from the nova shell is negligible. Hence, the continuum of the hot nova remnant could be observed and the interstellar reddening estimated from the dip at 2200 A. A color excess E(B-V) = 0.69

has been found, nearly equal to that determined for 55 Cyg, which is nearby V1500 Cyg. From a comparision of the intensity of the emission lines of the Balmer and Paschen series, Ferland (1977b) found E(B-V) = 0.50 +/- 0.05 consistent with the strength of the interstellar lines. This value gives a distance of 1.95 kpc +/-0.02 kpc, higher than the value of 1.35 kpc given by the nebular expansion parallax. The latter is probably more reliable, because methods based on the interstellar extinction and interstellar lines are affected from the irregular distribution of the dust and gas in the interstellar medium.

Copernicus observations, at a spectral resolution of 0.4 A, were made from September 1 to September 9 (Jenkins et al., 1977). The spectrum was not detectable at $\lambda < 2700$ A. Broad Mg II emissions were observed. After the 9th, the nova was no longer detectable with Copernicus. These authors discuss the absence of measurable ultraviolet radiation at shorter wavelengths: it suggests that the Mg II lines are formed by collisional excitation in the outer layers of the shell at T $\simeq$ 4,000 K, and the absence of emission lines of the abundant multiionized atoms indicate that the material at temperature between 25,000 and 50,000 K is less than 0.001 that producing the Mg II emission. They point out also that it is strange that no emission was observable as λ 1302 A, corresponding to the O I resonance line, while 8446 O I is a strong emission line. In fact, both these lines are explained with Ly Beta fluorescence: Ly Beta emission (1025.72 A, upper E.P. level 12.04 eV) overpopulates the upper level of 1025.72 O I (upper E.P. level 12.03 eV), and from that level $3d^1\ D^0$ a cascade down to $3p^3$ P and then to $3s^3\ S^0$ explains the emissions at 11287 A and at 8446 A; then a cascade down to $2p^4\ ^3p$ will produce the 1302 A emission. Now from the infrared observations of Gallagher and Ney (1976) and from the ultraviolet spectroscopic observations of Jenkins et al. (1977), one derives that the flux at the Earth of λ 8446 is of about 4×10^3 photons $cm^{-2}\ s^{-1}$, while the upper limit for λ 1302, after correction for the interstellar extinction is less than 31 photons $cm^{-2}\ s^{-1}$.

These two fluxes are irreconcilable. From the average luminosity of the central remnant of novae Strittmatter et al. (1977) estimated the number of ionizing photons emitted by the central source of V1500 Cyg and the optical depth of Ly Alpha. This is so high that a random walk of photons in the nebula will be accomplished in a time long compared with the age of the nova. For this reason, no strong Ly Alpha emission is expected, in agreement with Copernicus observations. For the same reason, one also expects that the optical depth at 1302 O I is high enough for the 1302 photons to have an escape time that is long compared with the age of the nova at the time of Copernicus observations, therefore explaining why this emission was not observable.

II.E. INFRARED OBSERVATIONS

Observations at 2 μm (Ennis et al., 1977) show that the Brackett Gamma line changes from absorption to emission about 5 days after maximum. It is in absorption when the 1-20 μm continuum is that of a black body and changes to emission when the continuum becomes that typical of free-free radiation.

Starting on September 16, several coronal lines were detected: [Fe X] 6374, [Fe XI] 7892 and [S VIII] 9911 are present from late September 1975 to January 1976; [Fe XIV] was not observed (Ferland et al., 1977) Hence, according to them, the temperature was placed between 10^6 and less than 2×10^6 K. As the coronal lines became fainter, the [Fe VII] 6087 strenghtened, indicating T $\simeq 2 \times 10^5$ K. O I and H Alpha are clearly formed in the same region of the envelope as indicated by the strict similarity of the profiles (see Figure 8.3) while the forbidden lines of multiionized iron have different profiles and must be formed in different layers (see Figure 8.4 and 8.5).

As we have seen in Chapter 6, the infrared light curves of V1500 Cyg indicate that the energy distribution until 3.2 days after outburst

is that typical of a blackbody with T varying from 10^4 to about 5,000 K. Later, the energy distribution curve changes gradually from that typical of a blackbody (approximated in the infrared by the Rayleigh-Jeans relation $F_\nu \propto \nu^2$) to that typical of free-free radiation ($F \sim$ constant). Figure 8-7 gives the flux at the Earth of Nova Cyg 1975 and, for comparison, the flux of Alpha Cyg.

The spectral energy distribution from near UV (as measured by Copernicus) to IR on September 2 is shown in Figure 8-8. The position of the maximum at about 0.8 μm indicates a color temperature of about 4,000 K.

The maximum in the light curve is reached at progressively later epochs with increasing wavelengths, according to the empirical relation Fmax = 31.31 August 1975 (UT) + 0.681 λ (μm).

During the phases of the thick shell, it is possible to estimate the distance of the nova by the following considerations (Gallagher and Ney, 1976): the flux at the Earth F_λ is known directly from the observations; the flux B_λ emitted per surface unit by the shell is found by fitting the observed energy curve with the planckian curve for the corresponding temperature. Hence, it follows: $F_\lambda = \theta^2 B_\lambda$ with θ angular radius of the shell. Now $\theta = R/d$, $d\theta/dt = (1/d)\, dR/dt = v/d$, where R is the linear radius of the shell, d is the distance of the nova, and v, the expansional velocity of the shell. The observations give θ, dθ/dt, and v; hence, the distance d can be derived. Since the expansional velocities range from 1300 to 2500 km/s, it is found 1.2 kpc < d < 2.3 kpc (i.e., a value including that derived by the nebular expansion as well as that derived from the 2200 dip—see Chapter 8, Sections II.D and II.G. Figure 8-9 gives the values of T and θ and the absolute magnitude computed for a distance of 1.5 kpc. At 3.2 days after outburst, when the shell is still optically thick and fits the blackbody curve for T = 5,000 K from 0.5 to 5 μm, the radius (for a distance of 1.5 kpc) is equal to 3 AU and the area of the shell is 3×10^{28} cm^2. If σ is the mass above each cm^2 of photosphere, since the shell is optically thick, but just about to become optically thin, it

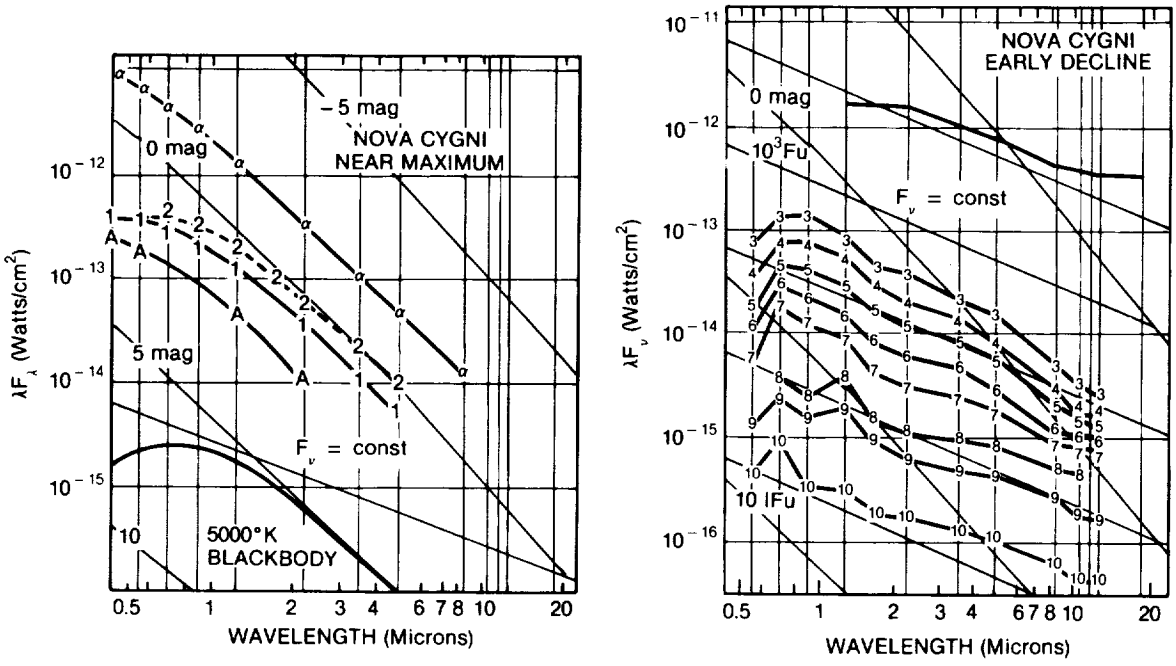

Figure 8-7. Energy spectra for V 1500 Cyg near maximum and during early decline. A:Aug. 29.8; 1:Aug.30.3; 2:Sep.1.1; α:α Cygni shifted by -2.5 mag; 3:Sep.2.0; 4:Sep. 2.4; 5:Sep.4.0; 6:Sep.6.1.; 7:Sep.9.1; 8:Sep.16.2; 9:Sep.24-25; 10:Oct.18-21. The transition from Black Body to free-free radiation is evident by comparing spectra no. 3 and No. 5. (from Gallagher et al. 1976).

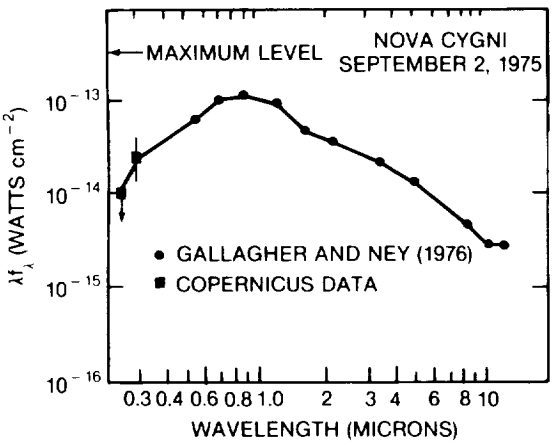

Figure 8-8. Spectral energy distribution for V 1500 Cyg measured on Sep. 2, 1975. (from Jenkins et al., 1977).

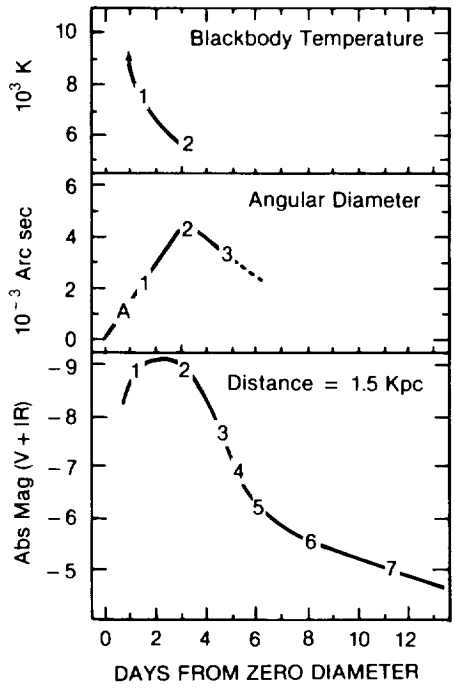

Figure 8-9. Black body temperature and angular diameter versus day from the zero expansion date (Aug. 28.9) and corresponding absolute magnitude (V+IR) for d= 1.5 kpc. (from Gallagher et al., 1976).

is reasonable to assume $\tau = \kappa\sigma \approx 1$. Hence, the mass of the ejected shell is about $3 \times 10^{28} \times (\tau/\kappa)$. For temperatures of about 5,000 K and density of the order of 10^9 cm^{-3}, $k \simeq 0.01$. If the gas in the outer parts of the shell becomes ionized, then $k \simeq 2$. Hence, the two limits for the mass of the ejected shell are obtained: 1.5×10^{28} g $< m < 3 \times 10^{30}$ g; the lower limit is in good agreement with the value derived by Wolf (1977) from the Balmer lines.

By combining all the available observations in the different spectral ranges at different epochs it is found that the luminosity of V1500 Cyg passed from 5×10^5 $L_\odot$ at maximum to 3×10^4 $L_\odot$ 100 days later, These values give a bolometric amplitude $\Delta m_{bol} = 3.05$ against a visual amplitude $\Delta m_v = 7.5$. Figure 8-10 gives the infrared light curves. The infrared energy distribution from August 30 to October 15 is shown in Figure 6.27c.

Although V1500 Cyg is generally considered a dustless nova, it shows a slight IR excess at 10 μm about 100 days after outburst. An excess is detectable also at 3.5 μm (Ennis et al., 1977; Szkody, 1977; Tempesti, 1979).

According to Bode and Evans (1985), this excess is consistent with the heating of dust close to the nova during the eruption. No significant excess is observed for $t < 120$ days. Between days 200 and 400, the excess increases monotonically. The dust temperature is of the order of 200 K. A previous interpretation of the IR excess at 10 μm was given by Ferland and Schields (1978a) who attributed it to a [Ne II] emission at 12.8 μm; in this case, however, the excess at lower wavelengths is not explained. A summary of all the observations made at the McDonald Observatory since the outburst through one year later is given by Ferland et al. (1986) (see Figure 6.14). They found that the remnant became a dominant contributor to the optical continuum only one year after outburst, while it was detectable in the ultraviolet, with the Astronomical Netherland satellite (ANS) by day 100 (Wu and Kester, 1977). Both the UV continuum on day 100 and the optical continuum on day 368 fit the same Rayleigh-Jeans tail ($F_\nu \propto \nu^2$) indicating: a) that the underlaying hot body radiates like a blackbody at $T > 10^5$, and b) that the hot body maintained almost constant luminosity and energy distribution for at least 268 days. The continuum emission in the optical and infrared, on the contrary, shows a flat distribution ($F \approx$ con-

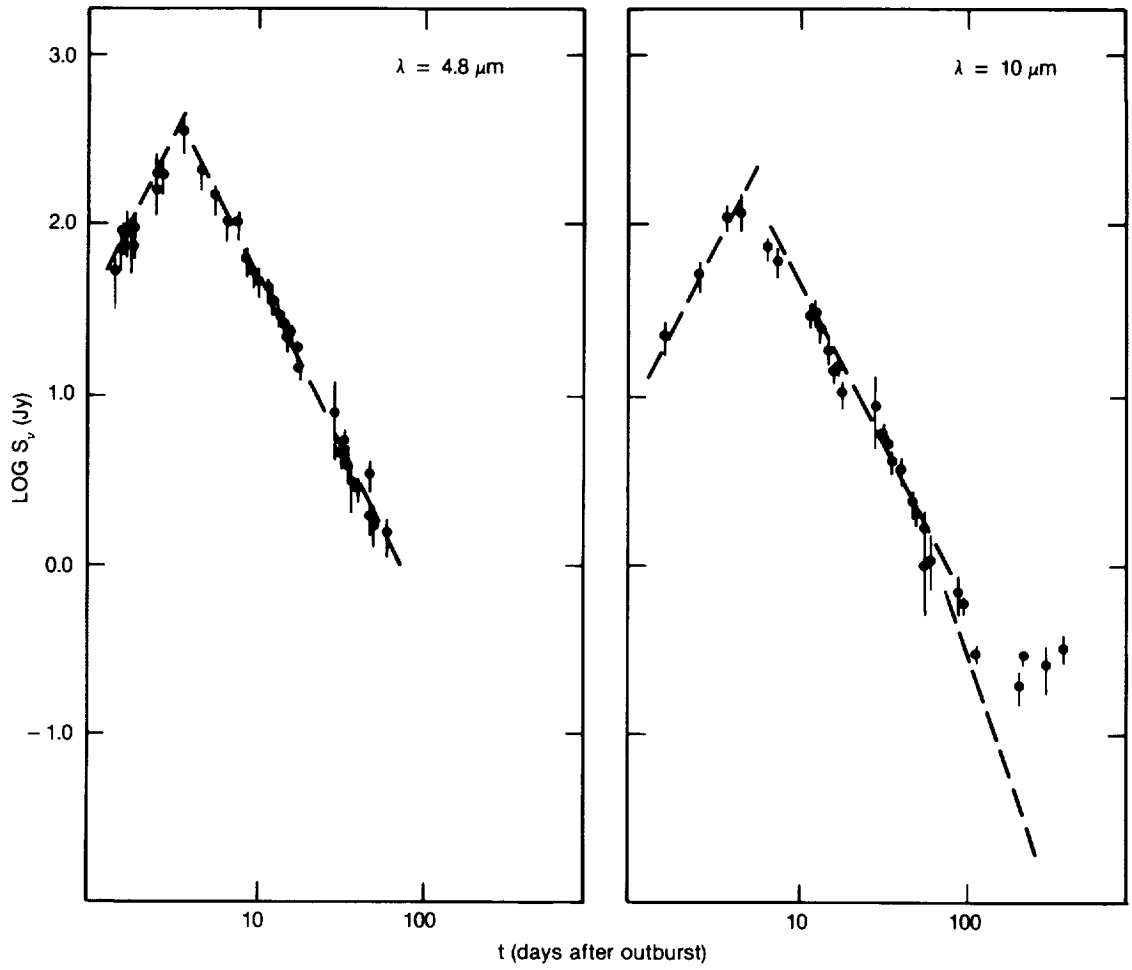

Figure 8-10. Infrared light curves for V 1500 Cyg. After day 300 from outburst an infrared excess is observed, especially evident at 10 μm, suggesting the formation of a dust shell. (from Ennis et al., 1977).

stant) (see Figure 8-11 from Ferland et al., 1986) dominating the nova spectrum from day 10 to day 100. Ferland et al. show that the gas at $T \approx 10^4$ responsible for the nebular spectrum is insufficient to explain this continuum and suggest that a contribution from the coronal line region, as well as the central object, must be added. In fact, from the H Alpha intensity, one can derive the combined free-free + bound-free emission of a low-density gas at temperatures $t=T/10^4$ for $0.5 \leq t \leq 2$: $vF(4800\ A) / F(H\alpha) = 1.23\ t^2\ e^{-0.663\ t}$ (see Osterbrock, 1974). Now Figure 8-12 from Ferland et al. shows that the free-free + bound-free contribution predicted from the intensity of H Alpha is lower by a factor of about 3 than the observed continuum emission. The hot underlying body gives also a contribution, which, by comparing the amplitude of the 3-hour-period light variation when the continuum is produced by the hot body only with that when the flat continuum was present, can be estimated to be of 10%. The only other contributor to the flat continuum is then bremsstrahlung from the hot gas ($T \approx 10^6$) originating the coronal lines. Figure 8-13 from Ferland et al. shows that the contributions of the hot body, the nebular, and the coronal gas are able to explain the observed continuum.

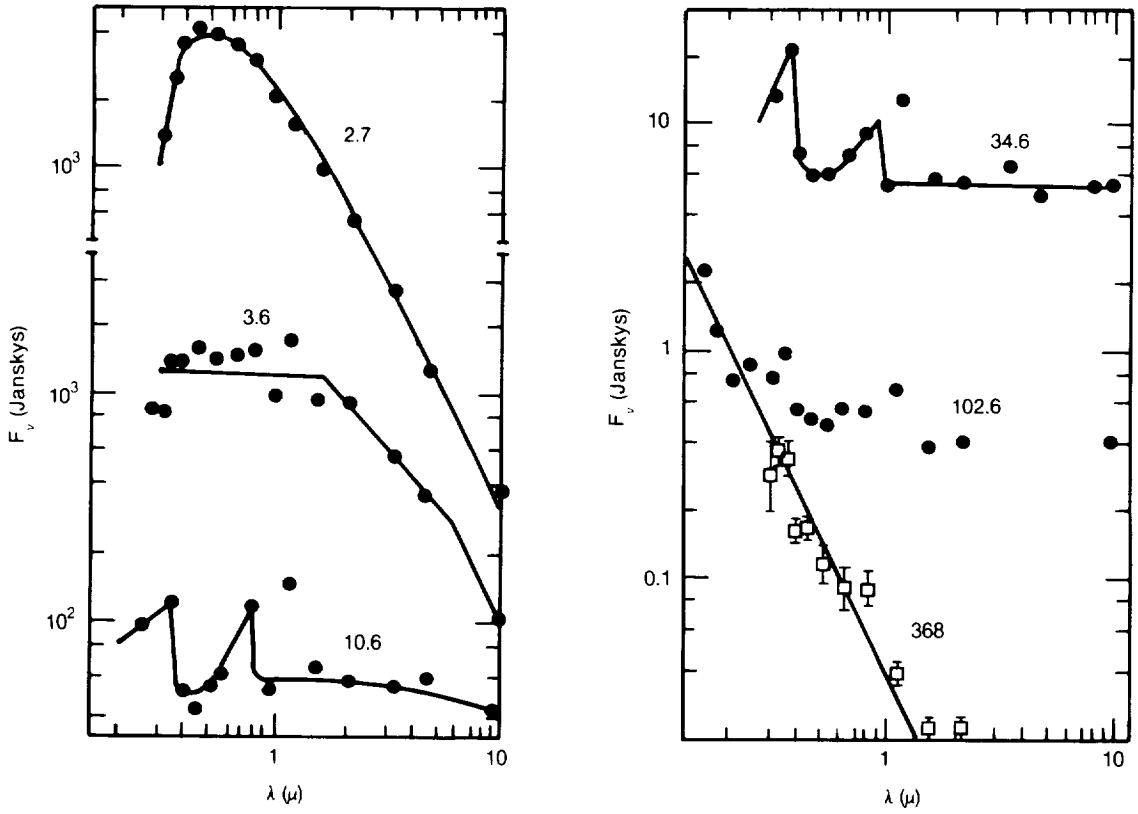

Figure 8-11. The composite energy distribution of the nova continuum is shown throughout the decline. The data are corrected for insterstellar reddening, and are taken from Ferland et al., 1986, from Wu and Kester, 1977 and from Ennis et al. 1977. The days after outburst are indicated. The squares and error bars are the data for day 368.

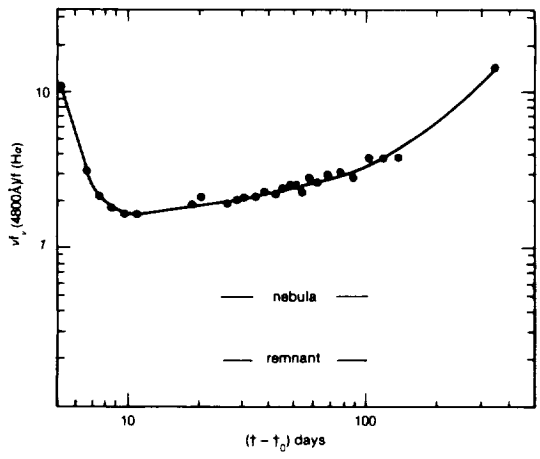

Figure 8-12. Ratio of the 4800 continuum to Hα as a function of time. The intensity of H α is used to predict the contribution of the nebula, and the intensity of the remnant continuum is predicted from Zanstra arguments. It is evident that a third contribution is required to fully account for the optical continuum.
(from Ferland et al. 1986).

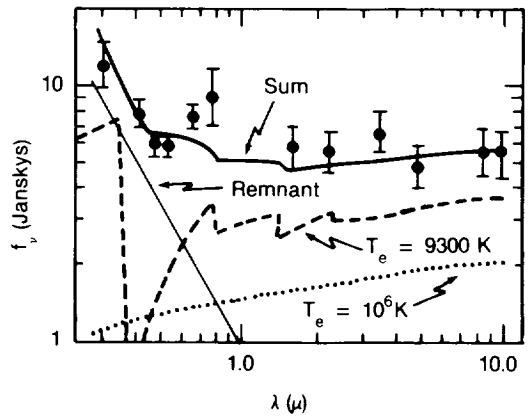

Figure 8-13. Continuum deconvolution for day 34.6. Reddening—corrected infrared and optical data are plotted. The contribution of a warm gas at 9300 K, plotted as a dashed line is predicted from the strength of Hα. A similar contribution from coronal gas at T≈10^6K, plotted as dotted line is fitted by matching the infrared continuum points; a hot Rayleigh - Jeans tail is added to fit the UV observations (solid line). The sum of all these contributions fits the observed data in a very satisfactory way.
(from Ferland et al. 1986)

II.F. RADIO SPECTRUM OF V1500 CYG

V1500 Cyg was observed at different frequencies with different radiotelescopes (see Figure 6.76): at 0.6, 1.4, and 5.0 GHz with the Westerbork Synthesis Radio Telescope, at 2.7 and 8.1 GHz with the Greenbank interferometer, at 10.5 and 22.5 GHz with the Algonquin 46-meter telescope, and at 90 GHz with the NRAO 11 m radiotelescope on Kitt Peak. Seaquist et al. (1980) show that the data are consistent with thermal bremsstrahlung from an expanding cloud of ionized gas. Radio and infrared observations can be interpreted not in terms of a shell of constant mass, but rather as an ionized zone moving outward through the shell.

II.G. THE SHELL OF NOVA CYG 1975

The shell became observable for the first time on direct photograph on August 27, 1979 (Becker and Duerbeck, 1980). The image of the nova (Figure 8-14) displays an extension into the NW quadrant, Since Beardsley et al. (1975) have excluded the existence of any star brighter than 21 mag in a circle of 10 inches around the position of the nova, this feature cannot be a close companion, but must be identified with the brightest part of the ejected shell. Hence, the mass ejection was strongly asymmetric, a behavior seen in other novae, in particular, in the fast nova GK Per. The mean expansion rate of 0.25 inch per year, compared with the expansional radial velocity of the principal spectrum, gives the distance of 1350 pc quoted above. Speckle interferometry of V1500 Cyg made by Blazit et al. (1977) 45 days after outburst gives an expansion rate of 0.26 inch per year in excellent agreement with the value obtained at a distance of 4 years from the outburst.

II.H. THE ELEMENT ABUNDANCE IN THE SHELL OF V1500 CYG

Ferland and Schields (1978b) have derived the chemical composition of the envelope by comparing the measured intensities of the emission lines of the nebular spectrum (observed between days 40 and 120 after the outburst) corrected for interstellar reddening E(B-V) = 0.51 with those predicted for an equilibrium photoionization model. The authors observe that the steady-state assumption is reasonably good during this phase of the outburst, because the recombination time scale is always short compared with the rate of decline of the nova. Several line ratios are indicators of the electron temperature and electron density, which vary between about 9500 K and 8400 K, and between 1.5×10^8 and 10^7 cm^{-3}, respectively, The model successfully predicts the intensities of He I, [OIII] and [Ne III], but underestimates the strengths of [Ne V] and [Fe VII], which may be produced in a mechanically heated "subcoronal" region. Table 8-1 gives the abundances derived from the nebular spectrum. Moreover, Ferland et al. (1986), using the determination of electron temperature and density made by Ferland and Shields (1978b) derive the abundance of argon from the only line present in their spectra, 7136 [Ar III].

Table 8-1. Chemical abundances of V1500 Cyg

Element	$\log N(V1500\ Cyg)/N_\odot$		
He/H	0.0		
C/H	1.4	+/-	0.2
N/H	2.0		0.2
O/H	1.3		0.1
Ne/H	1.3		0.2
A/H	<0.9		
Fe/H	0.1		0.3

Hence, helium and iron have solar abundances, while carbon, nitrogen, oxygen, and neon are strongly overabundant, and argon is less than a factor of eight of the solar value. The normal helium abundance is a characteristic common to several novae and not easily reconcilable with the excess of CNO. Colvin et al. (1977) suggest that the overabundant C,O,Ne are the result of convective mixing of the outer layer of the white dwarf with its carbon core. Helium and iron, on the contrary, would have the abundance of the material transferred from

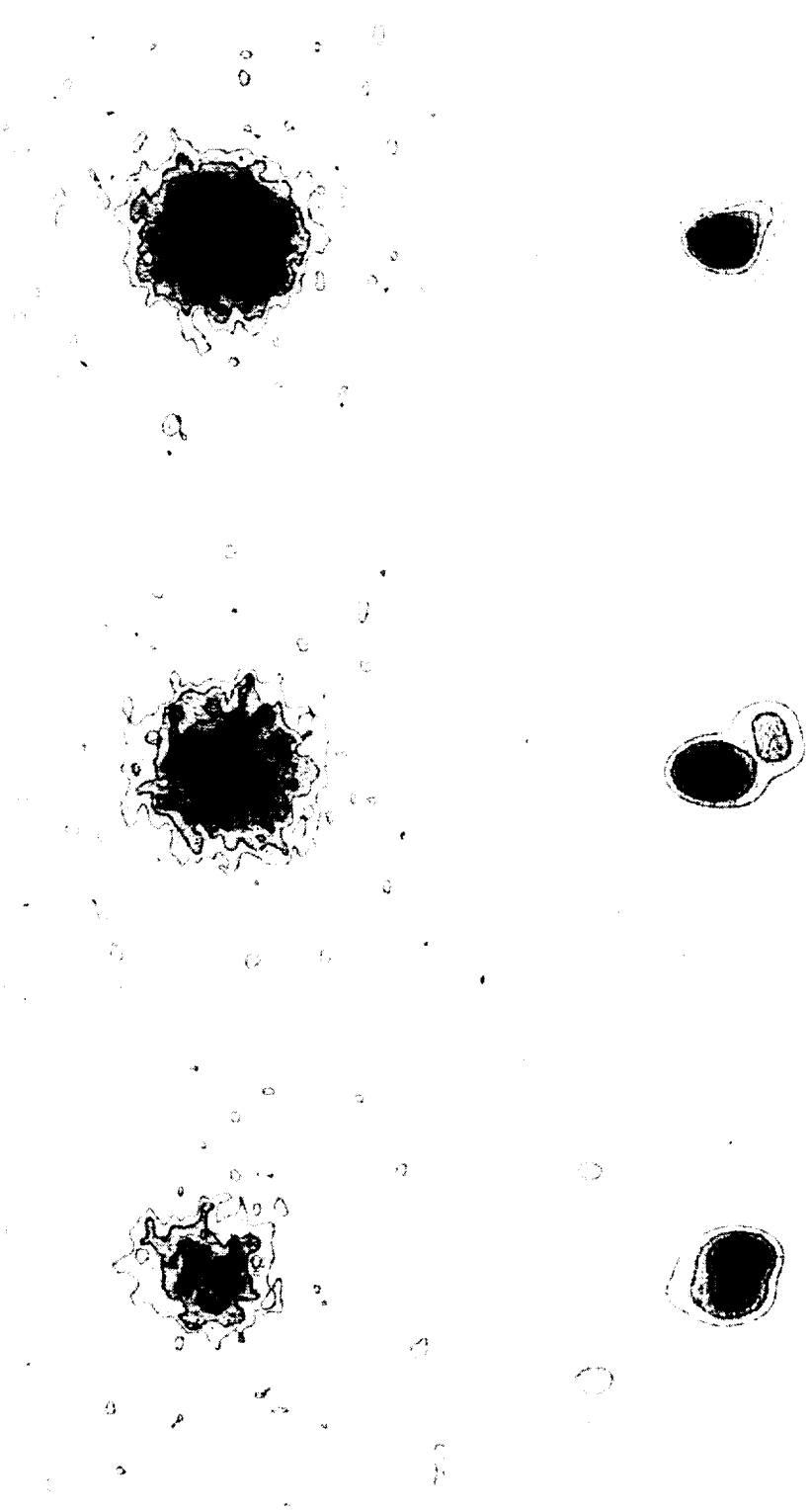

Figure 8-14. Density profiles (left) and deconvolved images (right) of the bright comparison star, the nova and the fainter comparison star (from top to bottom). North is up, west is to the right.
(from Becker and Duerbeck, 1980).

the companion to the white dwarf. The large abundance of nitrogen may result from proton capture during the thermonuclear runaway. For a complete discussion of these suggestions and theories of the origin of the outburst, see Chapter 7.

III. V603 AQL - AN HISTORY SURVEY
(written by Selvelli)

III.A. THE LIGHT CURVE

V603 Aql is the brightest member of the "classical" nova class having reached $m_v = -1.1$ at maximum and having now $m_v \sim 11.6$.

The light curve of its outburst, which started near June 9, 1918, was studied by Campbell (1919). Figure 8-15 illustrates the light curve of V603 Aql in the first 100 days after maximum. The "very fast" nova character of V603 Aql is based on the very short (2-day) time interval between the prenova phase and the maximum phase.

It is noteworthy that the maximum luminosity phase lasted a few hours only and was anticipated by a premaximum halt. The first decline phases were quite smoothed, with t_3 of the order of 10 days, and were followed by the oscillation phase, which lasted about 100 days and was characterized by the regularity of the oscillations with P~11 days. The last decline phases were instead characterized by a constant or weak variation in the light curve.

The luminosity of V603 Aql during the outburst phases has been studied by Payne-Gaposchkin (1941, 1957). Since the ejected shell is optically thick and Teff 10^4 K near maximum, the visual maximum luminosity provides a good estimate of the peak bolometric luminosity; the bolometric correction is small at this stage.

Figure 8-16 (from Gallagher and Starrfield, 1976) shows that if the maximum luminosity is to be maintained for a time of 100 days after maximum, the bolometric correction must be

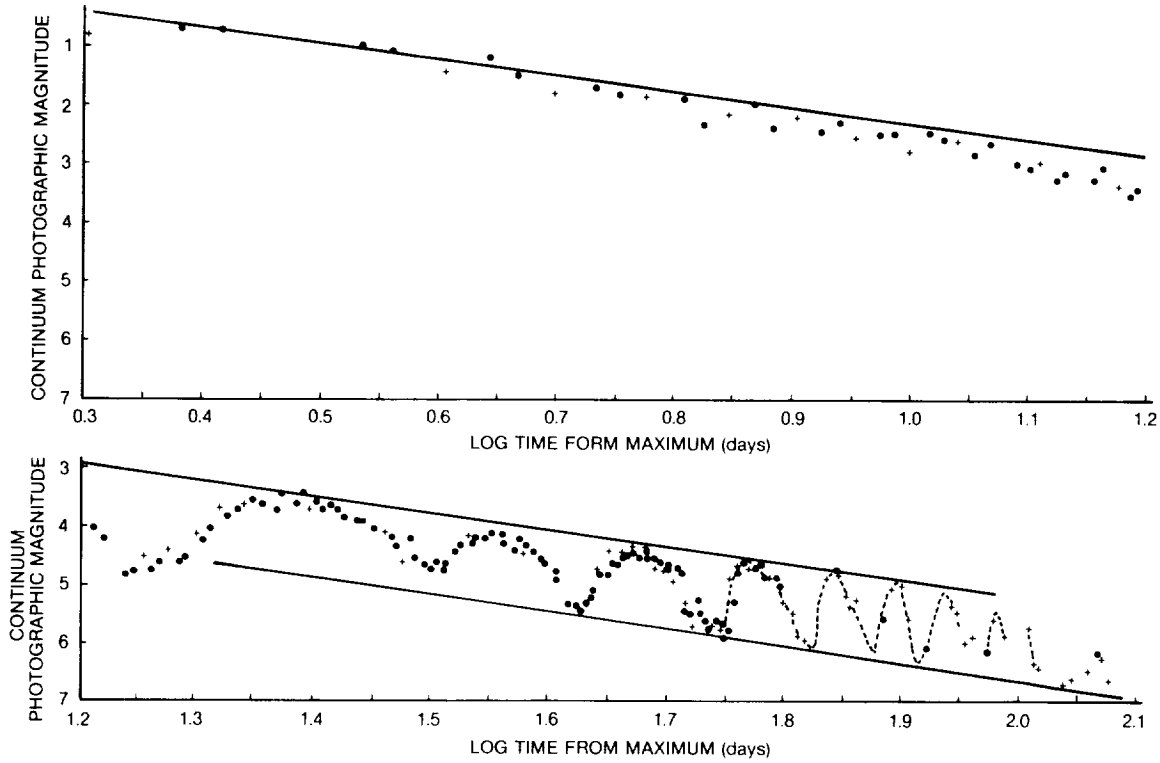

Figure 8-15. The continuum magnitude of V 603 Aql against log t from maximum. (From Friedjung, 1966a).

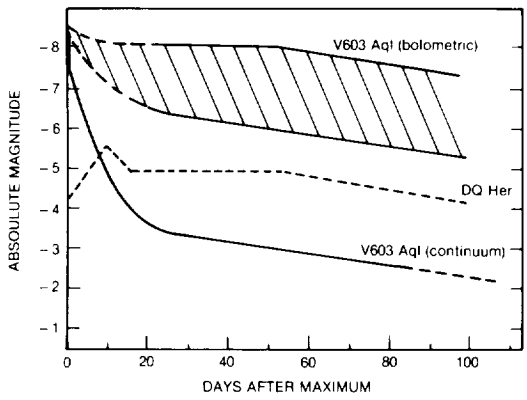

Figure 8-16. Smoothed photographic light curves of V 603 Aql and allowed range of bolometric absolute magnitudes. (From Gallagher and Starrfield, 1976).

higher than 6 magnitudes. Gallagher and Starrfield interpreted this as an indication of a decline in total luminosity, although the total amount of energy radiated under the assumption of constant L_{bol} of the order of L_{max} was estimated at about 8 x 10^{45} erg, a value which is approximately three times the total amount of kinetic energy and is similar to that found for slow novae (~10 times). Only the assumption M_{bol} ~7 during the interval from 10 to 100 days after maximum would give a ratio radiative energy/kinetic energy larger than one. If no bolometric correction is applied, this ratio is only one-tenth.

III.B. THE SPECTRUM IN OUTBURST

Objective spectra of the pre nova were reported by Cannon (1920). The energy distribution seemed to indicate a rather high temperature, but there was no evidence of emission lines. Several sharp absorption lines were seen, probably of hydrogen, and the spectral type was classified near Class A I. V603 Aql was also observed spectrographically during the first outburst phases. Absorption lines at maximum were violet-shifted by about -1300km s^{-1}. This spectrum was followed by the principal absorption spectrum, which showed similar features (resembling an F I star) but with higher velocities v_{out} ~-1500 km s^{-1}, thus producing an aspect of duplicity in the lines. Nearly at the same time with the presence of the principal absorption, bright emission lines of low excitation (H, NaI, CaII, FeII, etc.) appeared as superimposed to the absorption spectrum. This principal emission was gradually replaced by lines of increasing ionization and excitation. Ultimately, emission lines of NIII, NeIII, OIII, HeII, etc., appeared in the emission spectrum.

Gallagher and Starrfield (1976), using selected spectral features reported by Wyse (1939), have outlined the increasing level of ionization with the decline in luminosity (Figure 8-17). Lines from ions which appear shortly

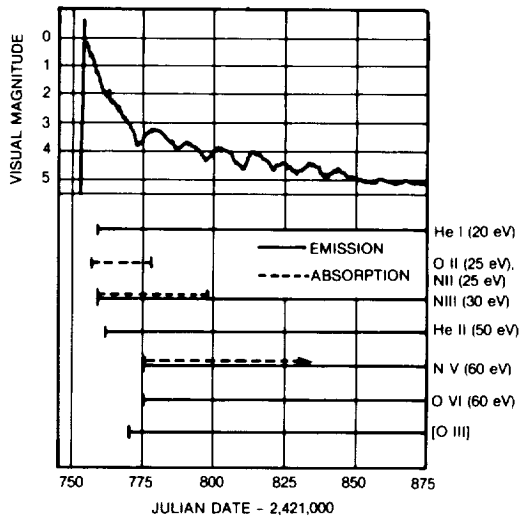

Figure 8-17. The appearance times for lines from major ions are compared with the visual light curve for V603 Aql. All of the data are from Wyse (1939). The pattern of increasing excitation with declining light is observed in most novae and suggests that ultraviolet energy redistribution following maximum commonly occurs.
(from Gallagher and Starrfield, 1976).

after maximum have excitation and ionization potentials of the order of 20 eV or less, while later features require much higher potentials (>50 eV).

The new system of lines of the diffuse-enhanced spectrum showed absorption features which were violet-shifted by about -2200 km s^{-1}, almost twice as much as in the premaximum spectrum. An even higher outflow velocity was present in the Orion Spectrum, which showed absorption lines (typically HeI, NII, OII) with velocities up to -4000 km s^{-1} Figure 8-18).

Payne-Gaposchkin (1957) has given a detailed description of the complex behaviour of the various absorption and emission systems.

As the nova faded, forbidden emissions became prominent, with a progressive strengthening with respect to the permitted ones. McLaughlin (1960), has provided a comprehensive description of the postnova emissions of V 603 Aql, including a detailed description of the behaviour of the HeII λ 4686 Paschen line emission. Nitrogen flaring, a secondary fluorescence originated from HeII Lyman alpha λ 303 was related to the increase in intensity of the 4686 emission line and was evident from the appearance of two wide and hazy emissions at 4100 Å and 4640 Å. It is remarkable that, as noted by Wyse (1940), most of the nebular light in 1919 and 1920 came from the OIII λ 4959-5007 doublet and, in second place, from the NII λ 6548-6584 doublet.

Payne-Gaposchkin and Gaposchkin (1941), from the absolute intensities of some lines and from the distance derived from the nebular expansion, have estimated the line luminosity for

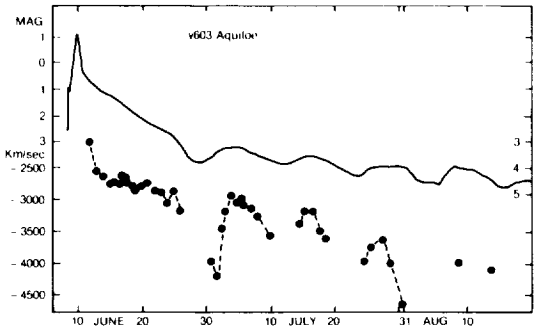

Figure 8-18. Radial velocities of Orion absorption system of V 603 Aql, correlated with light curve. (from Friedjung, 1966b).

H delta (log H_δ 36.65, Δ m = 3, and 35.85, Δ m = 6 with Δm counted from maximum) and for the [OIII] λ 5000 emission (36.99 at maximum).

Electron temperatures have been calculated from the usual OIII ratio (5007 + 4959) / 4363, and values of about 6500 K were derived. Estimates of the electron density, based on the surface brightness of H delta and the nebular radius, gave values ranging from 1 x 10^9 cm^{-3}, in the early phases, to 1 x 10^6 cm^{-3} in the early nebular stages. With the assumption $N_e \sim N_H +$, a lower limit to the mass of the shell ejected in the outburst was estimated in 10^{29} g.

Friedjung (1966b) has given a set of determinations of temperatures and radii of the ejected shell in the first months after the outburst. The estimates of the temperature were made using the methods developed by Zanstra, Ambartzumian, and Stoy and data from the literature and from archives. From this study, Friedjung found support in favour of an inverse T-R correlation. A clear relation between the characteristic velocities of the diffuse-enhanced and Orion spectra and the corresponding radii was also found (Figure 8-19).

III.C. THE STRUCTURE OF THE EJECTED SHELL

The expansion of the ejected shell and the nebular structure has been studied quite carefully by various authors. About 4 months after maximum, Barnard (1919) detected a nebular shell with a diameter on the order of 1" that expanded at a uniform rate. Wyse (1940), in his protracted photographic and spectroscopic monitoring, showed that the expansion rate was at about 1"00 per year during some 20 years. Wright (1919), from a series of exposures made by rotating the spectrograph, was able to demonstrate that the expanding shell was not spherically symmetric. From studies on spectrograms taken at Lick Observatory with the slit at different position angles, Baade (1947) proposed the presence of a system of three rings (equatorial belts) in parallel plans, and of two very large polar caps (blobs, condensations) that were apparently ejected in opposite directions along a common symmetry axis pointing nearly (16°) toward the sun.

Weaver (1974) has made the most exhaustive study on the development of the shell. From the slit-spectrograph images taken with the slit in a number of different position angles, he reconstructed the structure of the ejecta. The model he derived describes the nebula in terms of cones of emitting material and two polar jets. The axis of the cone system and the line of

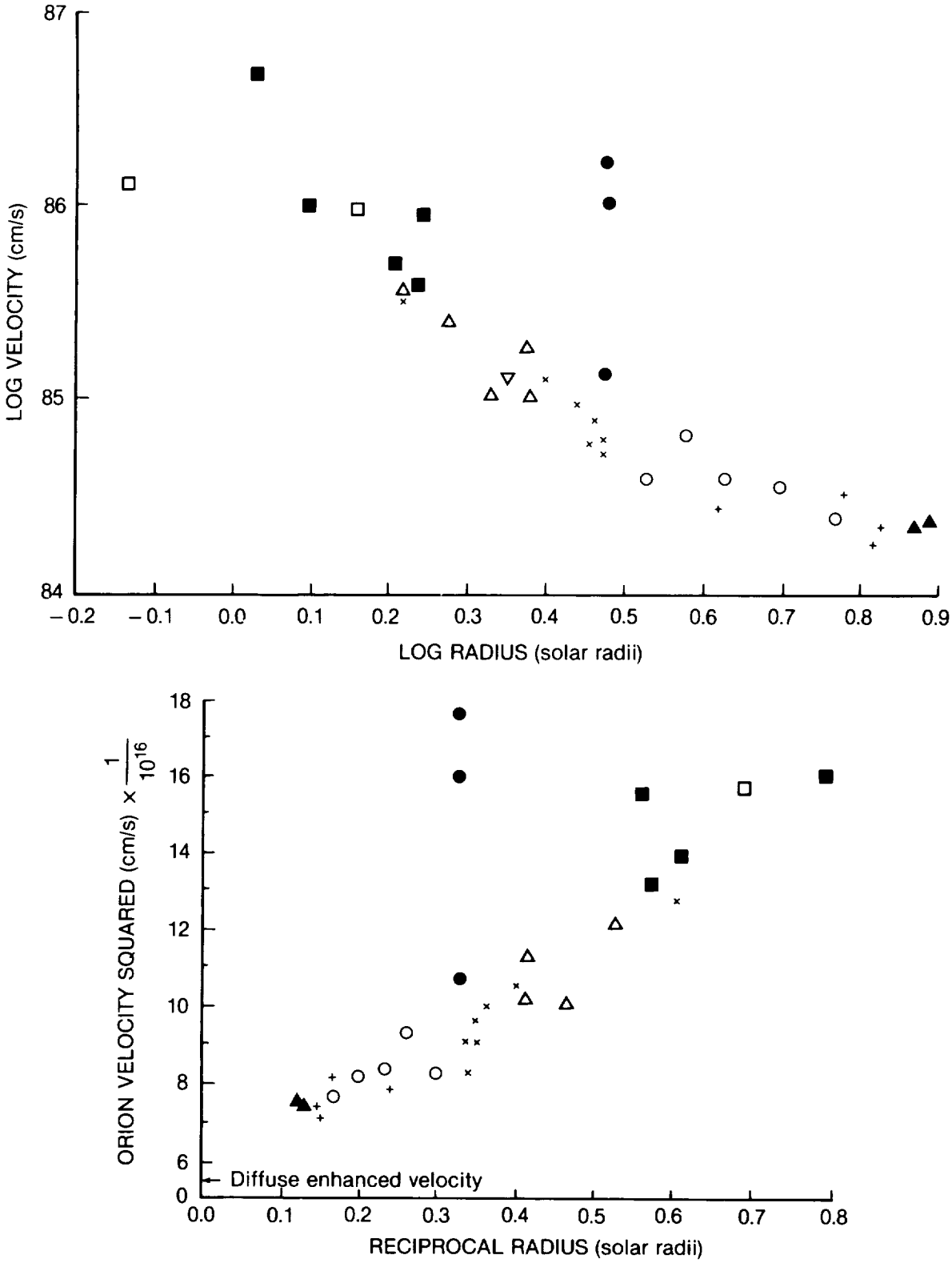

Figure 8-19. a) The relation of Orion velocity to radius for V 603 Aql.log t included between less than 0.80 (black triangles) and larger than 1.60 (black squares) and 1.73 (white squares). b) Relation between the velocity squared and reciprocal radius. Symbols for different epochs are the same as in a) (from Friedjung, 1966b).

sight are nearly perfectly aligned (angle less than 1°). Figure 8-20 gives a sketch of the morphology of the ejecta.

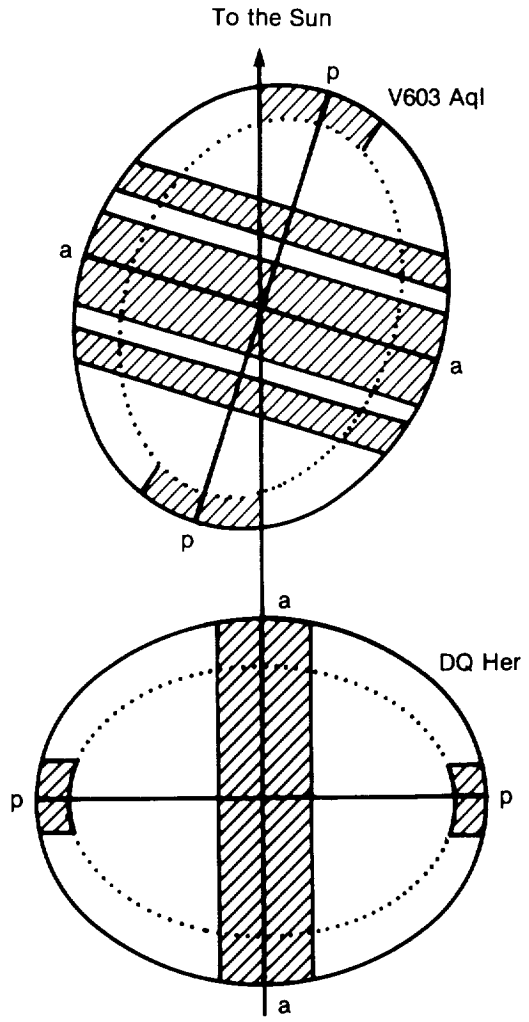

Figure 8-20. Morphological models of the principal envelopes of V 603 Aql and DQ Her.pp is the polar axis and aa the equatorial belt. (from Mustel and Boyarchuk, 1970).

III.D. UV AND X-RAY OBSERVATIONS OF V 603 AQL

The first UV observations of the old nova were made by Gallagher and Holm in 1974 (1974), using the 8-inch photometric telescopes of the OAO-2 Wisconsin Experiment Package (WEP).

They attempted also to observe other quiescent novae, but only V 603 Aql and RR Pic were positively detected. From the observed distribution, after correction for $E_{B-V} = 0.07$, Gallagher and Holm were able to estimate an empirical color temperature of about 25,000 K.

From the observed continuum distribution and the knowledge of the distance, a lower limit for the luminosity of about 8 $L_{\odot}$ was derived.

After the launch of IUE, V603 Aql was observed by several authors: Selvelli and Cassatella (1981), Drechsel et al. (1981), Lambert et al. (1980), Duerbeck et al. (1980a), Krautter et al. (1981), Ferland et al. (1982a), etc. (Figure 6-36 shows a typical IUE spectrum of V603 Aql.)

The remarkable differences from author to author in the temperature fitting to the continuum distribution have already been mentioned in Chapter 6. In this respect, it is worth mentioning that Lambert et al. (1980) in the first IUE observations of V 603 Aql noted a systematic disagreement between the OAO-2 and IUE values shortward of λ 1600 and suggested real variability in the continuum of the hot component.

Duerbeck et al. (1980) reported that the CIV 1550 emission was accompanied by a blue-shifted absorption indicating mass outflow. Selvelli and Cassatella (1981) used low-resolution archive data and original high-resolution spectra to look for a possible phase dependence in the continuum distribution (which could explain the differences in temperatures found in previous works) and to check the reality of the presence of P Cyg profiles in the resonance lines of CIV and SiIV reported by Krautter et al. (1981). One of the results of this study was the suggestion of the presence of rapid variations in the far UV and "eclipse-like" effect in the near UV for the high excitation lines, which seemed correlated with the orbital phase.

The high-resolution SWP spectrum was slightly underexposed. However, three emissions were clearly present, i.e., SiIV 1400, CIV

1550, and HeII 1640. They all present the same kind of profile, which appears to be a wide and shallow emission centered at the nominal wavelength. The half-half widths indicate velocities of around 900 km s^{-1} that cannot be ascribed to the orbital motion, which has lower velocities. It is remarkable that this high-resolution, deep-exposure spectrum (420 minutes) has not revealed any additional emission line besides the three emissions mentioned above (see also Figure 6-42) that are clearly evident in the low-resolution spectra. The absence of (sharp) intercombination emissions was interpreted as an indication that the nebular shell had essentially vanished.

The main shortcoming of this study was in the inhomogeneity of the data: the IUE spectra used were taken at different epochs, and phases were reconstructed assuming Kraft's (1964) period. Drechsel et al. (1981), instead, made an extensive set of observations monitoring the nova during almost two complete cycles, one entire IUE shift. A total of 8 SWP and 2 LWR spectrograms were obtained. UV (and optical) changes with a period in agreement with that of Kraft were detected and interpreted as related to the phase of the binary system. The emission line spectrum consists of two distinct groups: quite strong resonance lines such as SiIV, CIV, AlIII, MgII, and much weaker semiforbidden lines such as NIV 1486, NIII 1750, CIII 1908, and CII 2326. The presence of these latter lines, if confirmed, would indicate that the system is surrounded by highly diluted (nebular) matter. The strongest feature is the CIV resonance doublet λ 1550. Phase-dependent variations (by a factor of up to two) in the line intensity are clearly evident, especially for CIV, SiIV, HeII, and NIV 1486. The most pronounced changes occur near maximum light at about $\phi = 0.5$. The intensity is instead minimum near orbital phase 0 (Figure 8-21). The continuum variations with phase are smaller than the 0.3 mag observed in the visual (FES) light-curve. The fact that the variations in the optical continuum, UV continuum, and UV line emission are strongly correlated suggests that the main source of UV and optical radiation are located in about the same region of the system. This behaviour is in agreement with the optical photometric observations of Panek (1979), who showed gray variations in the light-curve. "Eclipse-like" effects (near phase 0.0) are not evident in the semi forbidden lines. This was interpreted as an evidence for the presence of diluted gas surrounding the whole system. These results are in disagreement with those by Selvelli and Cassatella (1981) who did not show presence of nebular lines.

A study similar to that of Drechsel et al. but focused on the LWR range (which was covered by two observations only in that study), was performed by Selvelli and Cassatella (1982). Five LWR spectra at low resolution were taken in a close sequence, to monitor the phase-related variations (since they covered about one orbital period), and one high-resolution LWR spectrum was taken in order to provide correct identifications and information on the emission lines shape. Actually, no stellar lines, either in emission or in absorption, were detected in the high-resolution spectrum, probably partly because of the fact that it was underexposed by a factor of about two, and mainly because the possible features, being very broad and shallow as in the high-resolution SWP spectrum described previously by Selvelli and Cassatella (1981), were not detectable. The five low-resolution spectra, on the contrary, have permitted an easy estimate of the presence or absence of spectral features. These data indicate that the emission lines are probably formed in the accretion disk and that there is no trace of any nebular contribution from the envelope ejected at the time of the outburst. (Figure 8-22)

About three fourths of the emission lines have been identified or tentatively identified as belonging to permitted, semiforbidden, and forbidden transitions of medium-high ionization species. The strongest emissions are Mg II λ 2800, OIII λ 2320, OII λ 2470, AI II λ 2669, probably Fe XII λ 2568 and 2578, O III λ 3047 and a few unidentified lines. In addition, all the lines of the He II Paschen series are present, together with the O III lines produced by the Bowen flourescent mechanism involving He Lyα λ 303.

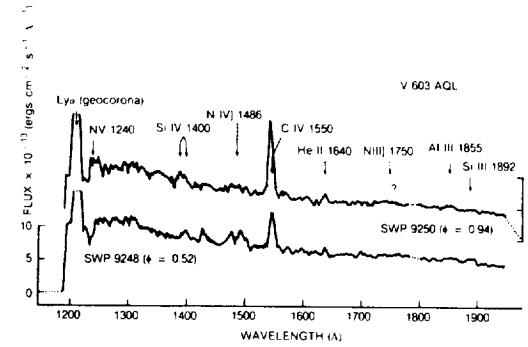

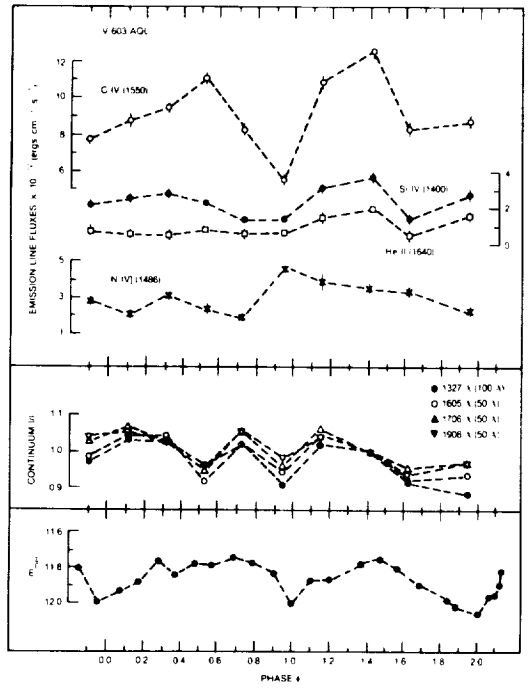

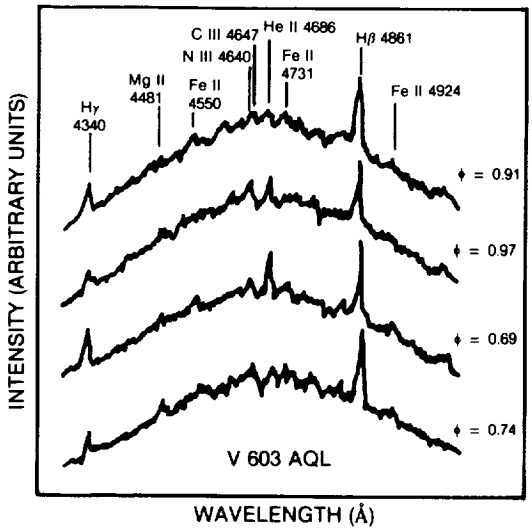

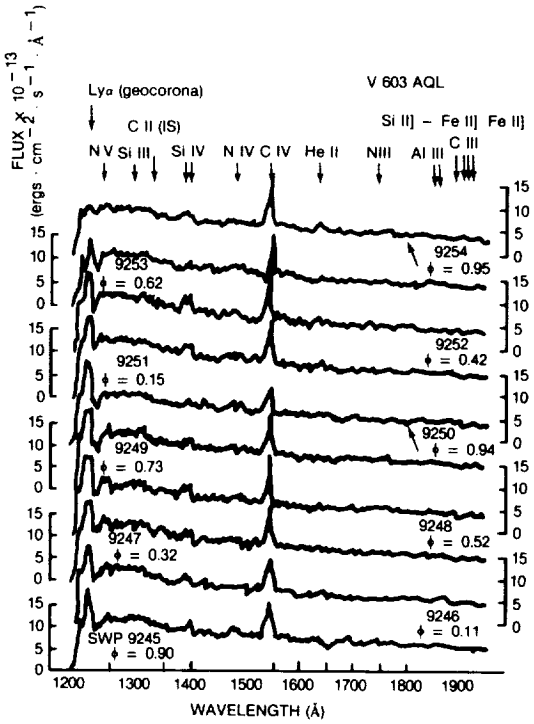

Figure 8-21. a) Two selected IUE short wavelength spectrograms of V 603 Aql obtained at orbital phase 0.52 and during the supposed eclipse at phase 0.94. Pronounced variations of the strengths of C IV 1550, Si IV 1400 and He II 1640 as well as N IV / 1486 - but in the opposite sense are evident. b) Comparison of the visual light curve (obtained with the Fine Error Sensor on board of IUE), at the bottom, with the emission line flux of four ions (top) and ultraviolet continuum light curves (center). c) IUE short wavelength spectrograms obtained during more than two complete orbital cycles. d) optical observations obtained with the ESO 3.6 meters telescope. Variations in the line strengths (e.g. He II 4686) and line profiles (e.g. H gamma) are noticeable.
(from Drechsel et al, 1980: Figs a, d; Drechsel et al. 1981: Figs b, c.)

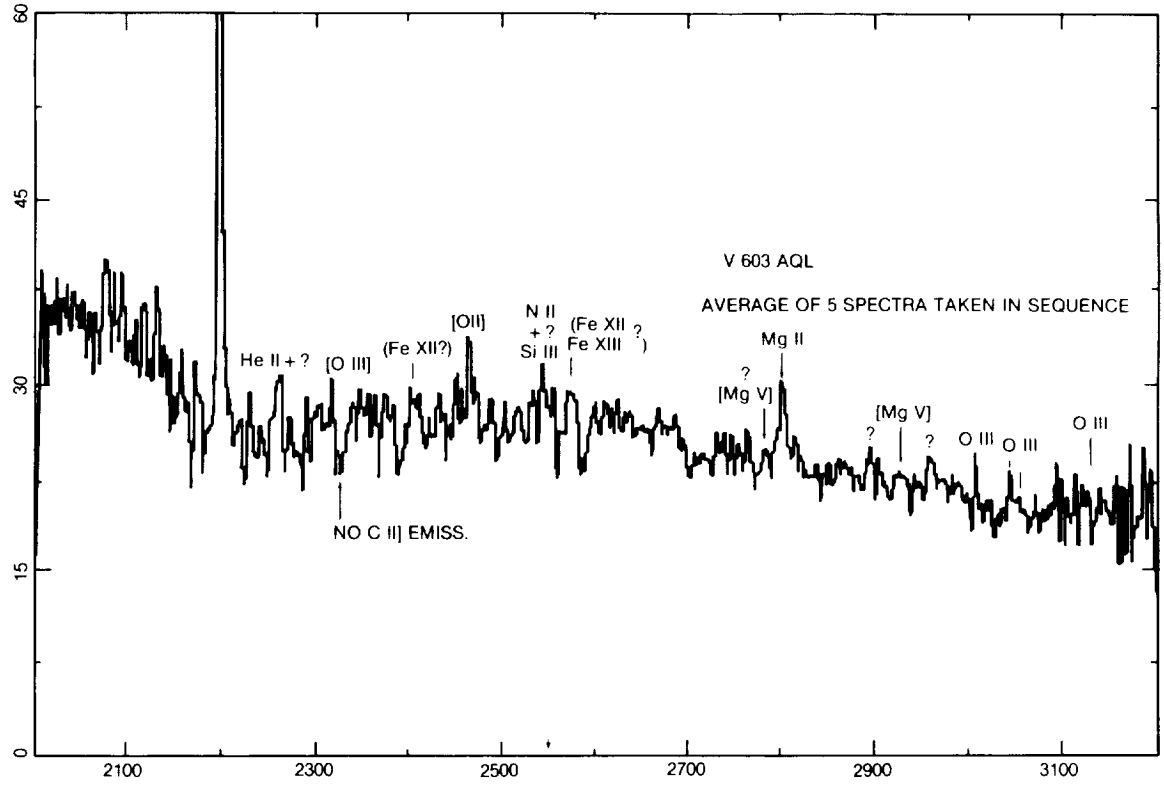

Figure 8-22. Average of 5 spectra of V 603 Aql taken in sequence in the IUE long wave range (2000-3100 A).

Selvelli and Cassatella (1982) have attributed to coronal lines many emission features lacking any other reasonable identification.

Actually, of the dozen coronal lines reported in the near UV range of the solar spectrum, all but one (Fe XI 2649) might be present in V603 Aql.

Figure 8-23 reports the values (not corrected for reddening) of the total flux below the continuum (i.e., $\int_{2000}^{3200} F_{\lambda}^{c}\, d\lambda$ in ergs cm^{-2} s^{-1}) of the Mg II emission intensity (erg cm^{-2} s^{-1}) and of the visual magnitude derived from the FES counts as function of the orbital phase (seeTable 8-2).

For the ephemeris, the value of P=0.1383d and the time of the principal minimum given by Herczeg (1982) have been assumed.

There are variations both in the lines (by a factor of $\simeq 2$) and in the continuum (by a factor of $\simeq 1.3$) in spectra taken in close sequence. It is questionable, however, whether these variations are intrinsically phase-related. The observed maximum of the Mg II emission and of the continuum around phase ~ 0 might be attributed to a transient phenomenon. This might explain the disagreement with the visible data and the previous far UV observations.

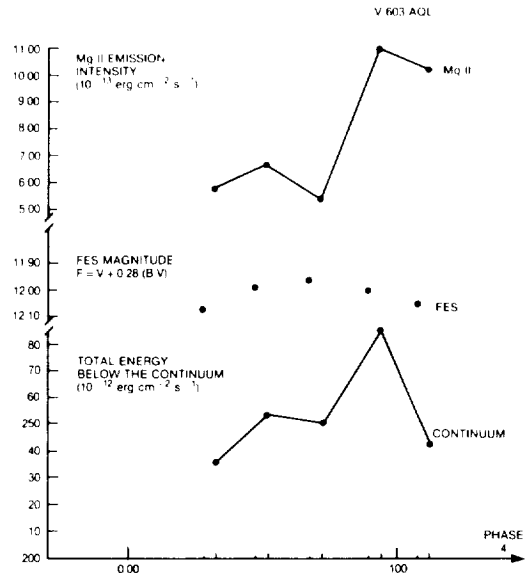

Figure 8-23. The variations observed in 5 spectra taken in strict sequence, in the long wavelength region.

TABLE 8-2.

VALUES OF VISUAL MAGNITUDE M_V(FES), MG II EMISSION, AND TOTAL FLUX BELOW THE CONTINUUM, FOR V 603 AQL AT DIFFERENT ORBITAL PHASES.

Phase*	m_v (FES)	MgII Emission (10^{-13} erg cm^{-2} s^{-1})	Total Flux below the continuum (10^{-12} erg cm^{-2} s^{-1})
0.281	12.11		
0.325		5.75	235
0.479	12.03		
0.522		6.70	253
0.678	12.00		
0.722		5.10	252
0.899	12.04		
0.942		11.00	285
1.097	12.09		
1.140		10.25	242

Surprisingly, the maximum in the near UV total flux and in the Mg II emission intensity occurs near phase = 0 (principal minimum in the visible), while at the other phases, the values of the quantities under study do not differ very much from each other.

Ferland et al. (1982) have made a quantitative analysis of the physical conditions in the continuum and line-emitting region of the system. After correction for E(B-V) = 0.07, the continuum follows a power-law close to the $\lambda^{-2.33}$ value expected from a "standard" disk. If the distance is of 380 pc, the total luminosity is of the order of 5 x 10^{34} erg s^{-1}. If this luminosity is generated in the accretion disk, the mass-accretion rate can be derived: $\dot{M}\sim10^{18}$ gr s^{-1}.

A study of the emission lines from ions like H, He, C, N, O, has led the authors to suggest that these lines are formed in a circumstellar "corona" with size comparable with the binary separation. The "corona" is heated by the hot radiation from the accretion disk. The large radius of the "corona" is required by the emission measure of the gas and by the presence of the NIV 1486 line, which has a critical density of about $10^{10.5}$. Ferland et al. (1982a) pointed out that several features of the model, in principle, were open to direct observational test. For HeII (produced across much of the corona) they expected a broad line with a fill-in center, while for lines such as C IV (produced only across an annulus), they expected a narrower, saddle-shaped profile.

Ferland et al. (1982) studied also the optical spectrum of V 603 Aql (Figure 8-24). The hydrogen emission lines show a flat Balmer decrement:

$H\alpha=0.99$, $H_\beta=1.00$, $H\gamma=0.86$, $H\delta=0.92$, etc.

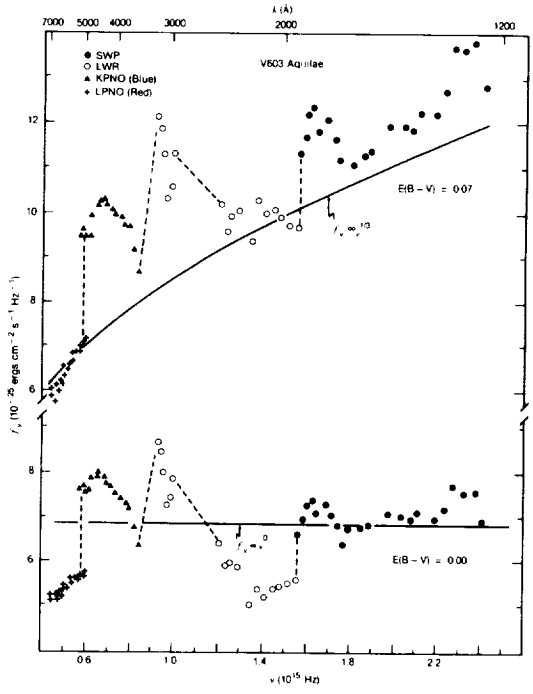

Figure 8-24. The lower panel shows the observed optical - ultraviolet continuous energy distribution. The upper panel shows the energy distribution after applying an interstellar reddening correction E(B-V)=0.07 mag. This reddening correction, which is consistent with the object's galactic position, brings the continuum to the form predicted for an optically thin accretion disk.
(from Ferland et al, 1982a)

*ϕ=0 corresponds to the principal minimum of the visible light curve. The phase associated with m (FES) is that corresponding to about 2 minutes before the beginning of the exposure. The phase associated with the spectral quantities is that of mid-exposure. (4 June 1981, GMT = 23y 09m 35s = JD 2444760.4652).

This anomalous behavior was interpreted in terms of emission from a small volume of dense gas (10^{13} cm^{-3}) on the surface of an accretion disk. The presence of N IV 1486 ($N_e^{crit} = 10^{10.5}$) however, is disturbing.

III.E. V603 AQL IN QUIESCENCE: HOW MANY PERIODS IN V 603 AQL ?

The binary character of V 603 Aql was discovered by Kraft (1964), by using high-resolution Palomar coude spectrograms at 38 Å/mm. From the RV changes in the Hγ and Hδ emissions, he determined a period of 3^h 19.5^m (0.13854 days). The RV curve has 2K = 75 km s^{-1}, and the emission lines have an intrinsic broadening of approximately 240 km/s (half-half width). The low 2K value suggested low system inclination, and, therefore eclipses or occultation effects were not expected.

The first photometric observations never covered one entire period; they just revealed strong flickering activity. (Walker, 1963; Robinson and Nather, 1977)

Time-resolved spectrophotometry (Panek, 1979) has shown that differences of 0.3 mag over time scales of ~10 minutes are common in V603 Aql. These variations are gray.

Rahe et al. (1980), during an 8-hour observing run with the IUE satellite, monitored the optical photometric behavior of V603 Aql by using the FES instrument (5.1-second integration times and about 20 points in the curve, separated by intervals of about 20 minutes).

The light curve they found (Figure 8-25) reveals the presence of three pronounced minima separated by a time interval, which is in agreement with the spectroscopic period found by Kraft. The presence of these minima was tentatively interpreted in terms of a partial eclipse of the accretion disk around the white dwarf by the late main-sequence component, or as an occultation of the hot spot by the disk itself.

Slovak (1981) made high-speed photometric observations of V 603 Aql starting on 15 June 1980, 5 days after Rahe's observations. The

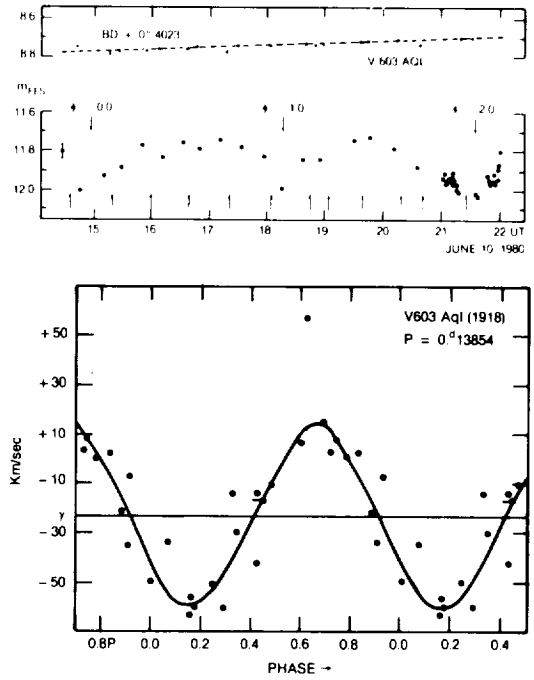

Figure 8-25. Visual light curve obtained with the FES (from Drechsel et al, 1980) and RV curve (only H gamma and H delta have been measured) (from Drechsel et al, 1983b).

new data were reduced, using a cross-correlation analysis, and power spectra were calculated to search for low-amplitude rapid oscillations, of the kind detected in DQ Her and V533 Her.

During the five observing runs, no evidence for regular eclipses or any other periodic feature was found. (Figure 8-26) This fact led to the conclusion that the variations reported by Rahe et al. (1980) may arise from the formation of transient features in the accretion disk.

This failure in the attempt to find regular eclipses was interpreted as a support to the indications of low system inclination derived from the spectroscopic data of Kraft and from the study of the nebula by Weaver (1974). Similar arguments were also adopted by Cook (1981) to reject the eclipse explanation of the minima observed in the light curve.

Surprisingly, new photometric observations by Haefner (1981) in summer 1981, revealed a repeating hump structure in the light curve. A periodogram analysis gave a period of

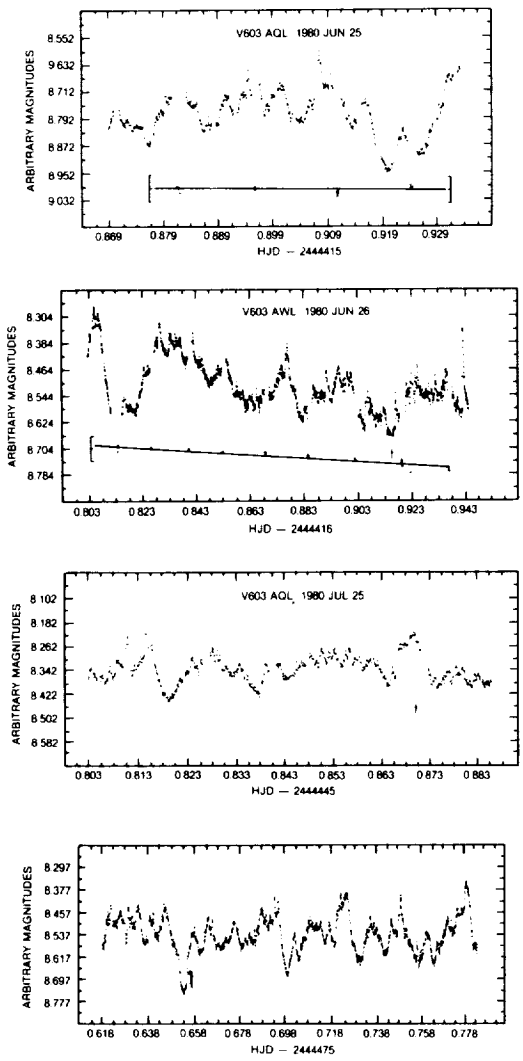

Figure 8-26. Light curves of V 603 Aql obtained during several nights, with a resolution of 6 s per point. Solid arrows denote predicted time of minimum light. On July 25 a hump occurs rather than an eclipse. (from Slovack, 1981).

0.144854 days, about 5% larger than the spectroscopic one. Haefner suggested that periodic features only can be identified when the mean light level of the system is low (V~11.9); otherwise, they might be masked by a strong flickering activity. In this respect, it is worth remarking that the observations by Slovak indicated V~11.4. New observations were made by Herczeg (1982) who also used data obtained in previous works in his attempt to clearly define the photometric period. He found, beyond any doubt, clear evidence of minima in the light-curve and suggested 0.13816 days as the best value for the period, leaving, however, a possibility for P = 0.13822 and P = 0.13828. Also, he pointed out the considerable observational difficulties produced by the strong photometric disturbances the star presents.

More recently, Haefner and Metz (1985) have presented a careful analysis of the data taken in mid summer 1981 with the ESO 50 cm telescope during long observing runs. The preliminary results presented by Haefner (1981) were confirmed: hump-like features instead of eclipse-like features, and a period of 3^h 28.8 (0.144854 days), which is about 10 minutes (5%) larger than the spectroscopic one [Kraft 3^h $18^m.9$].

No periodic variations during the whole observing time interval, which covered 117 periods, were detected. The observed hump structure (Figure 8-27) in view of the low inclination of the system, cannot find an easy explanation. Haefner and Metz have made also polarimetric observations. The measurements of linear and circular (P_c~2.7 10^{-4}) polarization revealed an unexpected, new period of 2^h 48^m.

There are, therefore, at least three periods that characterize the various observing modes of V 603 Aql.

On the basis of these results, Haefner and Metz (1985) have proposed a detailed model of intermediate polar, combined with a transitory eccentric disc to explain the different periodicities present in the system. A magnetic field of the order of 10^6 Gauss was derived from the degree of circular polarization.

Optical observations obtained in 1980 and with the ESO 3.6 m. telescope (Drechsel et al., 1983b) together with previous data taken by Kraft, have been used to determine more precisely the spectroscopic period. (Figure 8-28).

The power-spectrum analysis yielded P = $0^d.1381545$ in good agreement with the early determination of Kraft: P = 0.13854.

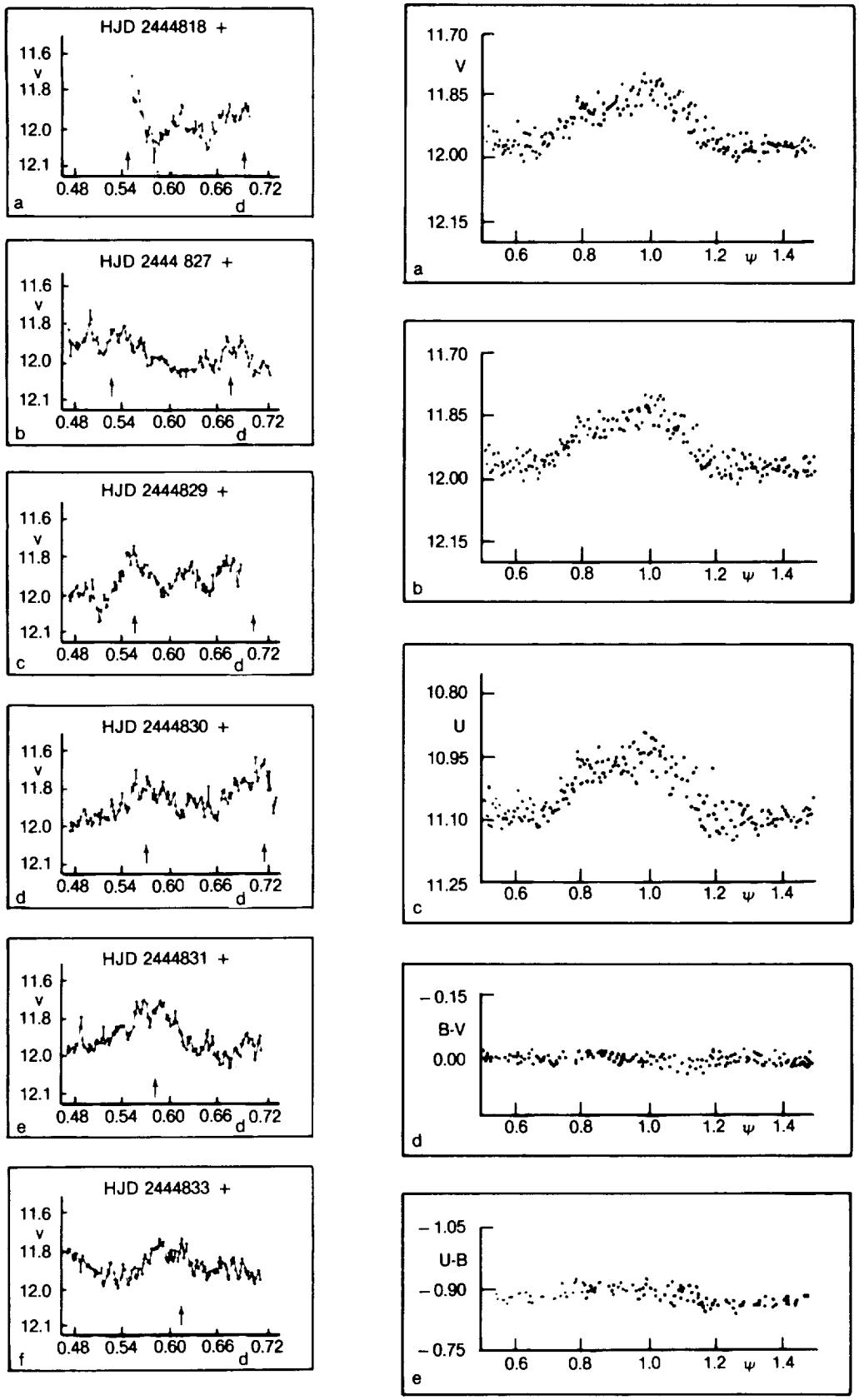

Figure 8-27. a) Selected photometric runs in chronological order V vs JD. Arrows indicate the predicted time of maxima. b) Average light curves and colors. (from Haefner and Metz, 1985).

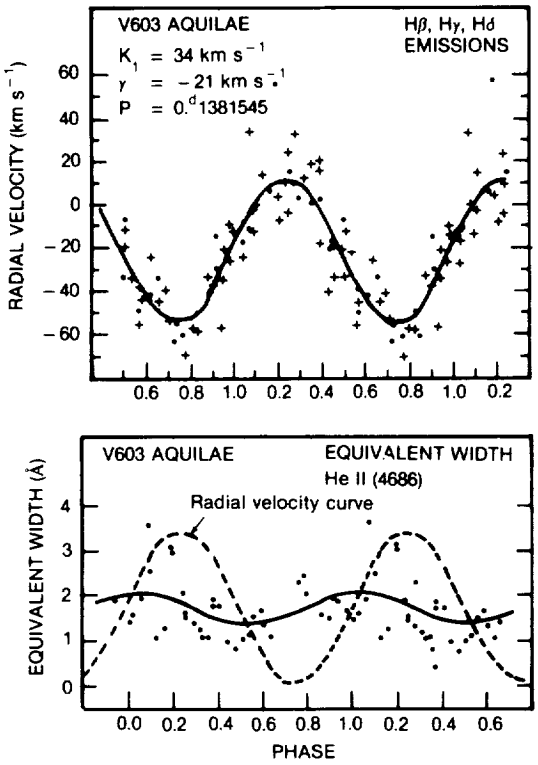

Figure 8-28. a) Radial velocity curve of the primary component of V603 Aql (crosses H Beta and H Gamma emission lines measured by Drechsel et al, 1983b), while the dots are earlier measurements by Kraft. b) equivalent widths of He II 4686 vs the phase. The dashed line is the RV curve shown in a). (from Drechsel et al, 1983b).

IV. CP PUP

(written by Bianchini)

IV.A. INTRODUCTION

CP Pup is one of the two brightest galactic novae ever observed; the other one is nova Cygni 1975. It reached photographic magnitude 0.5 on JD 2430675, rising from fainter than 17th magnitude. A large outburst amplitude, a very rapid development, though with modest expansion velocities, high terminal excitations with the simultaneous presence of very low excitation lines, such were the first peculiarities observed in nova Puppis 1942 (Payne-Gaposchkin, 1957). At light minimum, the nova has been found to be a close binary system having an unusually short orbital period below the 2-3 hour period gap for all cataclysmic variables (Bianchini et al., 1985a,b; Warner, 1985; Duerbeck et al., 1987).

We shall report here some relevant data for this nova at outburst and at minimum.

IV.B. THE OUTBURST

The outburst light curve of CP Pup shows a smooth early decline and a transition phase without oscillations (Figure 8-29). The star rose from fainter than 17th magnitude and so, at least after the rise, it had the largest range recorded for a nova. Now the old nova standstills at $m_v \sim 15$. The nova at maximum reached absolute magnitude -11.5 (Duerbeck,1981), so that it radiated for a large fraction of the outburst with a luminosity that surpassed the Eddington luminosity by two orders of magnitude. The velocity of decline of the light curve was as high as 0.37 mag/day. Such a large velocity of decline has been reached by the more recent very bright nova Cygni 1975 and also by the far less energetic recurrent nova T CrB, which also presented a similar rapid spectral development.

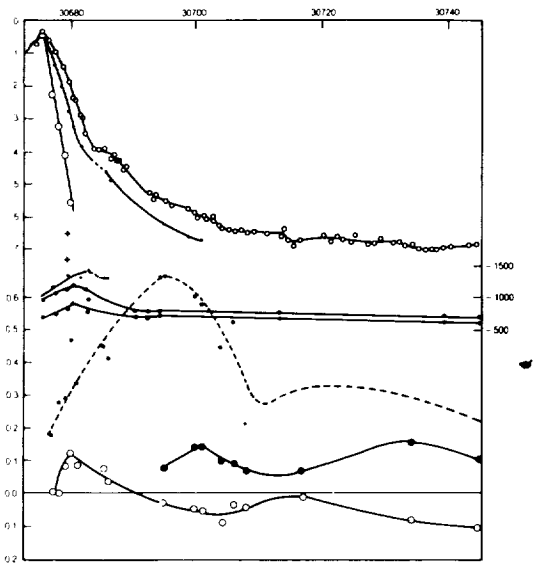

Figure 8-29. Above, the light curve of CP Pup 1942 in the photographic (dots), the visual (small circles), and the continuum (large circles). Middle, radial velocities from absorption lines (dots), red edge (half-filled circles) and violet edge (also half-filled circles) of bright lines. Ordinates are shown on the right. Bottom, logarithm of the ratio Hβ/Hγ (dots and broken line), the ratio V/R for the HeII 4686 (circled crosses) and for the Balmer lines (circle). Note that the curve of the HeII lines changes in the opposite sense to those of the Balmer lines. (from Payne-Gaposchkin, 1957).

Soon after the maximum, the spectra of CP Pup showed the presence of high-excitation lines of [OIII], [CaVII], [[CrIII], [MnVI], [FeVIII], [FeX] and [FeXI]. However, the same spectra revealed bright lines of [OI] OI, Na, CaII, Si, FeII, and [FeII], indicating the presence of a stratification of the ionized atoms around the star. We recall here the fact that high-excitation coronal lines are observed also in recurrent novae like, for example, T CrB. This demonstrates that the velocity of the photometric and of the spectroscopic development and the appearance of high-excitation emission lines are not related only to the rate of the energy output by the explosion. In fact, low-energy outbursts with large expansion velocities of very thin envelopes should also favor the formation of high-excitation lines. Moreover there exists only a very general correlation between the velocity of decline and the expansion velocity of the envelope of classical novae. Actually, the velocities derived from the diffused-enhanced spectrum and the Orion spectrum of CP Pup were not particularly large: –1600 km/s and –2000 km/s, respectively. When the envelope became optically thin, we observed a doubling of the nebular lines, due to the layers expanding towards us and those expanding in the opposite direction. These emission lines yielded an even lower value of the expansion velocity: 1100 km/s. The velocity derived from P Cyg profiles was of 1400 km/s. These differences can be attributed to the fact that the expansion velocity of the observed nebula is often lower than that derived from the blue-shifted absorption features that characterize the so called continuous wind-ejection phase of the decline. It is then possible that the bulge of the matter lost by the nova was not principally formed by the high-velocity wind produced during this relatively well-extended phase of the nova outburst.

However, the spectral development of CP Pup was really very fast. The diffuse-enhanced spectrum appeared four days and the Orion spectrum, five days after light maximum. The absorption spectrum was recorded for only fifteen days: it disappeared at the beginning of the transition phase, when the spectrum of a nova starts changing from a more stellar to a purely nebular one. This could suggest that the expanding envelope of CP Pup was not very massive.

The behaviour of the V/R reversals for the Balmer lines and for the HeII λ4686 emission is peculiar. The V/R ratio of the HeII line changes with time in the opposite sense to that of the hydrogen lines, but with the violet edge always the stronger. All this is shown in Figure 8-29. The V/R ratios for the H lines are initially larger than unity and become unity at approximately the end of the transition phase, just when the HeII λ 4686 emission becomes visible. It is then evident that hydrogen and HeII lines are produced in different regions around the hot central object. All these phenomena are actually the consequence of a unique basic physical process, that is the dilution of the expanding envelope and the consequent variation of the optical depths and the velocities of the regions that are responsible for the emission of the different ions. In 1947, the nebular spectrum was still strong, with very structured emission lines.

IV.C. THE NEBULA

The expanding nebula was for the first time observed by Zwicky (1956) when it had a radius of 2.78". Distance determinations based on several methods, including the nebular parallax, have been discussed by Duerbeck (1981), who gives the revised value of 1500 pc, based on new photographs of the nova (Duerbeck and Seitter, 1979). The nebula is shown in Figure 8-30. Its structure is, according to Williams (1982), "moderately symmetric, reminiscent of a wheel with spokes emanating from the center and extending out to a roughly circular rim." Williams (1982) has given a detailed spectroscopic study of the nebula when it was 14" in diameter. Two hours of exposure spectra of the nebula, taken in the blue and in the red spectral region, are presented in Figure 8-31. Table 8-3 gives the emission line fluxes.

Williams emphasized two peculiarities of the spectrum of the nebula.

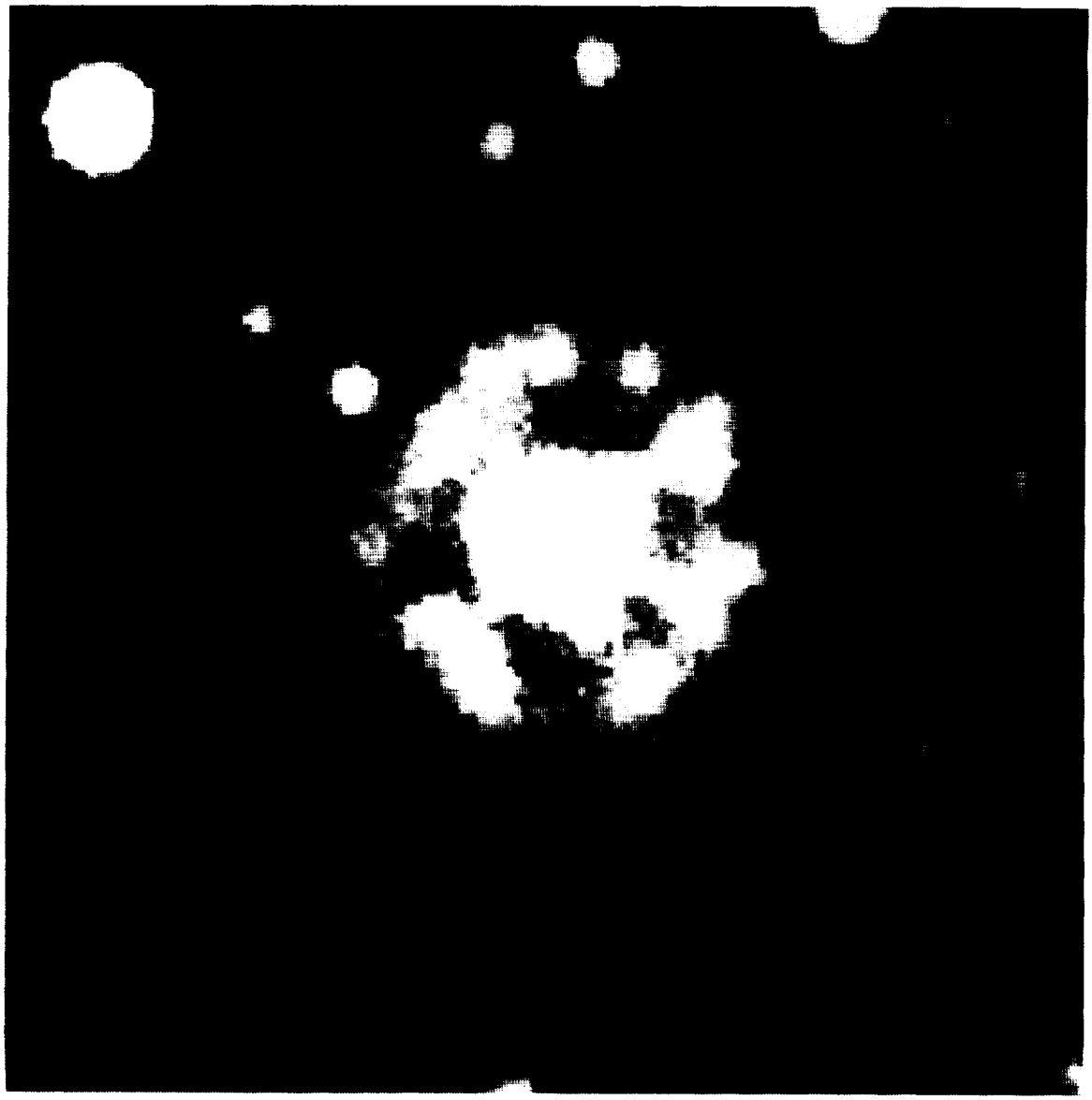

Figure 8-30. The shell of CP Pup 1942. H_α + [NII] CCD image taken by H W. Duerbeck with the 2.2 m ESO telescope.

The first is the presence of a broad emission feature at about λ3600, which might originate from Balmer continuum recombination of low-velocity electrons. If it is that, then the temperature of the nebula would be rather low, T = 800 K, for collisional excitation of the observed forbidden lines.

The second observed peculiarity is that the nebula contains permitted and forbidden lines of NII with comparable fluxes. Normally, forbidden lines of nebular spectra are 10^3 times the intensities of the permitted lines. The solution suggested by Williams is that excitation of all the levels occurs by recombination. Table 8-4 lists those transitions of the C,N,O elements which may produce the strongest optical lines in the recombination spectra of each of the five lowest ionization stages. Quantitative estimates can be made for the relative abundances of the H, He, and N elements, since line identifications and fluxes were well determined for ions of these elements. Assuming that lines are formed by recombination, and that the resonance lines are optically thin due to the very large differential expansion velocities for nova

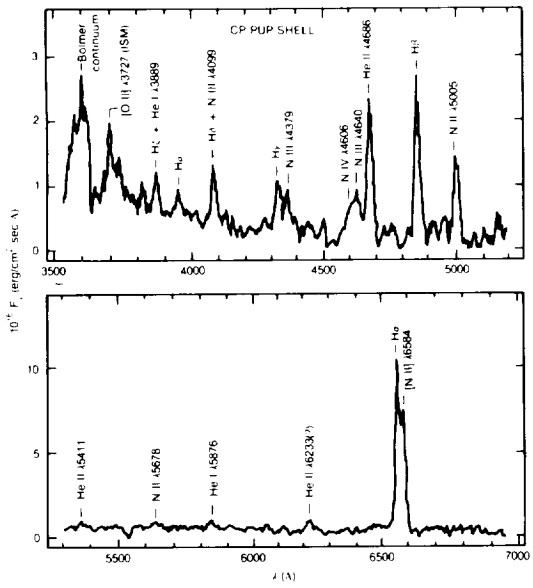

Figure 8-31. Blue (top) and red (bottom) spectral scans of the expanding shell of CP Pup obtained by R P Williams. Line fluxes are given in Table 1. (From Williams, 1982).

TABLE 8.3 (*)

EMISSION-LINE FLUXES FOR THE CP PUPPIS SHELL

Measured Wavelength (Å)	Line Identification	Relative Flux [3] (Hβ=100)
3638	H I Balmer cont.	...
3720	[O II] λ3727 (ISM)	21
3886	Hζ+He I λ3889	20
3969	Hε	13
4101	Hδ+N III λ4099	28
4341	Hγ	26
4380	N III λ4379	19
4608	N IV λ4606	
4640	N III λ4640	52
4682	He II λ4686	92
4860	Hβ	100
5004	N II λ5005	44
5407	He II λ5411	7
5672	N II λ5678	9
5875	He I λ5876	19
6233	He II λ6233 (?)	23
6560	Hα	300:
6580	[N II] λ6584	200:

[3]Fluxes of lines in the red (scan (λ >5300 Å) have been arbitrarily normalized such that Hα = 300. The absolute H β flux of the portion of the shell we sampled (~20% of the entire shell) was $F_{H\beta} = 5.8 \times 10^{-15}$ ergs cm^{-2} s^{-1}.

(*) From Williams (1982)

TABLE 8.4 (*)

STRONGEST OPITCAL RECOMBINATION LINES FROM CNO IONS[a]

Carbon	Nitrogen	Oxygen
C I ($2p^2\ ^3P$):	N I ($2p^3\ ^4S^0$):	O I ($2p^4\ ^3P$):
Triplets: none in visible	Quartets: $3s^4P$–$3p^4D^0$ λ8692	Quintets: $3s^5S^0$–$3p^5P$ λ7773
Singlets: $2p^2\ ^3P$–^1D [λ9849]	Doublets: $2p^3\ ^4S^0$–$^2D^0$ [λ5200]	Triplets: $3s\ ^5S^0$–$3p\ ^3P$ λ8446
C II ($2p\ ^2P^0$):	N II ($2p^2\ ^3P$):	O II ($2p^3\ ^4S^0$):
Doublets: $3d^2\ D$–$4f\ ^2F^0$ λ4267	Triplets: $3p^3D$–$3d\ ^3F^0$ λ5005	Quarters: $3s\ ^4P$–$3p\ ^4D^0$ λ4652
	Singlets: $2p^2\ ^3P$–^1D [λ6584]	Doublets: $2p^3\ ^4S^0$–$^2D^0$ [λ3727]
C III ($2s^2\ ^1S$):	N III ($2p\ ^2P^0$):	O III ($2p^2\ ^3P$):
Triplets: $4f\ ^3F$–$5g\ ^3G$ λ4069	Doublets: $4f\ ^2F^0$–$5g\ ^2G$ λ4379	Triplets: $3p\ ^3D$–$3d\ ^3F^0$ λ3266
		Singlets: $2p^2\ ^3P$–^1D [λ5007]
C IV ($2s\ ^2S$):	N IV ($2s^2\ ^1S$):	O IV ($2p\ ^2P^0$):
Doublets: $5g\ ^2G$–$6h\ ^2H^0$ λ4660	Triplets: $5g\ ^1G$–$6h\ ^1H^0$ λ4606	Doublets: $5g\ ^2G$–$6h\ ^2H^0$ λ4633
C V ($1s^2\ ^1S$):	N V ($2s^2S$):	O V ($2s^2\ ^1S$)
Triplets: $6h\ ^3H^0$–$7i\ ^3I$ λ4946	Doublets: $6h\ ^2H^0$–$7i\ ^2I$ λ4946	Triplets: $6h\ ^3H^0$–$7i\ ^3I$ λ4932

[a]The ground-state configuration of each ion is given in parentheses.

(*) From Williams (1982)

shells, Williams found that, for $T=10^3$ K, the He/H relative abundance of the CP Pup envelope is 0.12. Similarly, it resulted in N/H > 0.1. The strong abundance of N is characteristic of every classical nova.

IV.D. THE NOVA AT LIGHT MINIMUM-THE BINARY SYSTEM

The postoutburst apparent magnitude of CP Pup is ~ 15.0 mag; that is, at least three magnitudes brighter than it was before the outburst. This fact seems to be an exception, since Robinson (1975) has shown that the luminosities of novae before and after the outbursts are essentially the same. It is quite interesting, however, to note that a similar situation is occurring also to nova Cyg 1975. Why should these two very fast novae take such a long time to reach light minimum? It is possible that after an outburst, these systems remain for some time in a perturbed state either due to the secondary (high mass-loss), or to the white dwarf component.

CP Pup is a strong soft X-Ray source (Becker, Marshall, 1981; Cordova, et al., 1981a) and might be also variable by a factor of 10, at least, with a softer spectrum associated with a higher flux.

The old nova is now known to be a very-short-period binary system having the characteristics of the intermediate polar subclass of cataclysmic variables. This situation might perhaps explain the suggested excited state of the system, since one of the characteristics of intermediate polars is the presence in the system of some particular active regions that greatly contribute to the emitted radiation field.

Spectroscopic observations of CP Pup were carried out at the European Southern Observatory, La Silla, by Bianchini et al. (1985 a), Duerbeck et al. (1987) and Krautter (unpublished data).

The orbital period of CP Pup was independently discovered by the spectroscopic observations performed by Bianchini et al. (1985 a, b; see also Figure 6-2), and by the photometric observations carried out by Warner (1985b). Due to the poor signal to noise ratio of the spectra and also to the intrinsic strong variability of the nova, the modulation observed in the radial velocity curve couldn't give a precise determination of the period. For this reason, Bianchini et al. used several methods: line baricenters gave P = 0.0605 and P = 0.0571 days while line peaks gave 0.06115 days. The latter fit was probably clearer than the other ones and was adopted.

High-speed photometry performed by Warner (1985b) revealed a light curve whose morphology looks very similar to that of V 1500 Cyg (nova Cygni 1975), having a period of 0.06614 or 0.06196 days, that is slightly longer than the spectroscopic one (Figure 8-32).

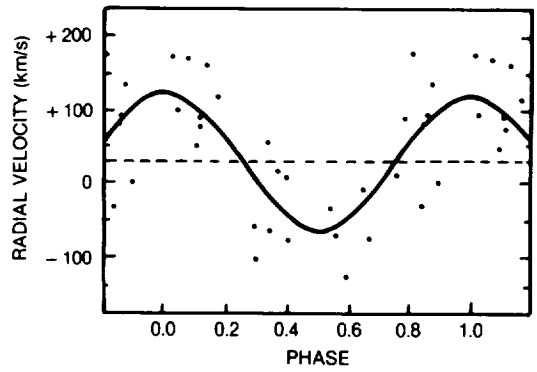

Figure 8-32. The radial velocity curve for the emission lines of CP Pup. (from Duerbeck et al., 1987).

Duerbeck et al. (1987) used Bianchini et al.'s (radial) velocities and 29 other ones determined from IDS spectra taken in December 1982. The spectroscopic period could then be refined to 0.061422 ± 0.000025 days, which is definitely shorter than the photometric period (1% and 7% shorter than the shorter and, respectively, the longer period found by Warner, and close to the original period proposed by Bianchini et al., see Figure 8.32). Thus, the behavior of CP Pup reminds us of Su Uma systems during superoutbursts, when the observed photometric periods of superhumps are systematically different by a few percent from the spectroscopic (i.e., orbital) ones (Warner, 1985b). Warner and Livio (1987) have sug-

gested that the period distribution of CVs below the period gap is characterized by a clustering of SU Uma's and Polars into separate period ranges. According to this scheme, the observed orbital period of CP Pup would fall in one of the period ranges favored by polars.

The amplitude of the radial velocity curve is determined by Duerbeck et al. (1987) to be 91.6 ± 17.6 Km/s (new data only), or 68.3 ± 11.0 Km/s (all radial velocity data). If this period and amplitude are interpreted as orbital motion, and since no eclipses were observed by Warner, Duerbeck et al. derive the following masses:

M (secondary) = 0.14 $M_\odot$, approximately an M7 V star

M (primary) $\leq$ 0.86 $M_\odot$ (all data)

$\leq$ 0.50 $M_\odot$ (new data only).

If the inclination of the system is estimated to coincide with some nebula features, i $\approx$ 30 ± 5°, then these authors obtain

M (primary) = 0.27 $M_\odot$ (all data)

= 0.12 $M_\odot$ (new data only).

These values are very low, much too low for any theoretical model of a white dwarf experiencing a TNR.

V. GK PER 1901
(written by Bianchini)

V.A. INTRODUCTION

Nova GK Per 1901 has been the first classical nova to be adequately observed from the early to the late stage. It was discovered by Rev. T. D. Anderson on February 21, 1901, before the light maximum, which was reached two days later, at visual magnitude 0.2. A detailed comparative description of all the available observational data of the nova during the outburst has been given by McLaughlin (1969). The photometric and spectroscopic evolution was that of a fast nova, with a speed of decline of about 0.13 magnitudes per day, an outburst amplitude of about 13.0 magnitudes, and an expansion velocity of the ejecta which ranged from 1000 km/s, for the Absorption I system, to 3800 km/s, for the Orion system. During the "transition phase", i.e., between 3.5 and 6.0 magnitudes below the light maximum, the nova presented strong light fluctuations which, unlike for other novae, were not correlated with the variations of the Orion absorption system velocity (Friedjung 1966c). The nebular shell surrounding the old nova presents an asymmetric shape, probably due to its interaction with a dense and structured circumstellar environment in which Bode et al. (1987b) have discovered the presence, around the nova, of an ancient planetary nebula remnant. The return of GK Per to light minimum was complicated by strong light fluctuations that lasted until the forties. Later, the old nova settled down to a more quiescent state, at about magnitude 13.0, but, since that epoch, the nova has shown occasional well-defined optical outbursts. Several of the peculiarities of GK Per at light minimum have been reviewed by Bianchini et al. (1986).

Probably, the most peculiar characteristics of GK Per as an old nova are its relatively long orbital period, almost two days (but this is still subject of controversy), and its dwarf nova-like behavior, which would place this object between the classical novae and the dwarf novae subclasses of cataclysmic variables.

From the beginning, GK Per was seen to be an exceptional object, and we can assert today that the study of the many peculiarities shown by this nova, both during the main outburst and at quiescence, has strongly contributed to the understanding of the nova phenomenon and of the long-term evolution of cataclysmic variables.

We wish here to emphasize some of the more unique aspects of this important nova.

V.B. PECULIARITIES OF GK PER DURING THE 1901 OUTBURST

Following the chronology of the events, the first peculiarity can be found by analyzing the behavior of the nova during the so-called tran-

sition phase which started at 3.5 magnitudes below maximum, when strong light fluctuations with a range from 1 to 1.5 mag and a period from 3 to 5 days suddenly appeared (Figure 8-33). This phenomenon lasted for more than 3 months. At each minimum of the light curve, the spectrum of the nova changed towards the nebular type with a weaker continuum and stronger high-excitation emission lines of [NeIII], [OIII] NIII, HeII, and the unidentified band at λ4726. At light maxima, these lines were weaker or even disappeared, indicating decreased temperatures and increased densities in the line-emitting region. In particular, the [NeIII] λ3869 and the [OIII] λ5007 emission showed variations of two kinds: (1) they invariably weakened at light maxima and became very strong in coincidence of the minima; (2) at each succeeding light minimum, these forbidden lines emerged in greater strength, and at each succeeding light maximum, their extinction was less complete.

At the end off the transition phase, the spectrum of the nova was purely nebular.

These phenomena are believed to be common to all those novae that show oscillations during their transition phase.

Two aspects of the oscillatory phenomenon in GK Per however, are, quite unusual and then worthy of note. The first is that the time intervals between successive light maxima varied with time in a sinusoidal fashion and that the period, amplitude, and mean value of this sinusoid increased with time. In other words, the light fluctuations had a period that was oscillating between two extreme values that were monotonically increasing with time, as shown in Figure 8-33.

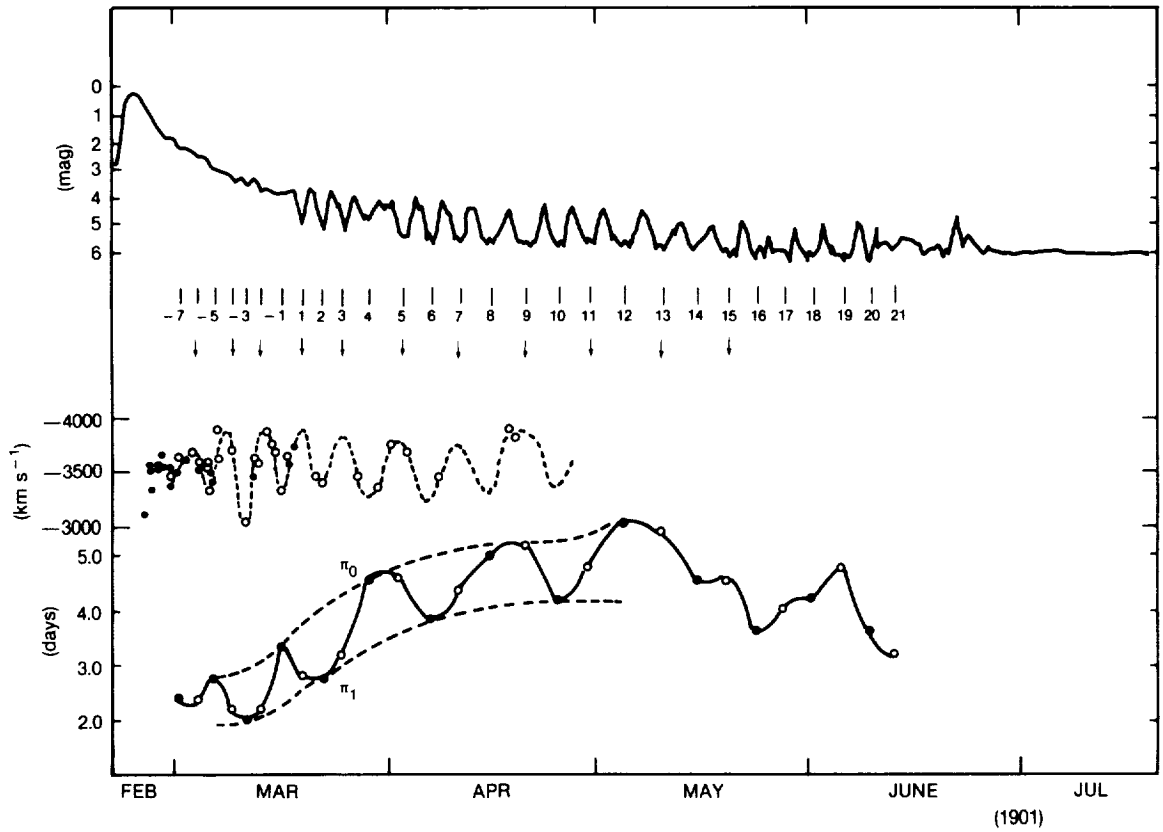

Figure 8-33. The oscillatory phenomenon during the transition phase of GK Per. Top pannel: the light curve of the early decline shows small amplitude oscillations, which might be correlated with the stronger oscillations of the transition phase. - Central pannel: the variations of Orion velocities (from McLaughlin, 1969) show that the negative maxima of the velocity of the ejected wind occur every two minima of the light curve. - Bottom pannel: the sinusoidal variation with time of the period of the oscillations. The period oscillates between two extreme values (dashed lines), which could represent the fundamental period and the first overtone of an n=3 radially pulsating, slowly expanding (v~2 Km/s) polytrope.

The second peculiarity of the transition phase of GK Per is that the radial velocity variations of the highly blueshifted absorption components of the diffuse-enhanced spectrum and of the Orion spectrum are not correlated with the light oscillations in the same way as for other novae. Friedjung (1966c) showed that the observed negative Orion velocities and the calculated photospheric radii—or the magnitudes—of some novae during the oscillations of the transition phase were inversely—directly, respectively—correlated; the only known exception seemed to be GK Per (see Figures 7-14, 7-15, and 7-16). A reanalysis of the photometric and spectroscopic data has revealed that a correlation similar to that known for other novae is still possibe for GK Per, provided that we assume that the negative maxima of the Orion velocities of this nova have a period that is all the time twice that of the light fluctuations. In Figure 8-33, we can, in fact, see that the negative maxima of the Orion velocities occur every two minima of the light curve. We can also note that the first decline of the light curve is not smooth but shows small amplitude oscillations that might represent the ideal backward extrapolation of the stronger oscillatory phenomenon of the transition phase. In fact, both the dependence with time of the maxima during the early decline and the correlation between the light minima and the negative maxima of the Orion velocities seem to have the same character as observed during the transition phase. Besides their different amplitudes, the principal difference between the small light fluctuations of the early decline and the larger ones of the transition phase is the appearance during the deeper minima of the latter phase of a genuine nebular spectrum. Thus, what we probably observe is the combined effect of an oscillatory phenomenon that starts immediately after the explosion of the nova and of the constant decrease with time of the density of the expanding shell. When a critical value of the density is reached, the outer expanding envelope becomes optically thin and the underlying pulsating object, whatever it might be, can be finally observed. This picture could actually agree with the fact that the two portions of the light curve immediately before and after the transition phase cannot be reconciled with a unique continuum slope. In fact, the first decline would fit only the maxima, while the second portion of the light curve seems to follow the slope indicated by the minima.

Since the light oscillation are not correlated in a simple way with the velocity changes of the Orion spectrum, we suggest that, at least in the case of GK Per, the light variations cannot be directly caused by changes in the velocity of the continuously ejected optically thick wind, as it is usually suggested for the other novae. The fact that the radial velocity changes of the Orion spectrum appeared rather large, even during the early decline, when only minor light oscillations were observed, could support the previous conclusion. Looking at Figure 8-33, one could even argue that these light oscillations start soon after the explosion with a period of about 2 days, which is close to the orbital period of the underlying binary system. Thus, the possibility arises that the luminosity fluctuations are triggered by binary motion inside a pulsating extended atmosphere, which is sustained by the radiation pressure produced by the hot central object. However, we do not observe the spectrum of such an expanded object but, more probably, that produced by a structured optically thick wind. We must then conclude that the physical mechanism responsible for the particular photometric and spectroscopic behaviours so far described is still not understood.

After the transition phase, GK Per settled down to a very slow decline towards its minimum light, which was reached several years later. As we have said, the spectroscopic evolution was typical of a fast nova with the normal sequence of slow changes from the nebular spectrum, where the [OIII] lines are predominant, to that typical of a cataclysmic variable, leaving the λ4686 and the Balmer emission as the strongest lines. A rapid fading of the nebula relative to the star was observed at the end of 1903 and during 1904, as shown by the weakening of [Ne III] relative to hydrogen and by the disappearance of [O III]. The historical mini-

mum of the visual light curve of the nova, m_v ~15, was reached in 1916. However, as we will see later on, since the mid-forties, the magnitude of the quiescent nova has remained at about m_v ~13.1.

V.C. THE PECULIAR EXPANDING NEBULA AND CIRCUMSTELLAR ENVIRONMENT

Another peculiarity of GK Per appeared in the autumn of 1901, when an apparent shell was seen to be expanding from the star at roughly the speed of light, such a high velocity being inferred from the apparent expansion velocity of the shell and an estimate of the lower limit of the distance to the nova that does not show any parallax effect. This shell is distinct from the shell of gaseous ejecta that was clearly seen only two decades later. Ka-pteyn first proposed that the high-velocity shell was due to a "light echo" from the burst of the nova light being reflected by interstellar dust. In all generality, such an apparently expanding nebula could be produced by the illumination of a sheet of material anywhere either beyond the nova or between it and the earth. In 1939, Couderc (1939) refined this model, showing that the illuminated dust seen by the earth at any time must describe an ellipsoid of revolution whose foci are the nova and the observer. On this principle, Couderc had calculated the location of the illuminated nebula, which resulted in a plane sheet placed between the nova and the observer at about 46 light-years from the nova and inclined about 45° to the line of sight. Actually, the presence of much circumstellar material is confirmed by the measures of the reddening, which can be easily determined from the intensity of the λ2200 dip observed in the UV spectra of the nova (Bianchini et al., 1986). The E(B-V) result was of the order of 0.35. The light echo was mainly visible south of the nova.

But the important discovery by Bode et al. (1987b) of an ancient planetary nebula surrounding the old nova has provided the basis for a new interpretation of the circumstellar environment and, obviously, of the evolutionary history of this interesting close binary system. The nebula was discovered by analysing several Infrared Astronomical Satellite (IRAS) images of the GK Per region. Extended emission was detected in both the 60- and 100-μm bands. Figure 8-34 shows the 100-μm map of the region with a superimposed sketch of the disposition of the mentioned 1901 light-eco. Bode et al. (1987) have estimated a grain temperature of about 22°K, a density of 2.2 g cm^{-3} and a total mass of the emitting dust of 0.058 $M_\odot$, which would imply a large mass for the gaseous component. Actually, new 21-cm HI observations performed by Seaquist et al. (in preparation) led to an HI mass of $\geq 0.6\ M_\odot$. This mass is 10^4 - 10^5 times greater than that found in classical nova envelopes. According to Bode et al. (1987), the ≤ 5 Km s^{-1} expansion velocity of the gas would suggest that GK Per, as a nova, is a relatively young object, not much older than 10^5 years, and the 1901 outburst might have been the first one from this system.

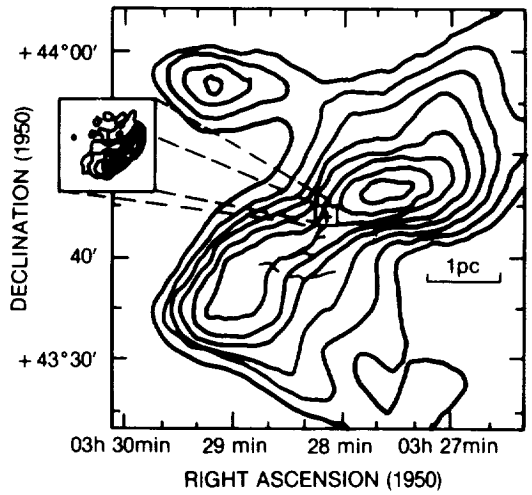

Figure 8-34. IRAS 100-μm map of the region around GK Per. Contours range from 1.5 MJy sr^{-1} to 55 MJy sr^{-1}. The position of the nova is marked. The inset shows a 5-GHz radio map of the nonthermal radio emission of the central interaction region of the expanding shell. Superimposed is also a sketch of the disposition of reflection nebulosity from a Lick Observatory plate taken on 12-13 November 1901 (from Bode et al., 1987b).

The nebula ejected by GK Per during its nova outburst is also peculiar. It has the shape of a prolate ellipsoid (Figure 8-35), but with

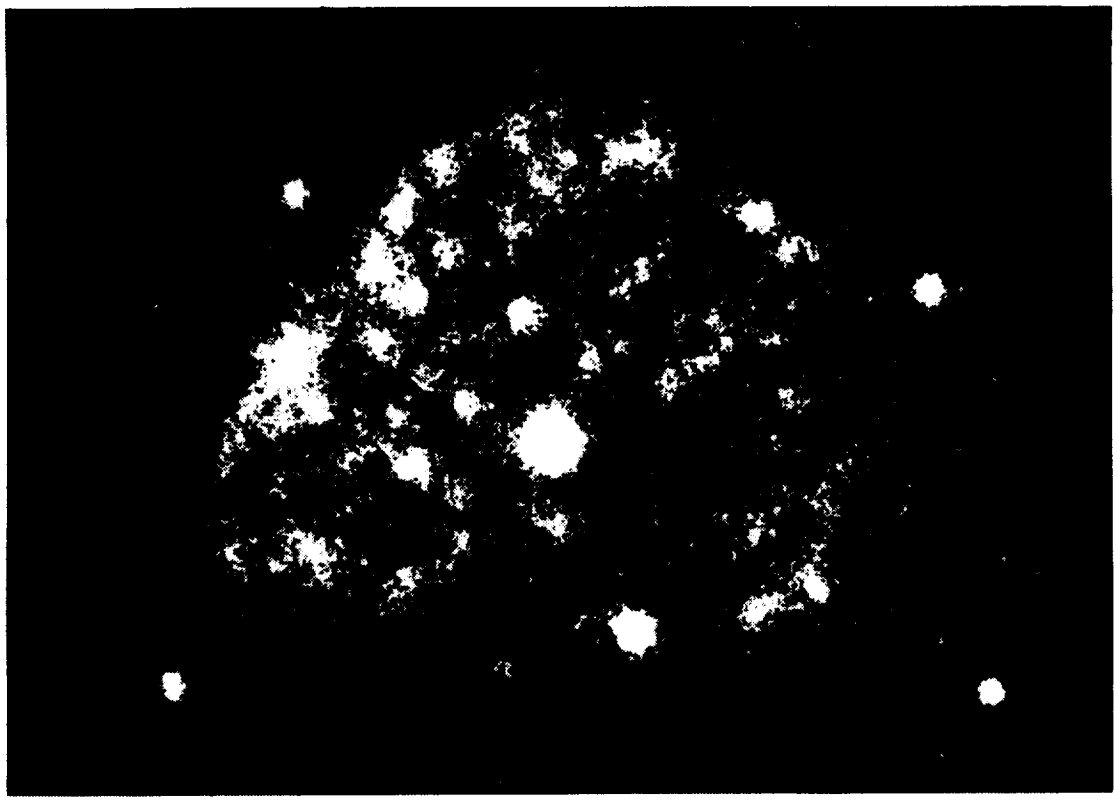

Figure 8-35. The nebula of GK Per. The distribution of matter is asymmetric and the material is concentrated into blobs. The interaction of the shell with the interstellar medium is responsible for the formation of the S-W front

the matter non equally distributed, the southwest portion of it being the more luminous. The material of the shell looks concentrated into blobs of variable size whose trajectories during the expansion can be determined by comparison of plate images taken at different epochs. The interaction of the expanding nova shell with the interstellar medium was discussed by Duerbeck (1987a) who determined the deceleration of the shell and more reliable distance to the nova: 390 pc. A detailed reconstruction of the three-dimensional image of the shell of GK Per was obtained, using more than 200 blobs, by Seitter and Duerbeck (in "An Atlas of Nova Shells", in preparation; see also Seitter and Duerbeck, 1987). Monochromatic images of the nebula taken by these authors revealed differences in the distribution of light concentrations from the different ions that do not exclude different chemistries for polar and equatorial regions as shown in Figure 8-36. Radio (Reynolds and Chevalier, 1984) and optical (Williams and Ferguson, 1983) observations revealed the presence on the nebula of shocks and turbulent processes which are similar, although far less energetic, to those acting in supernova remnants. In particular, the radio map of the shell (see Figure 6-77), shows that the emission is concentrated in the southern region of the sky around the nova, in complete analogy with all the preceeding results. It is then possible that the interaction of the ejecta with the interstellar material is, at least partially, responsible for the observed energetics.

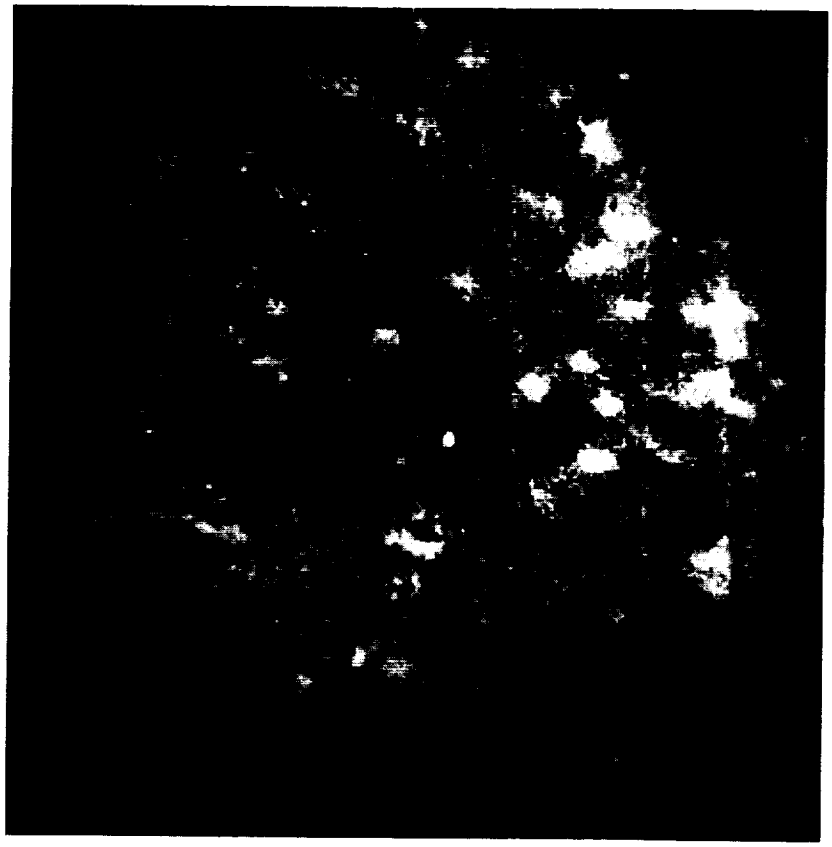

Figure 8-36. The [OIII] image subtracted from the Hα + [N II] image of the nebula of GK Per. North is to the left, west to the top (from Seitter and Duerbeck, 1987).

V.D. PECULIARITIES OF GK PER AS A CATACLYSMIC BINARY

The old nova GK Per was discovered to be a Close Binary System by Kraft (1964).

The results obtained by several authors have demonstrated that, among classical old novae, GK Per can be considered an exceptional object for the following reasons:

1) The most probable orbital period is unusually long. It has been subject of controversy (Kraft, 1964; Paczynski, 1965). Bianchini et al. (1981) found an eccentric orbit (e=0.4) and an orbital period quite close to that given by Kraft (P = 1.904 days). A more extended and detailed spectroscopic study of the radial velocity variations of both the white dwarf and the K2 secondary, done by Crampton et al. (1986), revealed circular orbits and a period of 1.996803 days (Figure 8-37). According to these authors, since no eclipse has ever been observed, the inclination of the system should be < 73° so that the most probable masses for the two components are M(K2) = 0.25 $M_\odot$ and M(WD) = 0.9 $M_\odot$ (Figure 8-38). Thus, apparently, only about one-quarter of the original mass of the K star remains. This also implies that the secondary is a slightly evolved star, perhaps stripped to its helium core.

More recently, this already uncertain scenario has been further complicated by a reanalysis of Crampton et al.'s original data carried out by Kurochkin and Karitskaya (1986). These authors found that the two-day variation itself is modulated with a period of 0.131623 days. The amplitudes of these smaller radial velocity variations are of only 15 Km/s for the absorption lines and 20 Km/s for the emission lines. If this shorter period is orbital, the masses of the two components could be 0.8 $M_\odot$ for the white dwarf, and 0.6 $M_\odot$ for the K star. Should this result be confirmed, then the two-day periodicity could be tentatively ascribed to the preces-

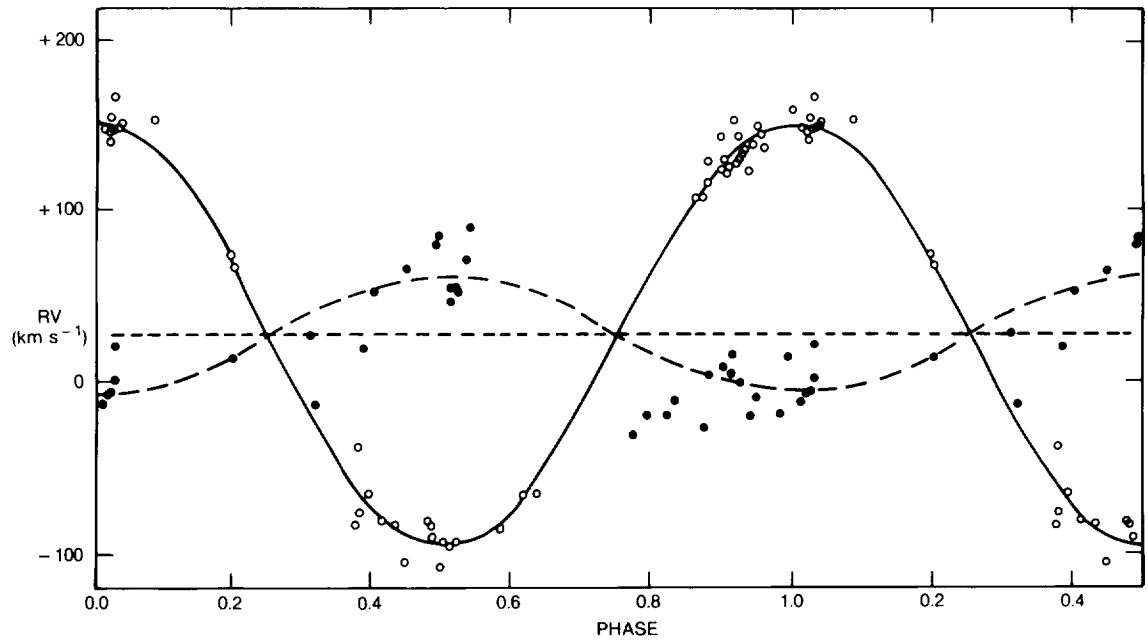

Figure 8-37. The radial velocity variation as a function of the orbital phase. Open circles represent the absorption lines, filled circles are measures of the positions of the wings of Hβ. Least-squares orbital fits are also shown (from Crampton et al., 1986).

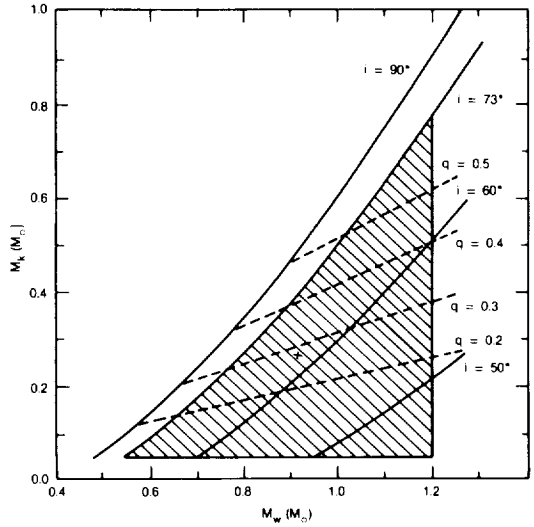

Figure 8-38. A diagram showing how the mass of the K star (M_k) varies with the mass of the white dwarf component (M_w) for different values of the inclination and mass ratio. Since eclipses have not been observed, i ≤73°, and M_w must be less than the Chandrasekhar limit, 1.2$M_\odot$. The cross marks the position of the most probable masses of the components (see text). (from Cramper et al., 1986).

sion of the eccentric, e = 0.4, orbit or to the presence of a third body. Needless to say, further detailed spectroscopic observations are badly required.

2) The nova at quiescence presents an outburst activity reminiscent of that of certain long-period dwarf novae, e.g., BV Cen. As an example, Figure 8-39 shows the light curve of the novae in the years 1969-1983. The duration of the optical outburst of GK Per is one or two months. The amplitudes range from one to three magnitudes. The outburst profiles tend to be symmetric, especially for the largest outbursts. The observed recurrence times are variable, but all of them seem to be submultiples of 2400 days. This sort of quasi-periodicity is illustrated in Figure 8-40. A classification scheme for the outbursts is suggested in Figure 8-41.

According to Bianchini et al. (1986) and Cannizzo and Kenyon (1986), most of the observational characteristics of the optical outbursts of GK Per can be explained by disc instability episodes starting from the inner edge of the accretion disc, where an unstable transition region is formed if the mass transfer rate from the secondary is slightly larger than 10^{16}gs^{-1}. However, as we will see, some observational facts are suggesting that we are probably still missing the correct interpretation of the out-

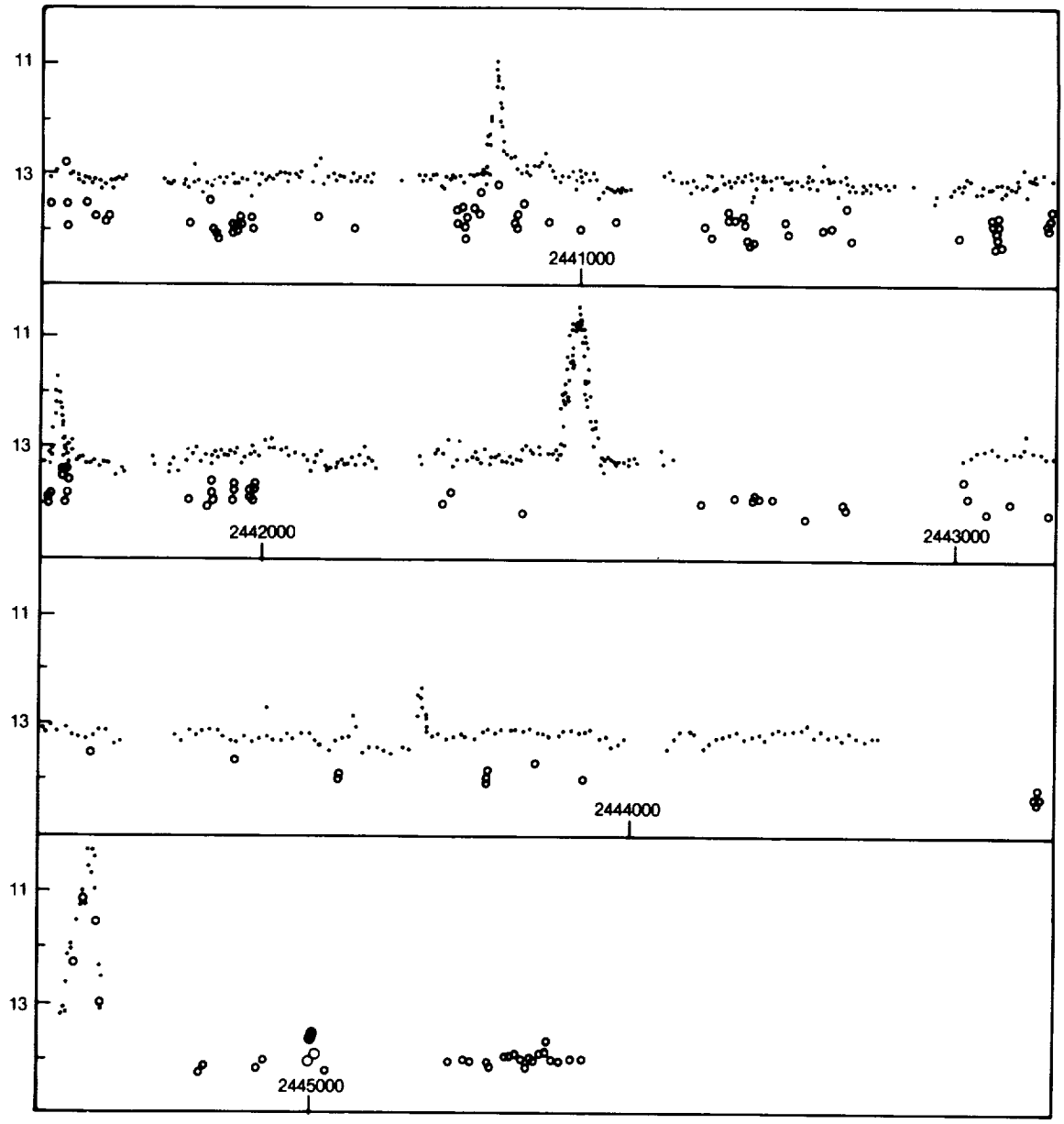

Figure 8-39. The light curve of GK Per in the years 1969-1983. Optical outbursts occurring in 1970, 1973, 1975, 1978, and 1981 are clearly visible (from Sabbadin and Bianchini, 1983). Circles: B; dots: v.

burst phenomenon in GK Per. The phenomenology connected to this important property of the old nova will be discussed further on in this review.

3) While most old novae are completely dominated in the blue spectral region by light coming from the accretion disc and the boundary layer, the spectrum of GK Per at light minimum (Figure 8-42), shows also the presence of a K2 IV-V companion (Kraft, 1964; Gallagher and Oinas, 1974). We note that the spectroscopic detectability of the secondary might be consistent with the assumption of the longest orbital period, since this would require the presence of a larger and brighter Roche-lobe filling secondary. It might be consistent also with the suggested low mass accretion rate, since this would imply a relatively low luminosity of the disc, at least compared to that of other classical old novae (Warner 1987a).

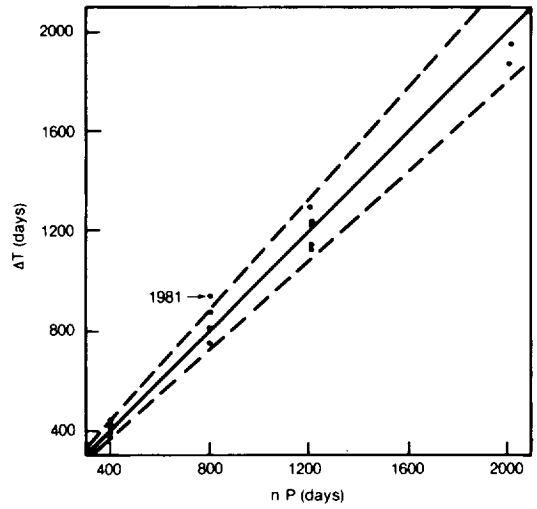

Figure 8-40. The $\Delta T=n(400\mp40)$ days relation between successive outbursts; only the 1981 outburst is clearly outside the error bar of ∓40 days (from Bianchini et al., 1986; except the point relative to the 1986 outburst).

4) In spite of the presence of high excitation emission lines, the UV continuum from the nova is unusually weak and flat. Bianchini and Sabbadin (1983) showed that the UV to IR continuum energy distribution, corrected for E(B-V) = 0.15, is peaked at λ3600. However, even applying a correction for E(B-V) = 0.35, as derived from the UV spectra of the nova in outburst, the continuum energy distribution in the UV remains rather flat and approximates that expected from the standard model of a semiinfinite accretion disc, i.e., F proportional to $\lambda^{-2.33}$, only during the optical outbursts (see Figure 8-43). Bianchini and Sabbadin (1983) suggested that the particular spectrum emitted by GK Per could be explained by assuming that the accretion onto the white dwarf is controlled by a magnetic field that is strong enough to disrupt the inner part of the accretion disc. Bianchini et al. (1986) suggested that the probable value of the mass transfer rate at quiescence is about 10^{16} gs^{-1}. This value of the mass transfer rate is rather low for a classical nova, but it would correspond to that needed by the theory if we assume that the outburst is produced by the disc instability mechanism starting near the inner edge of the disc and propagating outward as explained in Section V.E.4.

a)

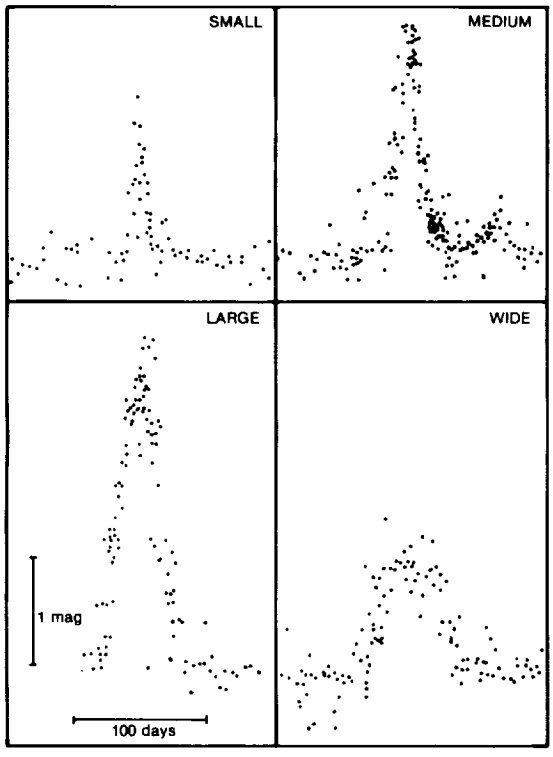

b)

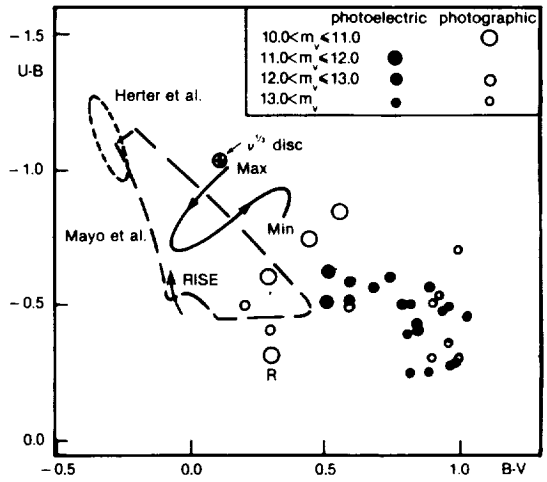

Figure 8-41. a) Average photometric properties of the four types of outbursts identified in the light curve of GK Per (from Bianchini et al., 1986). b) two color diagram.

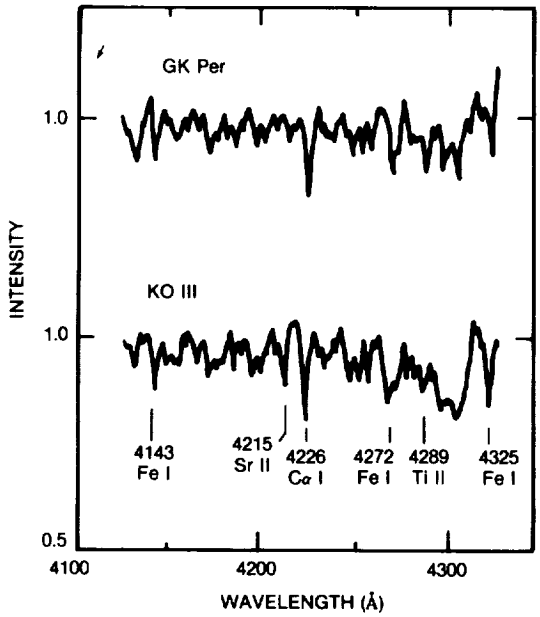

Figure 8-42. Portion of the mean spectrum of GK Per (upper) compared to that of a KO III star (lower) (from Crampton et al., 1986).

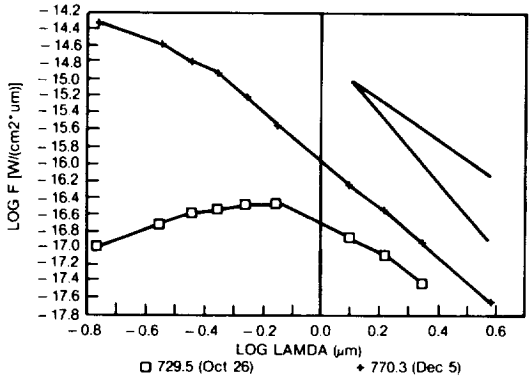

Figure 8-43. The UV to IR continuum energy distribution of GK Per at quiescence, corrected for E(B-V) = .1, and during the 1986 light peak, corrected for E(B-V) = 0.35. If we adopt E(B-V) = 0.35 also at light minimum the continuum in the UV becomes flat (see text). The $\lambda^{-2.33}$ and the λ^{-4} slopes are also shown.

5) GK Per is a hard x-ray transient. Although the near UV is faint, the x-ray emission from the nova is particularly strong and increases during the optical outbursts (King et al., 1979; Cordova et al., 1981b; Watson et al., 1985). The hard x-ray luminosity of the old nova at quiescence is between 2 x 10^{32} erg s^{-1} (Cordova and Mason, 1984) and 7 x 10^{33}erg s^{-1} (Bianchini and Sabbadin 1983). During an optical outburst, it can amount to about 10^{34} erg s^{-1} (King et al., 1979; Watson et al., 1985).

6) The old nova GK Per is an intermediate polar. During the 1983 large outburst, the nova was observed with the EXOSAT instrument by Watson et al. (1985), who detected a strong coherent modulation of the hard x-ray flux of about 80%, having a period of 351 s. Superposed to this, a longer term modulation on time scales of 0.8÷1.5hr was also observed (see Figure 8-44). The detection of the shorter highly coherent periodicity would then identify GK Per as a member of the so called 'intermediate polar' subclass of magnetic cataclysmic variables.

7) Part of the infrared radiation emitted by the system could come from the outer cooler regions of the accretion disc. Infrared observations (JHKL) performed by Sherrington and Jameson (1983) were interpreted in terms of the infrared radiation coming from the cool companion. However, several JHKL flux determinations secured at Asiago and TIRGO Observatories by F. Stafella and D. Lorenzetti show that, at some epochs, the nova may vary on time scales of few hours over a range of a few tenths of magnitude. As shown previously in Figure 8-43 the slope of the continuum energy distribution in the infrared does not change too much during an outburst and approximately fits that of the "standard" accretion disc model (a quite different behavior is observed in the UV). So we argue the infrared continuum is not principally produced by the cool secondary component of the binary system; most probably, the cooler outer regions of the large accretion disc, which is formed around the collapsed object, may give a significant contribution to the IR radiation field also

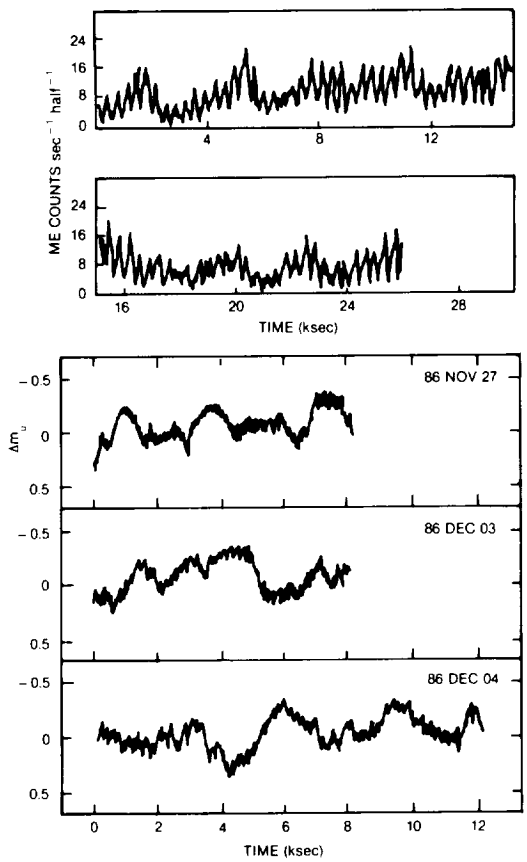

Figure 8-44. The EXOSAT hard X-ray light curve of GK Per during the 1986 outburst (from Watson et al., 1985) compared to the optical one (Stagni et al., in preparation). The 351 s coherent modulation is observed only in the X-ray region. The flickering observed in the U band, in fact, does not show any clear and steady periodicity. A .8-1.5-hr modulation can be seen both in the x-ray and in the optical.

at quiescence. This would again play in favour of the longest orbital period.

V.E. THE SMALL POSTNOVA OPTICAL OUTBURSTS OF GK PER

The most striking characteristic of the light curve of GK Per at quiescence is its nonquiescent character and, in particular, its "dwarf-nova-like" behavior. The amplitude, duration, rise, and decay times of the optical outbursts vary from case to case. As shown back in Figure 8-41, we can identify four types of outbursts. The rise to decay-time ratio is about 0.5 for "small" outbursts, like those that occurred in 1973 and 1978 ($\Delta m \sim 1.0$ mag); 0.7 for "medium" outbursts, like those of 1949, 1966, and 1970 ($\Delta m \sim 1.0$ mag), 2.0 for "large" outbursts, like those of 1967, 1948 (?), and 1950 (?) ($\Delta m \sim 2.0$ mag); and 1.0 for the "very large" ones, like those observed in 1975, 1981, 1983, and 1986 ($\Delta m \sim 3.0$ mag).

The best studied outbursts are those of 1981, 1983, and 1986. In particular, during the last one, coordinated UV, optical, and IR observations have been performed. In the following, we will discuss some of the main observational results so far obtained, pointing out those aspects of the known phenomenological scenario that we feel are more relevant to a physical interpretation of the outburst phenomenon.

Due to the long time intervals between two subsequent outbursts and the nonstrictly periodic nature of the phenomenon, most of our knowledge of the long-term light curve of GK Per comes from visual, photographic, and even photometric observations by amateur astronomers whose precious collaboration should be emphasized more often.

V.E.1. ON THE MULTIWAVELENGTH BEHAVIOR DURING THE OUTBURSTS

The only outburst for which extensive x-ray monitoring of the nova has been performed is that of 1978 (King et al. 1979). A reanalysis of all the available x-ray and optical data showed that, at least in that case, the x-ray flux reached its maximum level about 30 days before the rise in the optical (Bianchini an Sabbadin 1985). This cannot be simply explained as the effect of enhanced mass transfer rate produced by the disc instability mechanism. In fact, for inside-outbursts, like those observed in GK Per, the V and the x-ray light curves should present almost contemporary rising branches (Cannizzo et al., 1986).

Another peculiarity of the x-ray behavior is represented by the fact that during the 1978 one-magnitude outbursts, the luminosity of the nova in the 2 - 10 KeV range was $\simeq 5 \times 10^{33}$erg s^{-1} (King et al., 1979), which is comparable to that observed by EXOSAT, in the same energy

interval, during the larger outburst of 1983, that is when the star was two magnitudes brighter than in 1978!

IUE spectra of the nova taken by A. Cassatella during the 1986 outburst revealed that, although this optical maximum, in the visual, was only 0.2 - 0.3 magnitudes brighter than that of 1981, the UV fluxes of the continuum were brighter by a factor of two. The same occurred for the UV emission lines whose intensities resulted, on the average, twice as much as those observed in 1981.

These results are not completely accounted for by the standard disc instability model. In general, they only fit in the already proposed phenomenological scenario in which the outbursts should occur mainly in the inner, denser, and hotter regions of the accretion disc, probably starting near the boundary layer and the surface of the mass-accreting white dwarf (see also Section V.E.4.).

The visual and infrared light curves of the 1986 outburst are shown in Figure 8-45. No time delay between the two light curves can be clearly detected. We recall that no time delay was seen also between the visual and the UV light curves of the 1983 outburst (Bianchini et al. 1986). IUE observations of the nova during the 1986 outburst confirm this result.

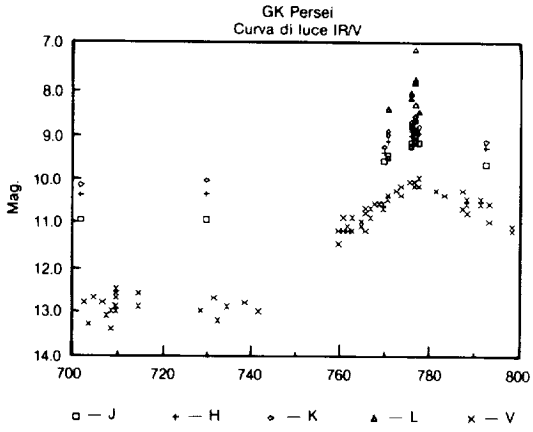

Figure 8-45. Visual, J, H, and K light curves of the 1986 optical outburst. No time delay is observed.

The UV to IR continuum energy distributions of the nova at quiescence and at the 1986 light peak, corrected for E(B-V) = 0.1 and E(B-V) = 0.35, respectively, are shown in Figure 8-43. At light maximum, the slope is not too far from that predicted by the theory for a semi-infinite disc even in the infrared, suggesting that the accretion disc of GK Per is quite extended and that a large portion of it has low temperatures also during an outburst. Alternatively, part of the infrared emission could come from the secondary, from the cold outer rim of the accretion disc and from the circumstellar material.

The pattern of the nova in the U-B vs B-V plane looks rather complicated, as shown by Bianchini et al. (1986). (Figure 8.41b).

V.E.2. SPECTRAL CHANGES DURING THE OUTBURSTS

Few optical spectroscopic observations are available for the 1986 outburst. More data were given for the 1981 and 1983 events. A description of the main spectroscopic changes observed in the optical region is given by Szkody et al. (1985) and Bianchini et al. (1986). The general trend is that of a strengthening of the central intensities of the high-excitation emission lines together with a general decrease of their equivalent widths. In other words, the outbursts occurred more in the continuum than in the emission lines. Bianchini and Sabbadin (1982) suggested also that the observed change in the width of the Hα profile might indicate that the radius of the outer optically thin portion of the accretion disc is about 8 x 10^{10}cm at quiescence, and 2 x 10^{11}cm during an outburst (Bianchini et al. 1982), as required by the disc instability model. In fact, a burst of the mass-transfer rate from the secondary would cause the disc to shrink and not to expand.

A particularly interesting behavior of the nova during light maxima is suggested by two optical spectra taken at the Asiago Observatory during the 1975 and 1983 light peaks. These two spectra show the presence of an unusual emission feature at λ4842. This does not seem to be a high radial velocity component of Hβ, since it is not observed at Hα; it can be tenta-

tively identified as the A1O head, similar to what is observed in Miras at maximum (Iwanoska et al. 1960). A portion of one of the two spectra indicating the line is displayed in Figure 8-46. Figure 8-47 reproduces a calibrated spectrum of the nova at light maximum taken by Szkody et al. (1985) in which the λ4842 emission might perhaps appear blended with that of H_β. We estimate that the line has a width of about 14 Å (FWHM) and an intensity about 0.3 that of H_β. The line has never been observed in any of the spectra taken after light maxima and at quiescence.

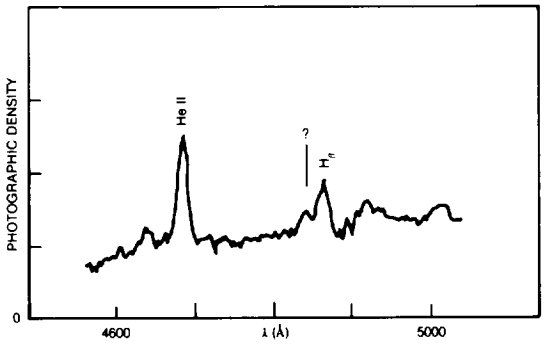

Figure 8-46. Portion of the plate spectrum taken with the 182-cm reflector of the Asiago Observatory during the light peak of 1975. The unusual emission at λ4842 is shown.

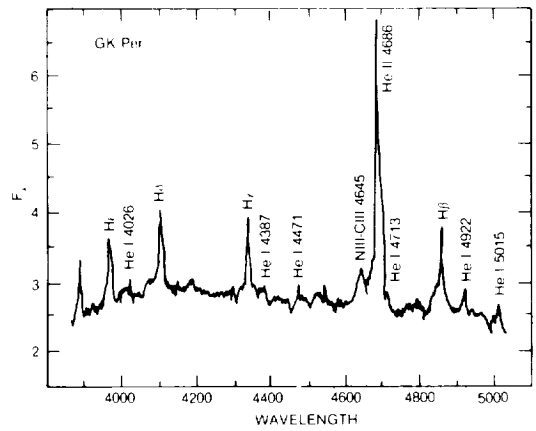

Figure 8-47. The spectrum of GK Per at the 1983 outburst maximum on 1983 August 15 UT (from Szkody et al., 1985).

IUE spectra of the nova taken during the 1981 (Bianchini et al., 1986) and the 1986 (Cassatella et al., work in preparation) large optical outbursts confirm the main character of the spectroscopic variability already observed in the optical region. In fact, only the central intensities, and not the equivalent widths of the principal UV emission lines, follow the outburst profile. An exception is represented by the NIV, SiIV, and OIII lines which have a dip at the very beginning of the rise; whereas, the UV continuum has a flare. Traces of [NeIV] 2423 and OV 1371 are observed during the rise and the light maximum. In general, the indication is that of an increase of the ionization during the rise to maximum. The constant presence throughout the outburst of the lower-excitation emission lines of [OIII] λ2471, [NIII] λ1750, [NIV] λ1487, and MgII λ2800 demonstrates that a stratification of the ionized elements is produced at all times. This requires the presence of an extended circumstellar envelope and /or of an anisotropy in the high-temperature ionizing source. We note, however, that the MgII chromospheric emisssion was almost absent during the UV spectra of the 1986 outburst, perhaps due to the presence of a much stronger UV ionizing radiation field. An IUE spectrum of the nova taken at the 1986 light peak is shown in Figure 8-48.

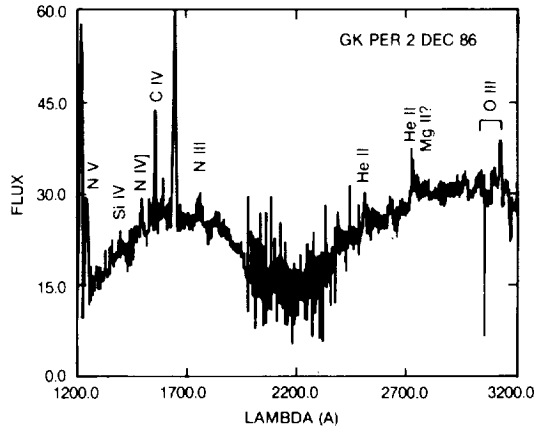

Figure 8-48. IUE spectrum of GK Per during the 1986 light maximum taken by A. Cassatella. The λ2200 dip suggests E(B-V)=0.35. At light minimum the dip seems to be less pronounced but the spectrum presents a rather poor signal to noise ratio so no conclusion can be driven.

Analysis of the behavior presented by some of the UV emission lines can give important information on the physics of the small outbursts of GK Per. The intensity ratios of resonance lines CIV (λ1549): NV (λ1238):SiIV (λ1394, λ1403) are changing during the outburst being

1:0.4:0.28 at light minimum, and 1:1:0.4 at light maximum. Bianchini and Sabbadin(1987) have tentatively explained this behavior by assuming that at light minimum, these three resonant lines are produced in a small volume around the white dwarf, having a radius of the order of that of the inner edge of the accretion disc, a temperature of a few 10^4 K, and a density of Ne > 10^{12}cm^{-3}. At light maximum, instead, a stratification of the ionization would imply for the different ions much larger but different emitting volumes.

Additional information about the physical mechanism of the outbursts is provided by the behavior of the OIII λλ3047,3133 and the [ArIII] λ3109 lines. The I(λ3133)/I(λ3047) intensity ratio is about unity at light minimum, at the start and at the end of the outburst, and about 6.0 during the rise and light maximum. For the OIII lines coming from the excitation of the oxygen by the HeII λ303.8 Ly_α (Bowen fluorescence mechanism), a typical I(λ3133)/ I(λ3047) ratio is about 5.6 (Saraph and Seaton, 1980). Our results suggest that the Bowen fluorescence mechanism might be operating only during the rise and the light maximum, while at quiescence and at the start of the outburst, the OIII energy levels could be selectively excited by collisions. In the spectrum of February 14, taken at the start of the 1981 outburst, we observe a bright emission of [ArIII] λ3109. This line is virtually absent in all the other spectra. Seven IUE spectra taken by A. Cassatella throughout the 1986 outburst (Cassatella et al., work in preparation) seem to confirm this particular behavior of the nova, because the [ArIII] λ3109 emission is detected only in one spectrum of the early rise. Since the ionization potential of ArIII is close to that of OIII, the ArIII forbidden line should come from the same region that also produces the OIII permitted line. However, collisions will prevent radiative decays from the ArIII metastable level for densities Ne > 10^8 cm^{-3}. For this reason, Bianchini and Sabbadin (1987) suggested that, at quiescence and during light maxima, the OIII emission lines are emitted by regions where the density is high enough to prevent the production of the ArIII forbidden lines. In particular, at quiescence, the OIII line-emitting region should be more concentrated around the white dwarf and the inner regions of the accretion disc, where densities can be relatively high so as to prevent the formation of the ArIII forbidden line. At the start of an outburst, instead, the luminosity and temperature of the central ionizing source increase, and the OIII ionization regions should be immediately pushed further out, towards lower-density regions, where the AIII forbidden line can be finally produced. This situation could be also favored by the suggested existence in the system of a very hot region, which explains the observed high-energy precursor to the 1978 optical outburst. However, if we assume that an outburst can also produce an increase of the wind from the inner regions of the accretion disc it is then possible that, soon after the start of an outburst, a substantial increase of the wind and, consequently, of the density of the circumstellar material might again prevent radiative decays from the ArIII metastable level. We note here that the lack of a P Cyg profile in the resonant lines during light maxima can be understood if we recall that a wind is predominantly emitted in directions perpendicular to the disc plane and that it can be observed only if the accretion disc is seen almost pole-on, i. e., the inclination of the binary system is rather low.

The 1986 IUE observations of the nova confirm the large color excess derived from the obervations of the 1981 outburst (Figure 8-48). The E(B-V), derived from the intensity of the λ2200 dip of the continuum, is about 0.35. It is not clear, however, whether such a reddening can be attributed also to the nova at light minimum (Bianchini et al. 1986).

As already mentioned, a rather peculiar difference was found between the UV spectra of the 1981 and the 1986 outbursts, that is the almost total absence in the 1986 outburst, of the MgII λ2800 chromospheric emission and its only appearance during the late decline. This particular behavior is perhaps understandable for what already has been said. In fact, the 1986 outburst implied much stronger UV, and possibly also x-ray, fluxes than the 1981 one. This

must have produced a higher level of ionization in most of the line-emitting regions included, perhaps, the region responsible for the chromospheric emission, i.e., the disc or the cool secondary star.

V.E.3. SHORT TERM PHOTOMETRIC VARIABILITY DURING THE OPTICAL OUTBURSTS

High-speed photometry of the old nova GK Per has been occasionally performed by different observers (Nather; Robinson; Bianchini; unpublished data), and the result was that the light curve could appear either smooth or flickered. Unfortunately, no systematic photometry has been performed before the 1983 optical outburst, when Mazeh et al. (1985b) and Steinle and Pietsch (1987) tried to detect the optical counterpart of the x-ray 351 s coherent modulation discovered by Watson et al. (1985) during the same outburst. Some small amplitude ($\sim$3%) periodicities in the optical, to be compared with the 80% modulation observed in the x-ray region, were actually detected, more often at slightly larger frequencies (360, 390, and 410 seconds), or close to the 350 s period but lasting only for a few cycles. High-speed photometry of the nova during the 1986 outburst (Stagni et al. 1987, work in preparation) didn't show any clear evidence for the existence of such periodicities. However, inspection of the light curves obtained in the different nights (an example is given in Figure 8-44) reveals the presence of periodicities of the order of 400 seconds lasting only for a few cycles, as found by Steinle and Pietsch.

This behavior means that the region producing the 351 s oscillations is very small and hot, as expected for the emission coming from the polar caps of a rotating magnetic white dwarf. The smaller amplitude of the modulation seen in the optical and its nonstrictly periodic nature could be attributed to the fact that the optical modulation originates from x-ray heating of a feature of the accretion disc that is not completely fixed or stable in the rotation frame.

The EXOSAT observations of the 1983 outburst (Mazeh et al. 1985b) revealed also the presence of a modulation of the x-ray flux on typical time scales of 0.8 hour. High-speed photometry performed by Stagni et al. during the 1986 outburst definitely confirms the presence of such a modulation as shown in Figure 8-44. Mazeh et al. (1985b) suggested that it might be generated by a bulge inside the disc, rotating around the compact star with its Keplerian velocity, and reprocessing the x-ray oscillation in the optical wavelengths. The observed periodicity should then be the beat frequency of the bulge orbital period and the x-ray one. Alternatively, Duschl et al. (1985) suggested the onset of the inner disc of a region that is unstable with respect to the mass flow rate which crosses it. The theoretical time scale of the modulation of the accretion rate should be of the order of 0.7 hour.

V.E.4. THE ORIGIN OF THE OPTICAL OUTBURSTS

Whether the optical outbursts of GK Per are to be considered as a genuine dwarf nova-like behavior is still a matter of discussion. Obviously, much depends on the definitions, classification schemes, and also on the particular theoretical models adopted to explain the dwarf nova phenomenon.

Two basic competing models are proposed to explain the dwarf-nova phenomenon (see also Chapter 4). The first model (Bath, 1973; Bath and Pringle, 1981) explains the brightening of the accretion disc as due to a sudden increase of the mass-transfer rate from the secondary component. The second model suggests that accretion discs themselves may be unstable (Smak, 1971; Osaki, 1974; Hoshi, 1979; Meyer and Meyer-Hofmeister, 1981, 1982; Cannizzo et. al., 1982; Mineshige and Osaki, 1983; Faulkner et al., 1983; see also Chapter 4.III).

We have already said that the disc instability model can account for most of the observational properties of GK Per during the optical outbursts. Cannizzo and Kenyon (1986) pro-

posed for GK Per an accretion disc limit cycle mechanism and placed the transition region, which is responsible for the onset of the outburst, at the very inner edge of the disc. Bianchini et al. (1986) proposed that the mass-transfer rate within the binary system is modulated by the presence in the secondary of some kind of activity, and that the unstable transition region in the inner regions of the accretion disc could be formed only when the mass-transfer rate from the secondary becomes larger than $10^{16} gs^{-1}$.

For bursts starting at small radii of the disc, the light curves observed at different wavelengths should have more rounded and symmetric profiles with no relevant time delays between them (Cannizzo et al. 1986). Actually, the outbursts of GK Per tend to be symmetric, and no appreciable time delay has been observed between the UV, the visual, and the infrared light curves. We know that smaller outbursts have a more asymmetric profile but, unfortunately, only their visual light curves have been observed so far.

However, we have seen that some observational results seem to contradict the standard disc instability model. For example, the detection of strong hard x-ray fluxes prior to the onset of the 1978 optical outburst strongly indicates that the outburst originates in the hotter central regions of the accretion disc or on the surface of the white dwarf, but also contradicts the theoretical prediction that no relevant time delay of the outburst profile should be seen at any wavelength. Other important discrepancies between the theory and the observations have been already pointed out in Section V.A.

The $T = n(400 \mp 40)$ days relation (n = 1,2,3,5; as we have seen, 4 seems to be absent), which gives the observed time intervals between two consecutive outbursts, suggests the existence of a mechanism capable of producing these particular recurrence times. This mechanism could be represented by the presence in the secondary of cycles of activity that modulate the mass-transfer rate and trigger the onset of the disc instability mechanism with the observed recurrence times.

However, we must be very cautious when applying the standard disc instability model to the very inner regions of the accretion disc of GK Per. In fact, the inner radius of the disc is controlled by the magnetic field and could be close to the corotation radius (Duschl et al., 1985). Thus, the physical situation in this region must be rather complicated, and much more refined models are required.

V.F. THE LONG TERM LIGHT OSCILLATIONS OF GK PER AT QUIESCENCE

The return of the nova to light minimum did not occur monotonically but through a number of strong light fluctuations. The historical light curve covering the years 1901-1983 is discussed by Sabbadin and Bianchini (1983). The main characteristics of the long-term light curve of GK Per at minimum can be summarized as follows:

1) The preoutburst light curve (Robinson, 1975) shows that the nova was fainter than 13.8 mag for several years and that it brightened in the range of 12.8-13.4 mag in the two years just prior to its eruption. We can then conclude that the nova had essentially the same luminosity before and after the explosion and that variations of, at least, 2 magnitudes were probably present also in the preoutburst light curve.

2) The historical minimum, $m_v \sim 15$, was reached in 1916, but this low luminosity does not correspond to that of the normal quiescent state of the nova, which is 2 magnitudes brighter. Instead, it is surprisingly close to the reddened apparent visual magnitude of a K2 IV-V star at the distance of the nova. Thus, we suggest that GK Per, at the end of the explosive episode, passed through a sort of mini-hibernation phase with little or no mass-transfer rate from the secondary. In fact it is possible that the strong heating of the deep layers of the secondary by hard radiation emitted during the nova explosion enhanced the mass loss from the secondary so much that at the end of the explosion the star had to shrink inside its Roche-lobe. The light fluctuations observed at that time should then

be mainly caused by intrinsic variability of the secondary while it was trying to fill again its Roche-lobe.

3) During the twenties and thirties, the visual magnitude of the nova was continuously fluctuating between magnitudes 14.2 and 12.0 on typical time scales of 40, 80, and 400 days. During this period of time, we observe an increase of the nova mean luminosity and, during the forties, the nova was hardly found fainter than magnitude 13.

4) From 1948 till the present time, we see a very slow decline of the luminosity; now the nova spends most of its time in quiescence and, at intervals of hundreds of days, shows enhanced outbursts. As an example, Figure 8-39, shows the light curve of the nova in the years 1969-1983.

5) The analysis of the data, including the more recent 1986 outburst, indicates that the observed optical maxima present a particular type of semiperiodicity, in the sense that the intervals, ΔT, between two consecutive outbursts can be expressed by the relation: $\Delta T = n(400 \pm 40)$, where n ranges from 1 to 5, although 4 seems to be excluded. Figure 8-40, presents the suggested relationship and shows that all points, except the 1981 outburst, which occurred 984 days after the 1978 one, are within their error bars of $\simeq$ 40 days.

6) The plot of the annual mean magnitude in the period 1917-1986 (see Figure 8-49) might suggest the presence of a longer term modulation of the outburst activity of GK Per. Fourier analysis revealed the presence of a main cycle of about 2500 days, but a smaller modulation at about 1300 days is also possible. This result has been tentatively interpreted by Bianchini (1988) as the effect of the presence in the secondary of a solar-type cycle capable of changing the mass-transfer rate within the binary system by a factor of 2.8. The cycle is more evident in the light curve of the period 1917-1940, that is, while the nova was recovering from the historical minimum. This might be due to the fact that solar-type cycles in CVs are better observed in systems having low-mass accretion rates (Bianchini, 1988). During the seventies and the eighties, the magnitude of the nova has been around 13.15, still oscillating on time scales of 1300 and 2600 days between magnitudes 13.0 and 13.2. However, in the period 1950-1988, a slow decline of the out of outburst-luminosity, at a rate of 0.018 mag/yr, could also be suggested. We note here that the observed 2400-, 1200-, 800-, and 400-day, time intervals between the optical outbursts of GK Per could well be connected with the 2400- and 1300-day modulations observed in the long term light curve of the nova. In other words, it is probable that all these periodicities are physically correlated. For example, they could be explained as the effect of the presence in the secondary of solar-type cycles. Bianchini et al. (1986) proposed that since 1950, the accretion disc of GK Per, due to the particularly low-mass transfer rate from the secondary, is fully convective and stable most of the time and that a cyclic increase of the mass transfer rate from the secondary is responsible for the onset of the unstable transition region near the inner edge of the accretion disc. In particular, a cyclic increase of the mass transfer rate might be caused by the periodic alignment of nonradial g-modes on the surface of the cool star. As a consequence, several periodicities should be observed, in coincidence with the periodic alignments of different groups of sets of modes. These periodicities should result in submultiples of the time interval between two consecutive alignments of all the sets. Such a long period could be tentatively identified with the observed 2400-day light modulation.

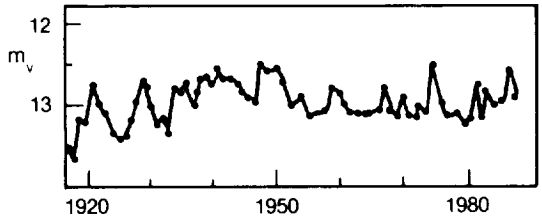

Figure 8-49. Annual mean visual magnitude of GK Per in the years 1917-1986. Fourier analysis reveals the presence of a quasi periodicity at about 2400 days. Similar periodicities have been found also in other Cataclysmic Variables. They could be ascribed to the effect of solar-type cycles in the secondary.

VI. V1668 CYGNI 1978, A MODERATELY FAST NOVA

(written by Hack)

V1668 Cyg 1978 was discovered on September 9, 1978, independently by Collins (1978) and by Shao (1978). It is the first nova whose development has been followed completely, from premaximum to the nebular phase, both in the ultraviolet with IUE and in the infrared.

VI.A. PHOTOMETRIC OBSERVATIONS

It reached maximum brightness on September 12, 20 with V = 6.2 (Kolotilov, 1980). The absolute magnitude is very uncertain; from the degree of interstellar reddening, values ranging between -6.2 and -8.3 are derived (Klare et al., 1980), while the relation between the fastness of light decrease and absolute visual magnitude $M_v = -11.5 + 2.5 \log t_3$ gives $M_v = -8$. In about 3 months, the nova decreased from V = 6 to V = 11, and the energy radiated amounted to about 3 x 10^{44} ergs. The photometric observations in U,B,V by Duerbeck et al. (1980b) show how the position of the nova varies in the two-color diagram (Figures 8-50 and 8-51). The temperatures derived by the colors, together with the values of the luminosity, permit to derive the loci occupied by the nova in the logT-logR diagram (Figure 8-52), where T and R represent the values of the pseudophotosphere. During the first 8 days after maximum, T varies from 8,000 K and 18,000 K, and R, between 100 and 25 solar radii, while the luminosity remains almost constant. On September 12-14, the UV and visual continuum energy distribution is similar to that of an F5 star.

Photoelectric observations in UBV were obtained in 1978 by Piccioni et al. (1984) from 2 to 60 days after outburst , and others were obtained in August 1981, when the magnitude was about 17, showing the presence of fluctuations of a few hundreths of magnitude (Figure 8-53) and time scales ranging from a few minutes to 2 hours.

Kaler (1986) has made simultaneous observations in the visual continuum (y magnitude in the Stroemgren system) and with the wide H

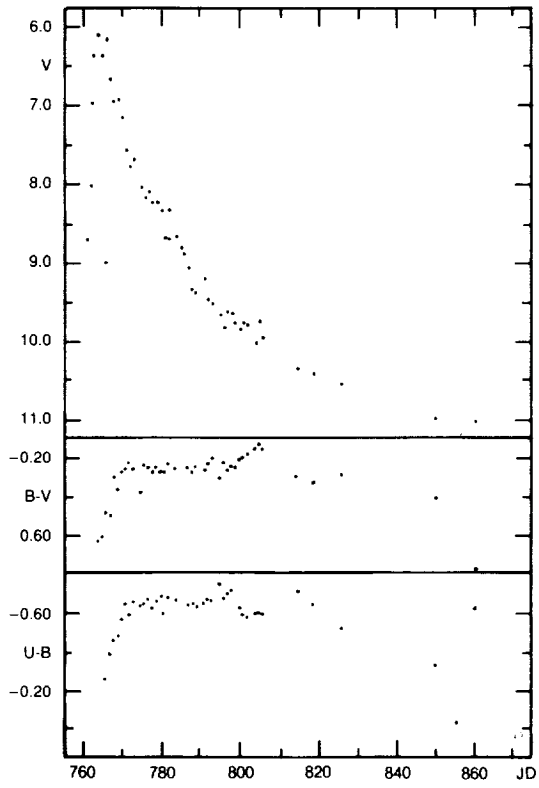

Figure 8-50. Light and color curves of Nova Cygni 1978.
(from Duerbeck et al., 1980b).

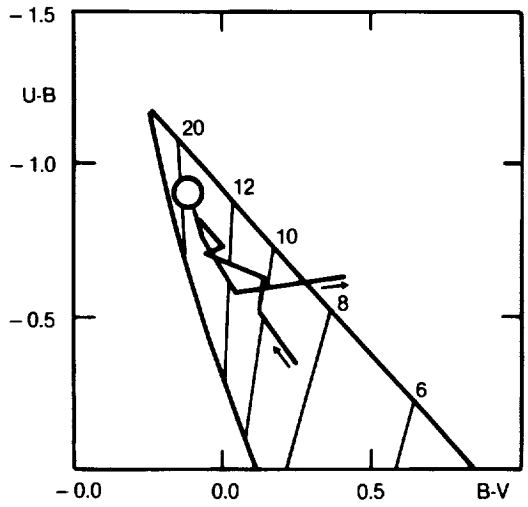

Figure 8-51. Path of Nova Cygni 1978 in the two-color diagram, corrected for interstellar extinction. Supergiant and blackbody sequences, and lines of constant temperature (in 10^3 K are shown.
(from Duerbeck et al., 1980b).

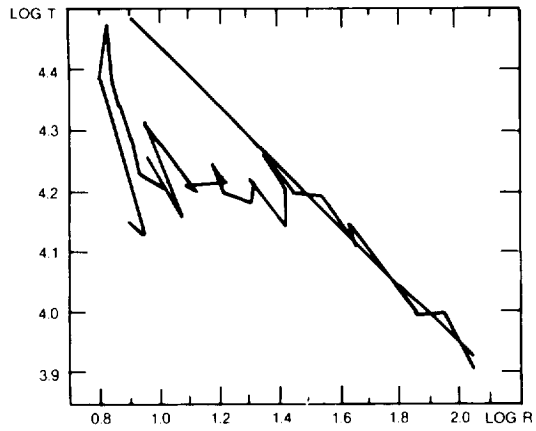

Figure 8-52. Nova Cygni 1978 in the T-log R diagram. For 8 days after maximum the nova stays at constant luminosity (corresponding to a line with a slope of 45°). (from Duerbeck et al., 1980b).

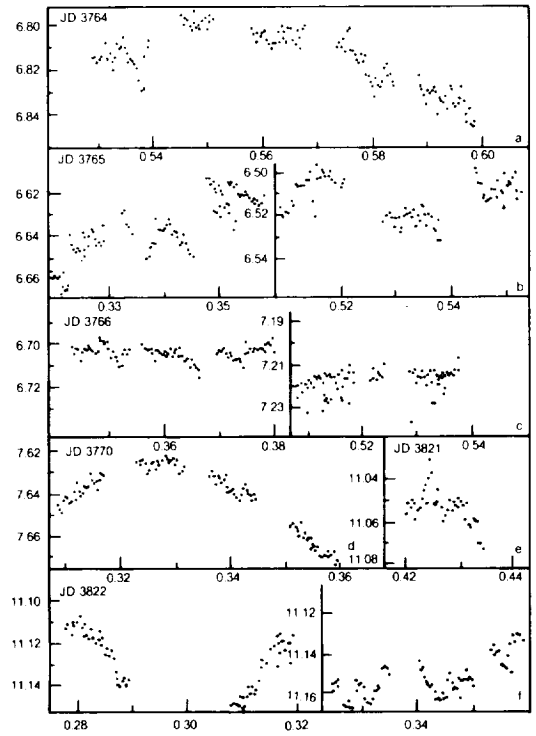

Figure 8-53. Examples of B light variations of Nova Cygni 1978 during its early decline. Each dot represents the mean magnitude over one minute. (from Piccioni et al., 1984).

Beta filter w (including the H beta and [O III] emissions). The two light curves separate rapidly after 50 days from outburst (Figure 8-54). At 311 days after outburst, the continuum has declined by 9 mag while the w emission has declined by 4.7 mag only. Hence, the decline of

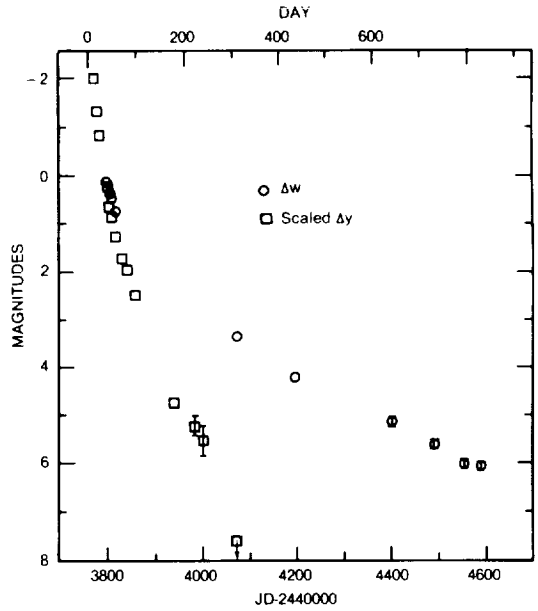

Figure 8-54. Hβ-wide (Δw) and Stroemgren y (Δy) light curves for Nova Cygni 1978. The ordinates are the nova minus comparison magnitude differences. The Δy curve is scaled to Δw for September 26, 1978, to show the differences between the two. The decline of Hβ is much slower than that of the y continuum. (from Kaler, 1986).

the star (indicated by y) is much faster than that of the nebula where [OIII] is produced.

Polarization measurements have been made by Piirola and Korhonen (1979) from 6 to 55 days after outburst. They observe an increase of polarization from 1.6% to 1.9% between October 1 and 11, 1978, i.e., in the same period when the dust formation phase (October 7-15), indicated by the infrared observations (Gehrz et al. 1978) started.

VI.B. SPECTROSCOPIC OBSERVATIONS

Spectra obtained near maximum and for several weeks after outburst have been obtained by Kolotilov (1980), Ortolani et al. (1978) and by Klare et al. (1980). The latter show the full sequence of spectra from September 13 to December 18, giving an instructive example of the kind of variations occurring in the spectrum of a nova (Figures 8-55 and 8-56). Three main emission components at about -500,- 45, and + 500 km/s are observed for several weeks on

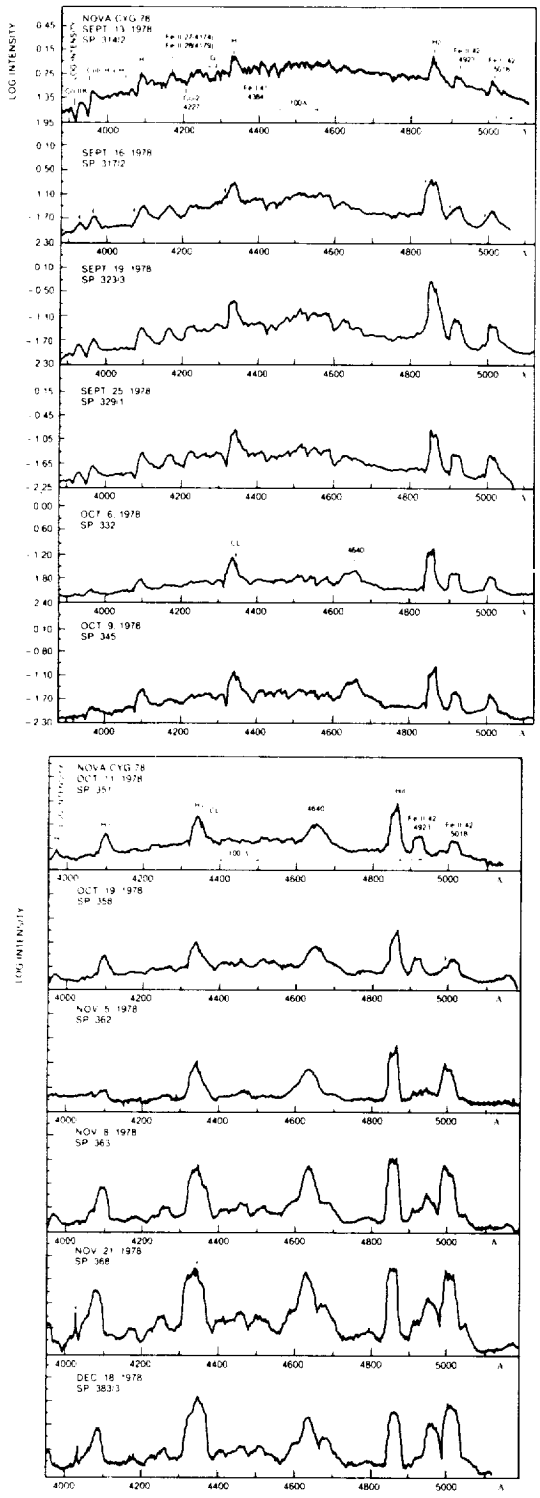

Figure 8-55. The photographic spectrum of V 1668 Cyg: a) from September 13 to October 9. CL = Emissions due to city light. b) The same spectral region, from October 11 to December 18. A P Cyg profile is still visible on October 11 at H Beta, Gamma, and Delta and is completely disappeared on November 5. The multiple structure of the emissions is evident. (from Klare et al., 1980).

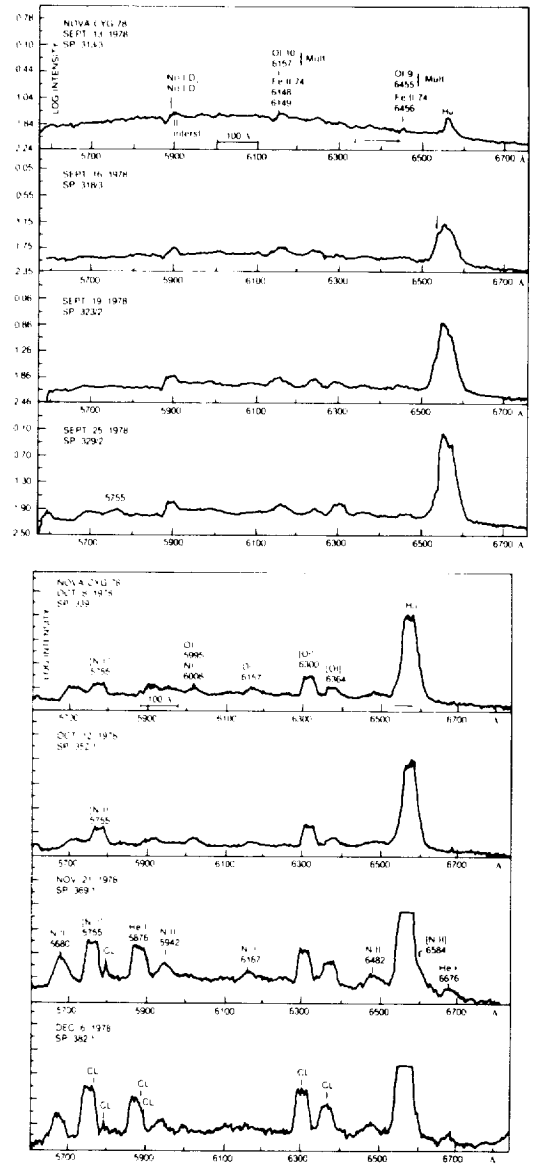

Figure 8-56. The red spectrum of V 1668 Cyg. a) from September 13 to September 25, b) from October 8 to December 6. CL = emissions due to city light. (from Klare et al., 1980).

October and November (Kolotilov, 1980), and more complex structures, indicating the presence of two main shells expanding at about 500 and 150 km/s, are evident along the 3 months after outburst (see Klare et al. 1980). During the first few days from outburst, P Cyg profiles are evident, with expansion velocities increasing from -600 km/s (principal spectrum), to -1700 (diffuse-enhanced) and -2100 km/s (Orion spectrum).

Comparison of the visual and ultraviolet

spectra show that lines of comparable excitation appear at about the same epochs in both wavelength ranges. The only exception is 1640 He II (E.P. 48.3 eV), which is present already on the spectrum of September 19 (7th from the outburst), while 4686 He II (E.P. 50.8 eV) only appears at November 5 (54th from the outburst), reaches maximum intensity on Novermber 21, and is still strong on December 18. However, the low-resolution spectra of IUE show that on September 19 (Figure 8-57a), the O I line at 1302 is present. Hence, it is possible that the emission at 1640 is due, totally or partially, to the semiforbidden line of O I at 1641. Figure 8.57 and 8.58 show the low-resolution UV spectrum on September 19 and October 17, 1978. The great strength of the ultraviolet nitrogen lines is noticeable. Comparison of the nebular spectrum of the nova with those of planetary nebulae suggests that nitrogen is in excess in the nova ejecta by a factor of 200 (Stickland et al., 1981) relative to the solar abundance.

Ultraviolet observations were made on the early phases of the outburst by Wu et al. (1978), who observed the nova on September 13.4 and then from September 15 to October 8; by Cassatella et al. (1979), who observed it on September 14.98 and then on September 28 and October 10 (Figures 8-59, 8-60, 8-61), and by Stickland et al. (1979), who obtained an extended series of spectra from September 11.7 to March 24, obtaining spectra preoutburst, at early decline, in the transitional stage and the nebular stage, which are the object of the quoted paper (Stickland et al. 1981). From visual data obtained on September 12-14, Ortolani et al. (1978) estimated a spectral type F5 Ib, which agrees with the UV energy distribution. On the same dates, the narrow absorption lines have an expansion velocity of -630 km/s. On September 16-17, Ortolani et al. observe only wide diffuse absorptions at the blue edge of the emissions with velocity of -630, -700 km/s. On September 28, emission lines of Fe II, Cr II, and Mn II are broad and symmetric. The half width (FWHM) of the Balmer lines indicates a larger expansion velocity, -1550 km/s. At least another system of emission lines, characterized by an expansion velocity of 525 km/s is present through the O III fluorescence lines at 2688, 2984, and 3333 Å. The structure of the Mg II resonance doublet (Figure 8.61) is complex, with two absorption components, one sharp (FWHM = 55 km/s) and shortward shifted by - 80 km/s; the other is broader (FWHM=270 km/s) and shortward shifted by -1160 km/s with an emission wing. The presence of a few resonance lines of Mn II, Fe II, Mg I, which are very sharp (FWHM = 30 km/s, just slightly above the resolving power of the IUE camera) and shortward shifted by -95 km/s, suggests that an outer shell is present.

The spectrum in October shows a higher degree of excitation and ionization (as indicated by the presence of emissions of 1640 He II, Fe III, Si III, O III) and the flux in the continuum is about twice as strong as that in September, indicating the usually observed shift of the flux to the ultraviolet, probably due to the unveiling of the hot object as the ejected envelope becomes optically thin.

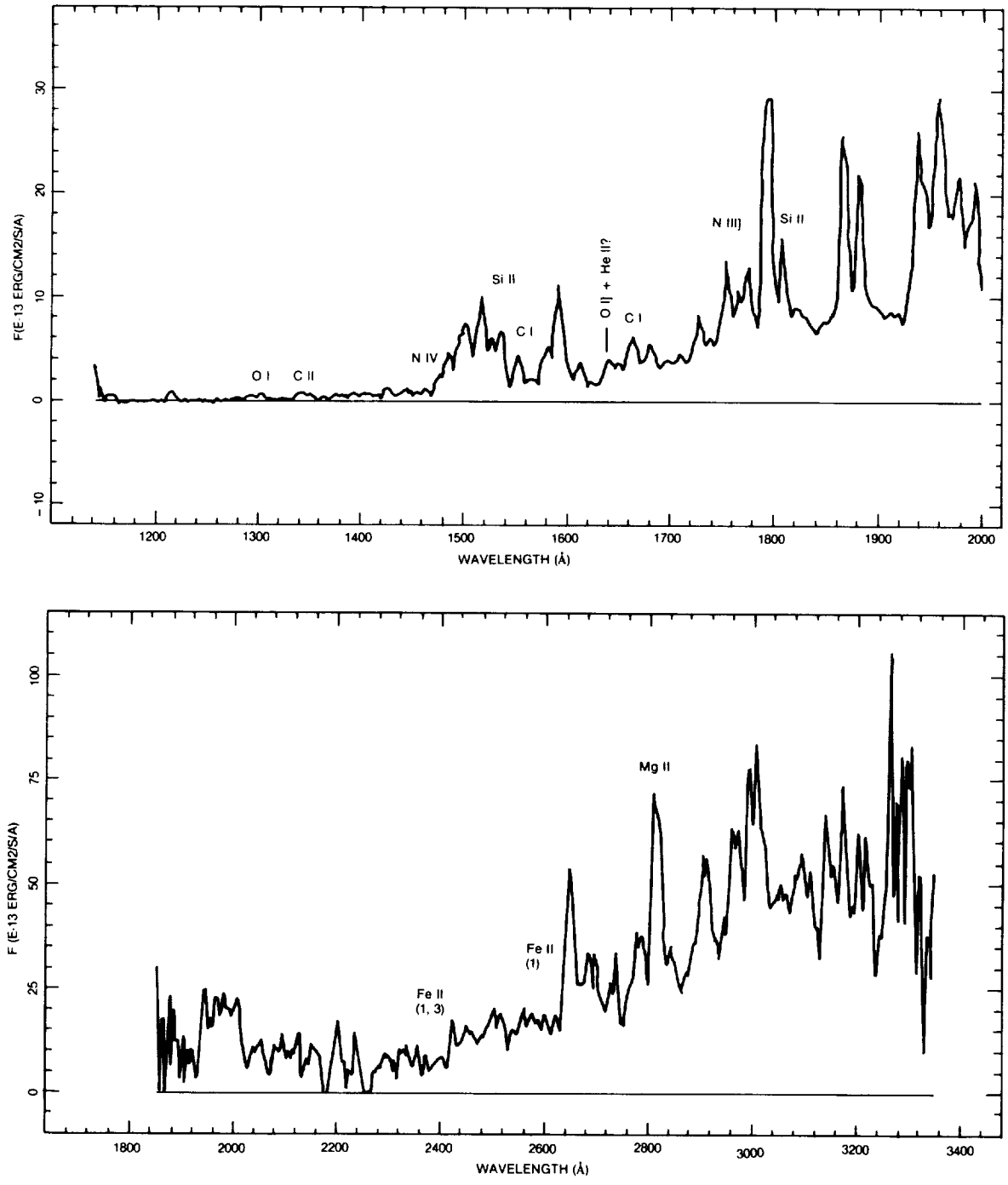

Figure 8-57. The ultraviolet spectrum (obtained with IUE) of V 1668 Cyg in the early decline stage (day 7 from maximum). a) short-wave range, b) long-wave range.
(from Stickland et al., 1979).

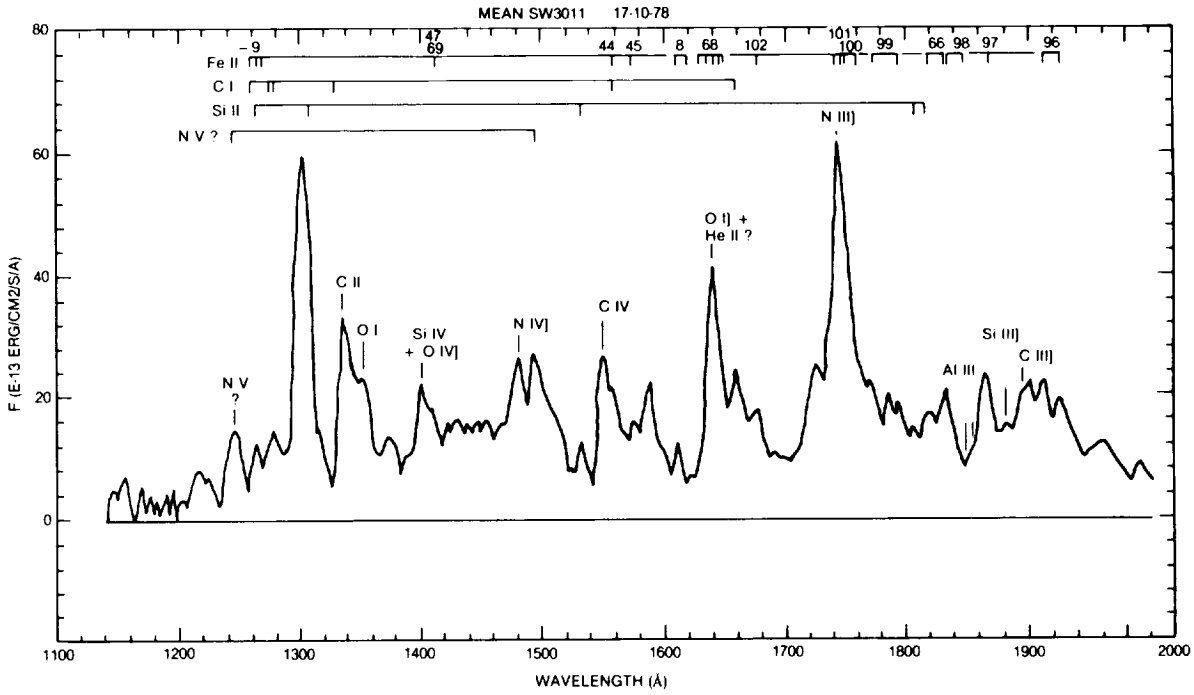

Figure 8-58. Short-wave spectrum of V 1668 Cyg in the transition state (day 35). (from Stickland et al., 1979).

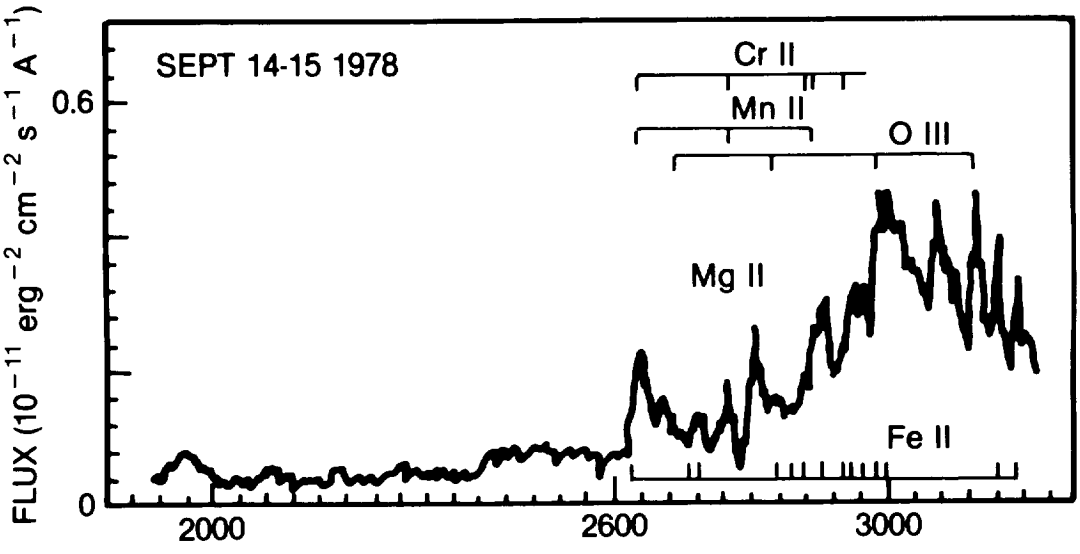

Figure 8-59. The absolute energy distribution (not corrected for reddening) in the IUE long-wave range, two days from maximum. (from Cassatella et al., 1979).

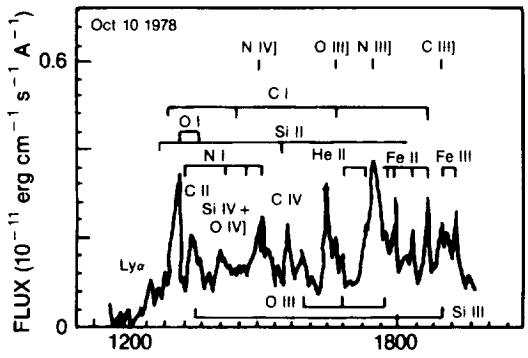

Figure 8-60. The absolute energy distribution (not corrected for reddening) in the IUE short-wave range on October 10. (from Cassatella et al., 1979).

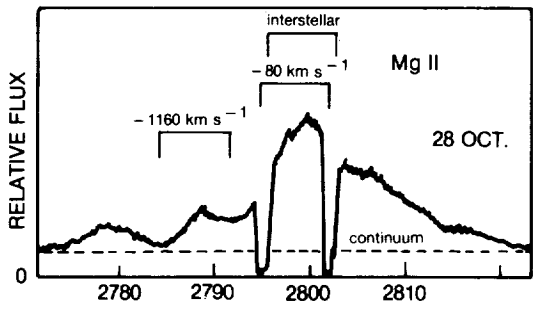

Figure 8-61. The Mg II doublet feature from the IUE high-resolution spectrum of September 28. The two broad Mg II lines at -1160 km/s are very broad, with a half-width at half maximum of 815 km/s. (from Cassatella et al., 1979).

VI.C. THE NEBULAR PHASE

The results of the study of the nebular spectrum (the first nebular spectrum was observed on November 6, 56 days after maximum) are summarized by Stickland et al. (1981). Their main results are the following. The reddening derived by the λ2200 feature is E(B-V) = 0.40 +/- 0.10 in good agreement with the value derived by the optical observations, which gives a mean value of 0.35 +/- 0.08. Electron temperature, electron density, and abundances are derived by the ratios of several nebular emission lines.

Collisionally excited lines are sensitive to the electron temperature while recombination lines are only very slightly dependent on T_e. Hence, the ratio between a line formed by recombination and another formed by collisional excitation of a same ion is independent of the abundance and of N_e (if collisional deexcitation is negligible), and dependent only on T_e. In the case of forbidden lines, which are present in the visual spectrum of novae, collisional deexcitation is not negligible; hence, the ratio of permitted to forbidden line of a same ion depends also on N_e. The situation is better in the UV. Stickland et al. (1981) used the following ratios to derive T_e: C II 1335/C II 2326 and CIII 2297/C III 1909, where the permitted lines are formed by recombination and the intercombination lines are formed by collisional excitation. Temperatures in the range 2 x 10^4 and 5 x 10^5 K are found. Although this method may seem the best way to derive the electron temperature, the application of it to planetary nebulae gives too high values. Another method is to use the ratio of the recombination line of 1717 N IV to the collisionally excited line 1240 N V. These three ratios give values of the electron temperature ranging from 9200 to 13,300 K on day 70 from outburst; from 9810 to 15,100 K on day 88 and from 8440 to 13,700 K on day 304.

Electron densities are derived by the ratios of intercombination lines to forbidden lines. Since intercombination lines fall in the ultraviolet and forbidden lines in the visual, lines from the two spectral ranges must be used. The ratios 2140 N II]/ 5755 [N II] and 1663 O III] / 5007 [O III] give N_e = 8 x 10^7 cm^{-3} on day 88.

The abundances of C, N, and O relative to He are obtained from the UV spectra, while the optical observations by Klare et al. (1980) have been used to derive the helium ionization and the He/H ratio. From these data, it is found that the ratio of CNO atoms in the shell relative to H is larger than the solar value by a factor of 30.N, in particular, is enhanced by a factor of 200.

Figure 8-62 shows the UV nebular spectrum.

Starrfield et al. (1978) have predicted that the rate of energy produced during the runaway is determined by the initial abundance of the CNO elements, and that the ejection of a shell becomes possible only if the CNO abundances

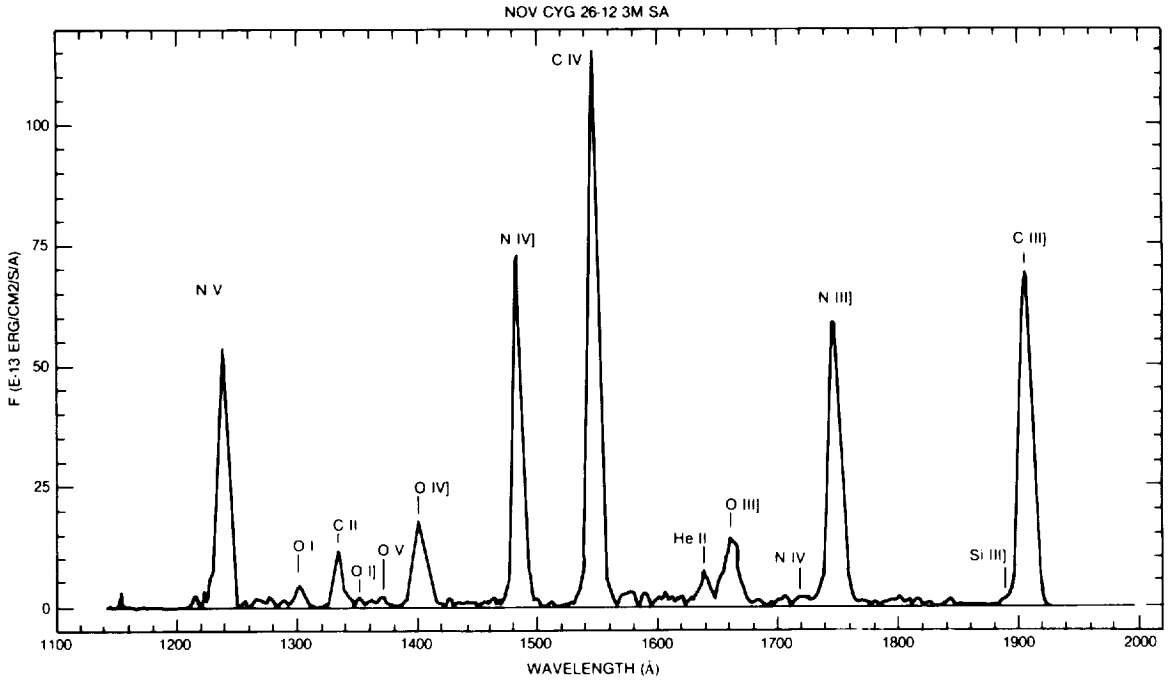

Figure 8-62. Short-wave spectrum of V 1668 Cyg in the nebular stage (day 105 from outburst). (from Stickland et al., 1979)

are substantially larger than the solar abundances. If this mechanism is operative, their computations show that the ejected material will have enhanced CNO abundances, and the abundance of N will be relatively enhanced to C and O: hence, the results found for Nova Cyg 1978 seem to confirm the theory of the thermonuclear runaway. The total luminosity of the remnant has an approximate constant value L = $1.7 \times 10^4 L_\odot$ from day 13 to day 27 after outburst, with an output of radiant energy of 8×10^{43} ergs. A total energy of about 3×10^{44} ergs has been emitted since the instant of the outburst. The mass of the ionized gas in the ejected shell is about 10^{29} g, and its kinetic energy of the order of 6×10^{44} ergs.

VI.D. INFRARED OBSERVATIONS

Gehrz et al. (1980b) have monitored V 1668 Cyg from the visual band V to 19.5 μm for 120 days after outburst. We have seen in Chapter 6 that V1668 Cyg is an intermediate case between slow novae-like FH Ser or NQ Vul (type DQ Her) which exhibit a transition phase with a deep minimum in their light curve and very fast novae-like V1500 Cyg. V1668 Cyg presents an intermediate behavior also in the infrared. In fact, infrared observations have shown that the formation of a thick dust shell in slow novae explains the deep minimum during the transition phase of the light curves. While the majority of slow novae form a thick dust shell, and fast novae do not show evidence of it, V1668 Cyg gives evidence of the formation of a thin dust shell. Figure 8-63 shows the infrared light curves. At the beginning of the expansion (4.5 days after outburst), the energy distribution was characteristic of emission from an optically thick photosphere at T = 7400 K (see Figure 8-64), and the luminosity in this phase varies as t^2 : in fact the flux at a given wavelength is $F_\lambda = 4\pi R^2 B_\lambda$, where B_λ is the Planck function and $R \approx vt$ with v expansion velocity; it follows that $F \propto t^2$. Then the expansion continues and the envelope becomes optically thin. Now in a thin shell of constant thickness and expanding at constant velocity, the flux varies at t^{-2}. In fact, the radius is still given by R = vt; the volume of the shell $V = 4\pi R^2 dR = 4\pi(vt)^2 dR$; the density of the shell $\rho = M/V \propto t^{-2}$. Now, the flux of a thin shell is proportional to its optical depth and therefore to its density; it follows $F \propto t^{-2}$. Hence, we have a first period

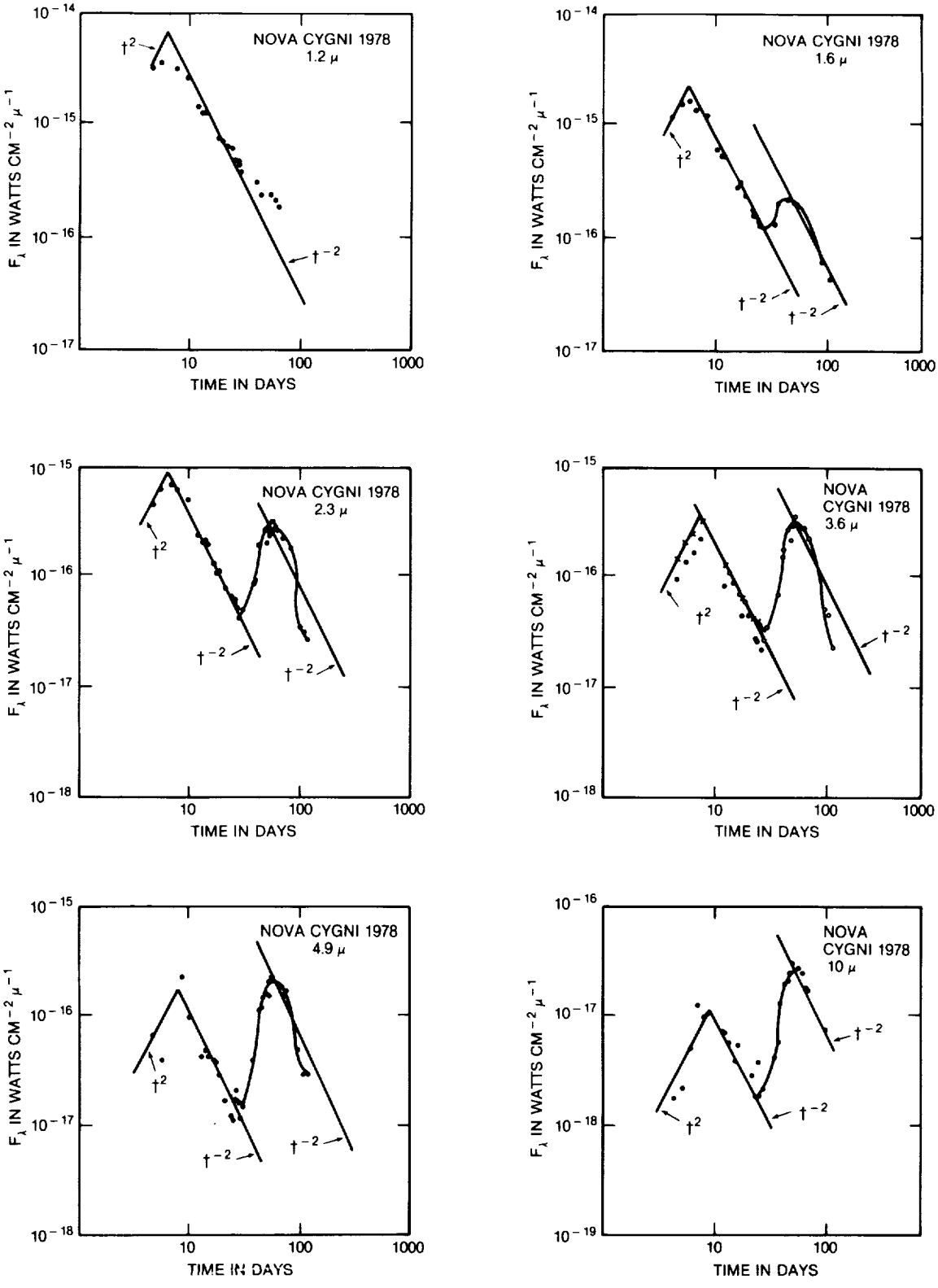

Figure 8-63. Flux versus time at different infrared wavelengths. The straight lines indicate the periods where F varies at t^2 or as t^{-2}.
(from Gehrz et al., 1980b).

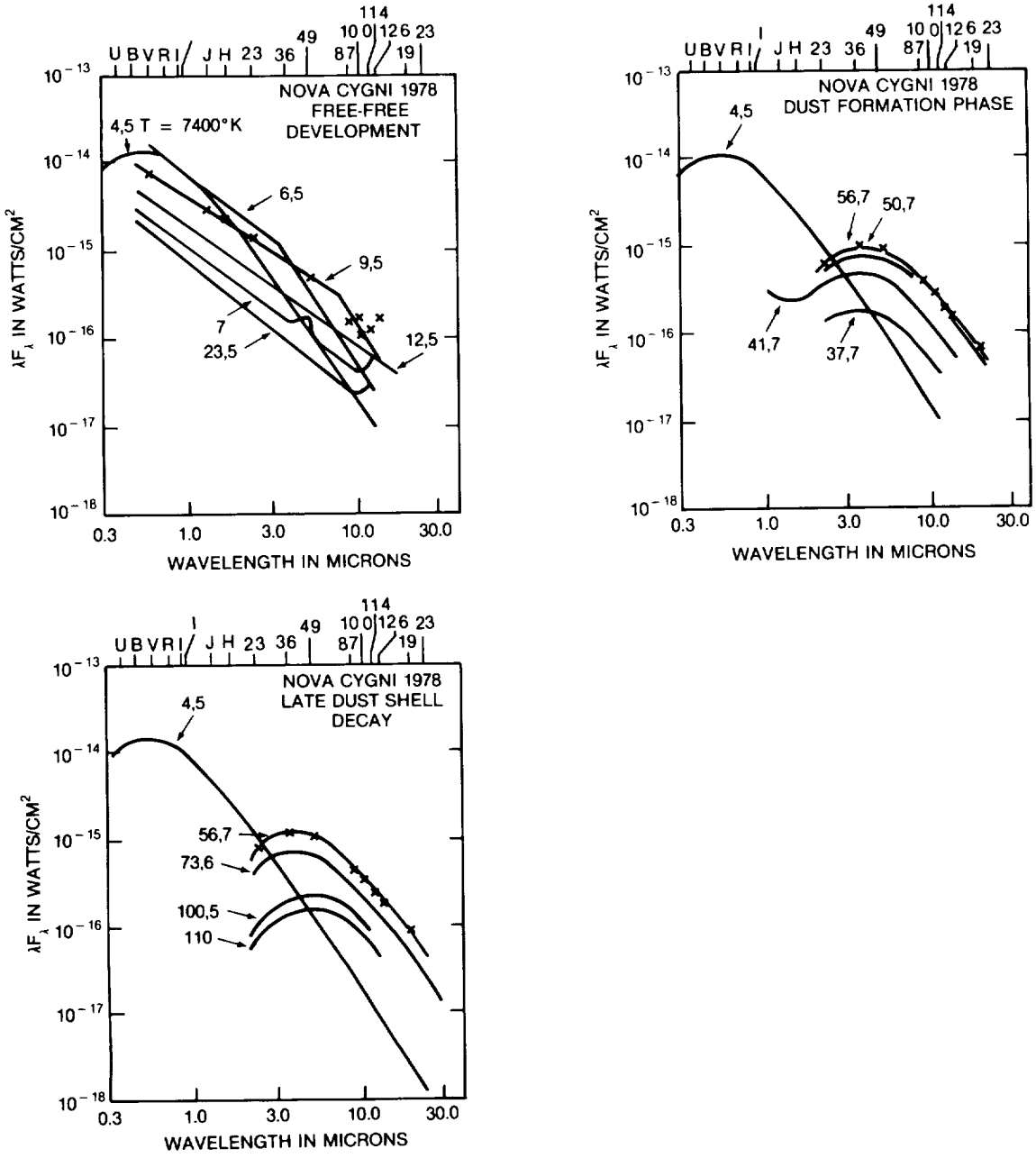

Figure 8-64. Following the expansion of the optically thick gas (the pseudophotosphere-when the energy curve is well fitted by a 7400K blackbody), three major phases follow: a) free-free development; the shell became optically thin at short wavelengths on day 6. During day 6 to day 10 the Rayleigh-Jeans tail advances towards the long wavelengths as the shell density decreases because of the expansion. By day 12.5 the spectrum 1.2 μm to 20 μm is that of a thin free-free emitting gas. b) Dust formation phase; dust grains are condensing by day 35 when the shell temperature has fallen to 1100K. From day 35 on the spectrum is that of a cool blackbody. c) late dust shell decay: after maximum infrared light, the flux from the shell decays because grain growth ceases and the shell optical depth decreases due to expansion. The shell has cooled to 850 K by day 110.
(from Gehrz et al., 1980b)

when the pseudophotosphere emits like a blackbody at T = 7400 K. The temperature remains constant, and the radius increases until day 6. From day 6.5 to day 12.5, we have a free-free emission phase; the energy distribution gradually evolves into spectrum typical of an optically thin gas. Since the absorption coefficient of a thin gas increases with the wavelength, the gas of a given density behaves like a thin gas at short wavelengths and as a thick gas at long wavelengths. Hence, the Rayleigh-Jeans tail moves toward longer wavelengths as the shell becomes less dense because of the expansion. Figure 8-64 shows that on day 6.5, the Rayleigh-Jeans tail starts at about 3.5 μm, while on day 9.5, the Rayleigh-Jeans tail start at about 8.7 μm, and 12.5 days after outburst, the spectrum has the characteristic shape of that of a thin shell in the whole observed infrared range. After day 35, we observe the start of the grain condensation phase: the flux increases again with time (see Figure 8-63) and the energy curve is represented by a blackbody curve for T = 1100 K (Figure 8-64). Hence, the angular diameter Θ_{BB} can be derived by the observed flux at the earth F and the blackbody flux B: $F = B\,(R/d)^2 = B\,\Theta^2$ (Figure 8-65). As

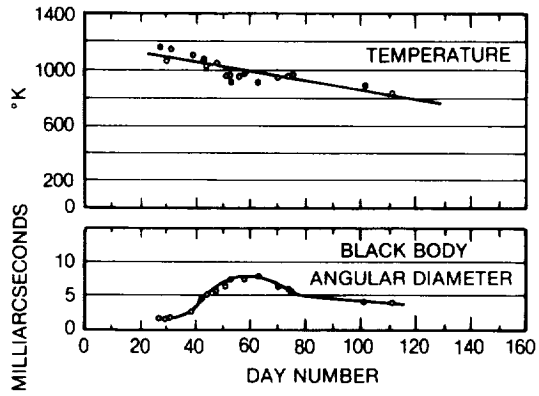

Figure 8-65. Shell temperature and angular diameter variations.
(from Gehrz et al., 1980b).

grain growth progresses, the shell flux reaches a maximum on day 60. After maximum infrared flux, there is a decay as the grain growth ceases and the optical depth of the shell decreases due to the expansion: the flux decreases again as t^{-2} (see Figure 8.63).

VII. FH SER

(written by Duerbeck)

VII.A. THE LIGHT CURVE

The outburst of FH Ser (N Ser 1970) was discovered on February 16, 1970 by M. Honda. It is a moderately fast nova with a DQ Her-type light curve, fairly similar to the nova XX Tau, and it is the first nova to be observed in the UV, optical, infrared, and radio regions more or less continuously.

The prenova magnitude was V = 16.1. FH Ser was discovered on its rise to maximum, which was reached at visual magnitude 4.4 on February 18.5. The decline occurred smoothly until about April 16, when it became very dramatic. An UBV light curve between outburst and 1979, making use of all previously published data and new ones, is shown in Rosino, Ciatti, and della Valle (1986) (Figure 8-66, 8-67, 8-68).

VII.B. SPECTROSCOPY

Spectroscopic studies of FH Ser were carried out by Wagner et al. (1971); Anderson, Borra, and Dubas (1971); Burkhead, Penhallow, and Honeycutt (1971); Walborn (1971); Hutchings, Smolinski, and Grygar (1971); Ciatti and Mammano (1972); Stefl and Grygar (1981); Rosino, Ciatti, and della Valle (1986). The absorption spectrum shows two main components, the principal and the diffuse-enhanced spectrum. Each of these has two subcomponents. (Figure 8-69). A general increase of the radial velocity was observed in the first 60 days, i.e., before the onset of dust formation, with an acceleration of about 0.02 m s^{-2}. The redshifted emission components of the Balmer and nebular lines lost much of their strength during the dust-forming phase, and in most other lines (O II, Fe II, N II...), there were no detectable redward components (Hutchings and Fisher, 1973; Rosino et al., 1986). This indicates that the dust formation occurred in the shell itself, i.e., the radiation from the receding layers was severely absorbed by dust in the approaching layers.

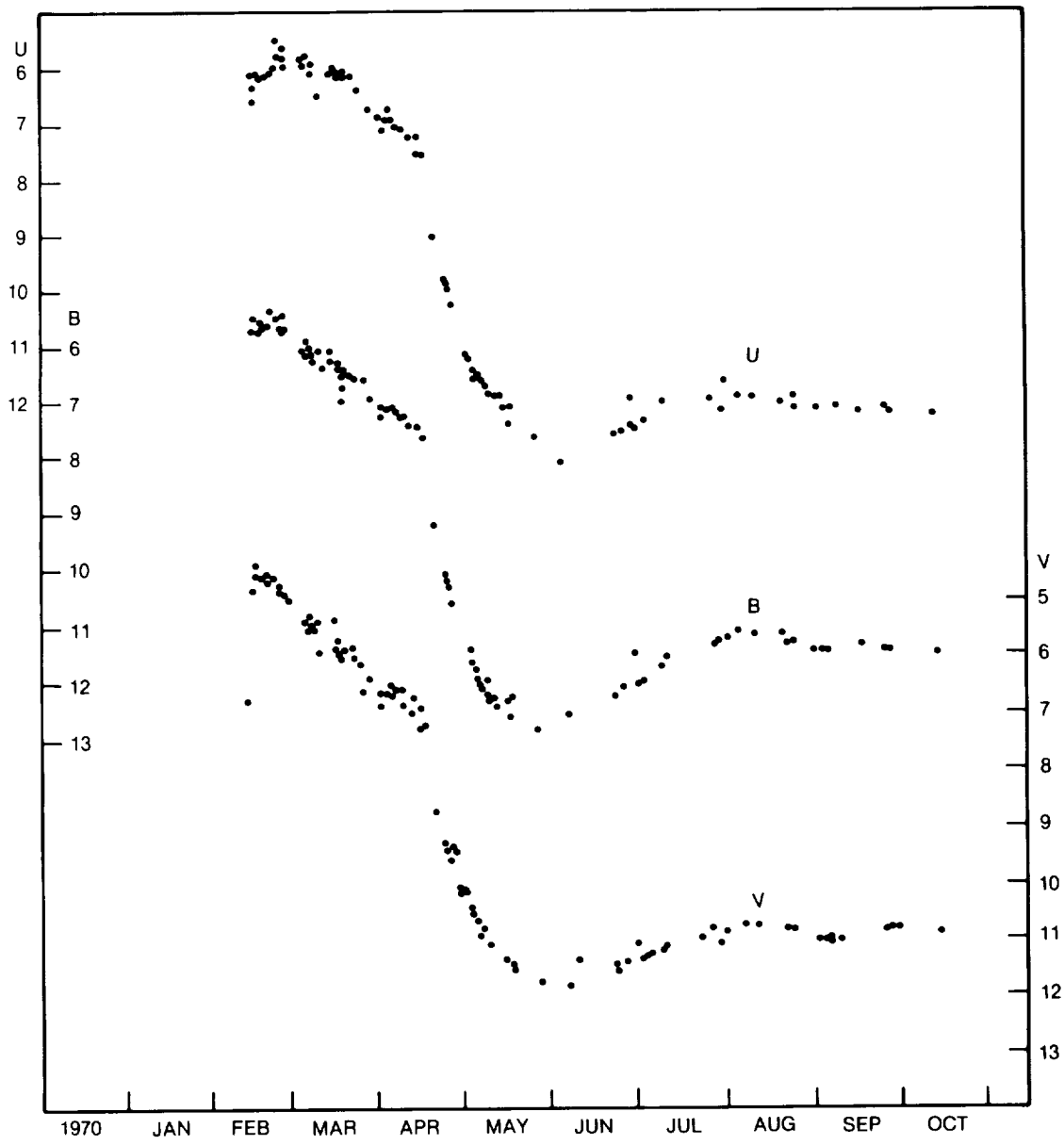

Figure 8-66. UBV light curves of FH Ser around maximum (Rosino et al., 1986).

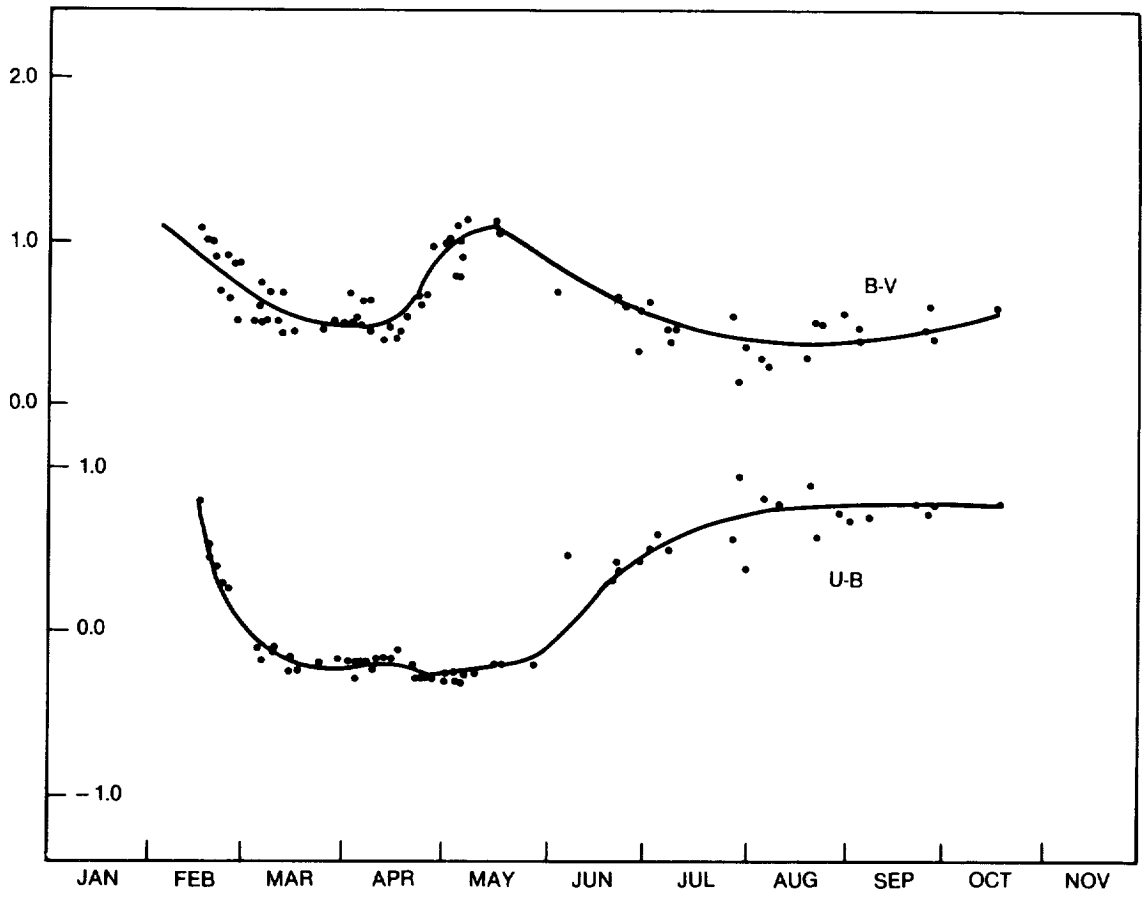

Figure 8-67. Colour curves of FH Ser around maximum (Rosino et al., 1986).

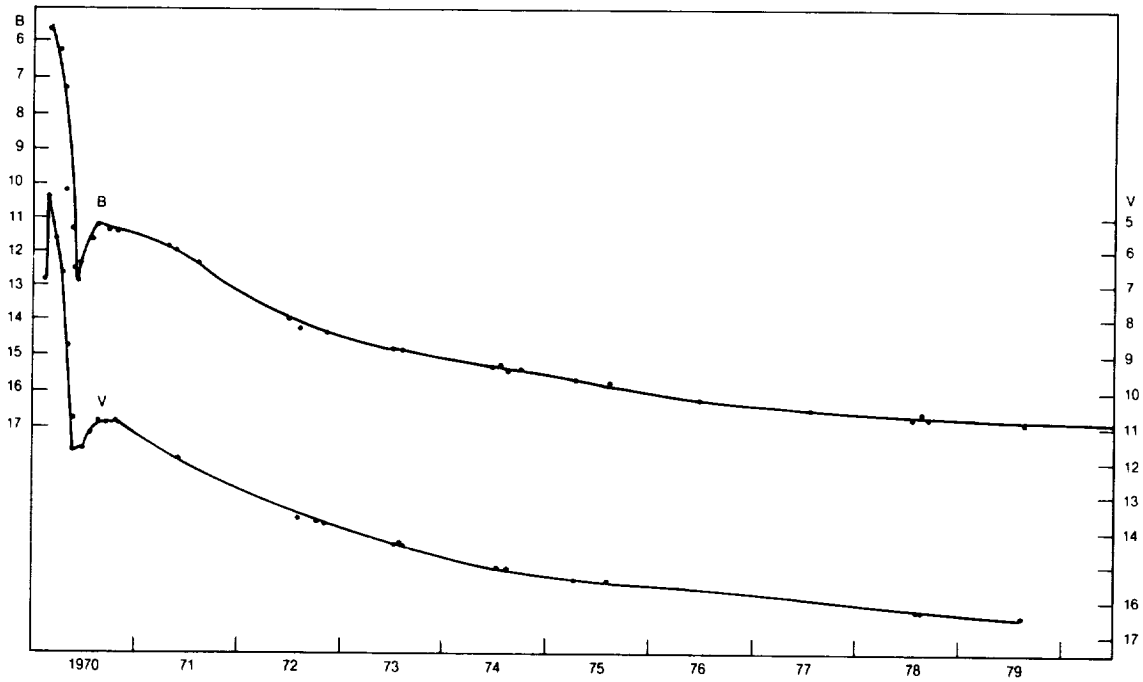

Figure 8-68. Extended B, V curves of FH Ser (Rosino et al. 1986).

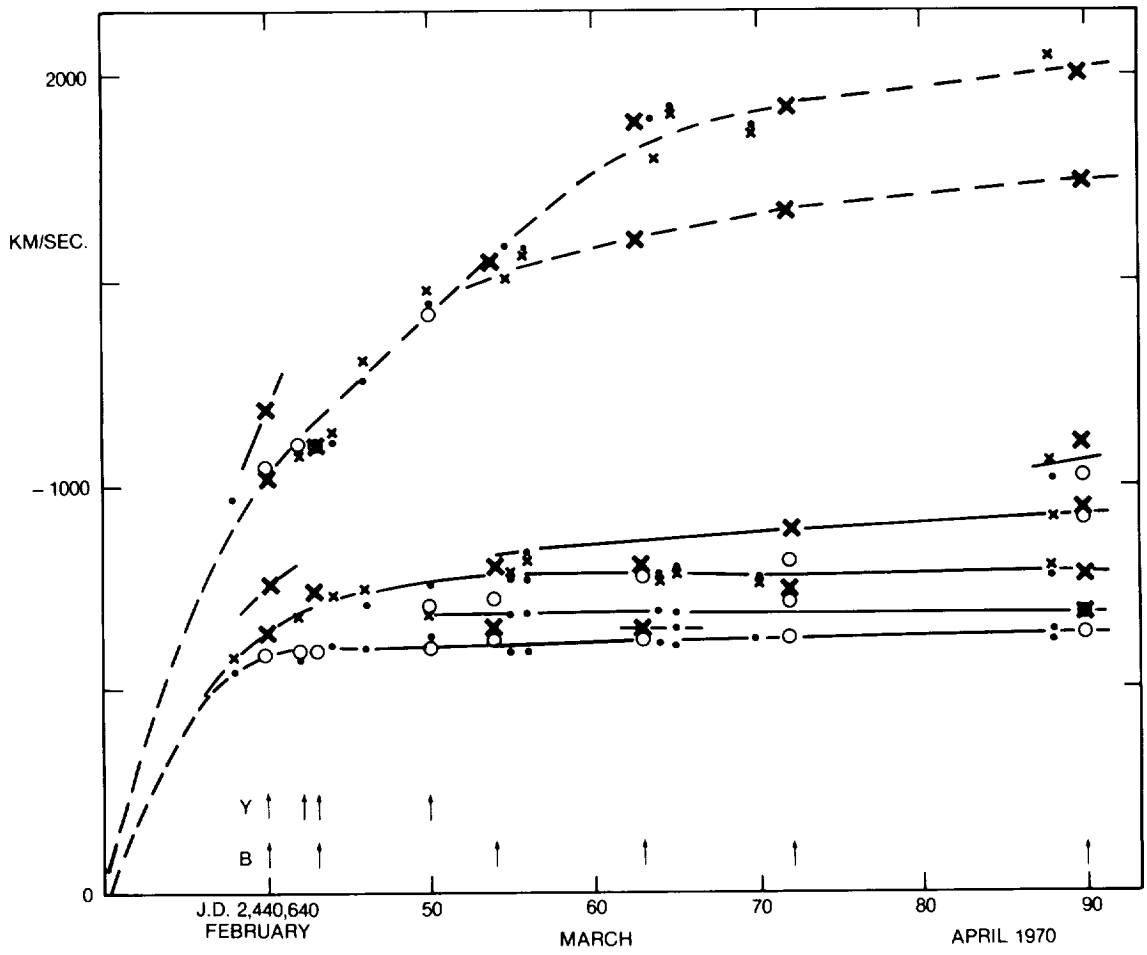

Figure 8-69. Absorption velocities in FH Ser. Crosses refer to Balmer lines, dots to metallic lines. The splitting of the principal and diffuse enhanced spectra into two (and later into four) components is clearly seen (Hutching et al., 1971).

A coronal line, [A X] 5535, was suspected by Anderson et al. (1971) on a spectrum taken August 13, 1970. Rosino et al. (1986) note that the nova attained its highest degree of ionization in March 1971, when they suspect lines of [Ni VIII] 4446, 4493, [Ni IX] 4332, 4404, [Fe XIV] 5303, and [A X] 5535. [O III] were also very strong in that phase.

VII.C. INFRARED OBSERVATIONS

Infrared observations were carried out by Hyland and Neugebauer (1970) and Geisel, Kleinmann, and Low (1970). Geisel et al. present light curves for .5, 1.25, 1.65, 2.2, 3.4, 5, 10, and 22 μm, which show clearly that the luminosity longward of 2 μm increases at the time when the light decreases at shorter wavelengths, which can be explained by formation of dust, which is heated by the central source. At peak infrared luminosity, the nova can be described as a spherical shell of unit emissivity radiating at 900 K, and having a diameter of 6.5 x 10^{14} cm (= 0.07") at a distance of 1.2 kpc, which may be an upper limit. Data taken from a more recent study are found in Section VII.F.

VII.D. RADIO OBSERVATIONS

Radio observations of FH Ser by Hjellming were analyzed by Seaquist and Palimaka (1977), and by Hjellming et al. (1979). They assumed a model in which the entire shell is ejected instantaneously and thickens as a consequence of velocity dispersion in the shell

(Hubble flow model). Two different geometrical assumptions, a spherical model and one consisting only of two polar caps, lead Seaquist and Palimaka to acceptable fits to the observed temporal change of radio radiation at 8.1 and 2.7 GHz, and to the spectral distribution of the nova remnant at a given moment (see Figure 6-76).

From the radio data and a Hubble flow model, a mass of 4.3 x 10^{-5} $M_{\odot}$ is deduced for the spherical shell, which has a temperature of 10^4 K and a distance of 730 pc.

VII.E. ULTRAVIOLET OBSERVATIONS

Ultraviolet filter photometry in the ranges of 1430 and 4250 Å and low-resolution spectral scans in the range of 2500 - 3600 A was carried out by the OAO-2 satellite (Gallagher and Code, 1974). The measurements were obtained from maximum to the onset of the rapid decline in April. (Figures 8-70, 8-71, 8-72, 8-73). Some additional UV lines are identified here.

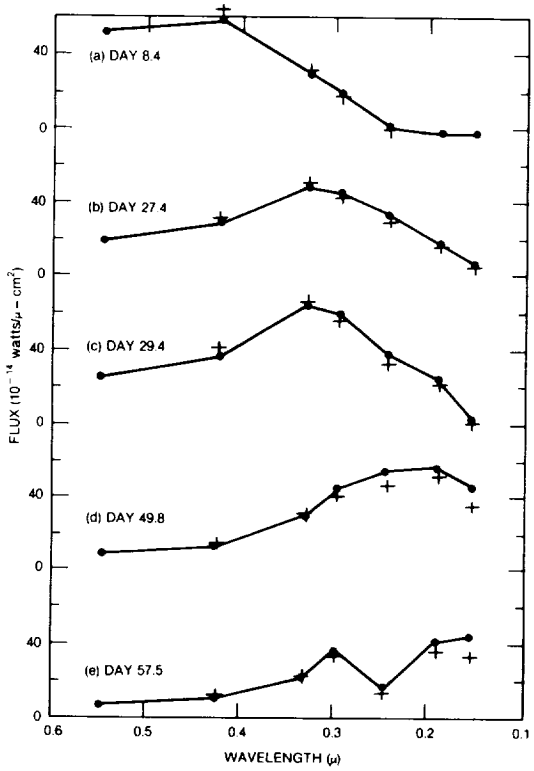

Figure 8-70. Flux distribution of FH Ser as measured by WEP photometry on board of OAO-2, corrected for an extinction of E(B-V) = 0.8. Crosses and dots refer to old and new calibrations (Gallagher and Code 1974).

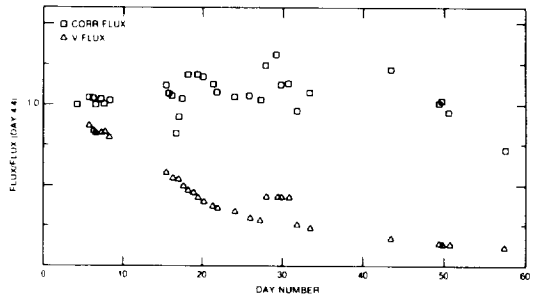

Figure 8-71. Integrated total flux as measured between 1550 aand 5460 A and corrected for extinction (open squares), and V flux (open triangles) (Gallagher and Code 1974).

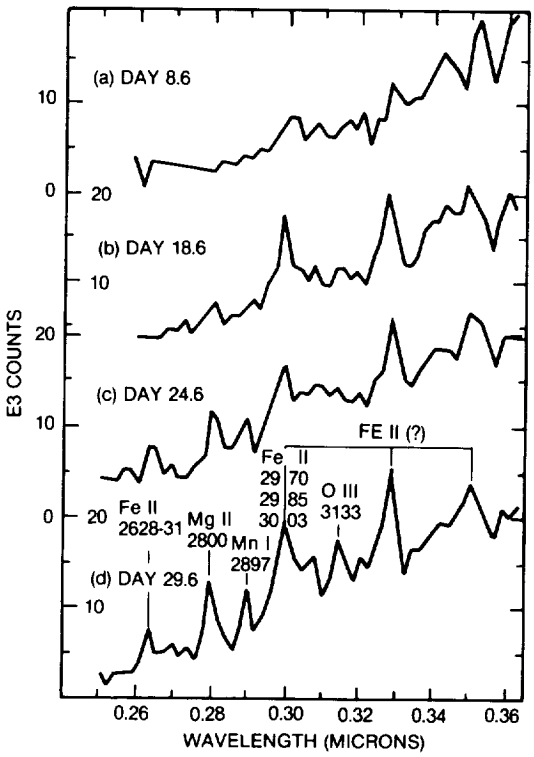

Figure 8-72. Spectral scans of FH Ser made with the spectrometer 1 on board of OAO-2 for times up to and including the "flare" in the light curve. The data have been corrected for the relative response of the scanner (Gallagher and Code 1974). Additional lines are identified.

VII.F. DISCUSSION

The most important result is that the nova did not decrease in total luminosity by a factor of 10 some 53 days after visual maximum, as implied by the V observations, but continued at almost constant luminosity. As the visible light declined, a compensating redistribution in flux

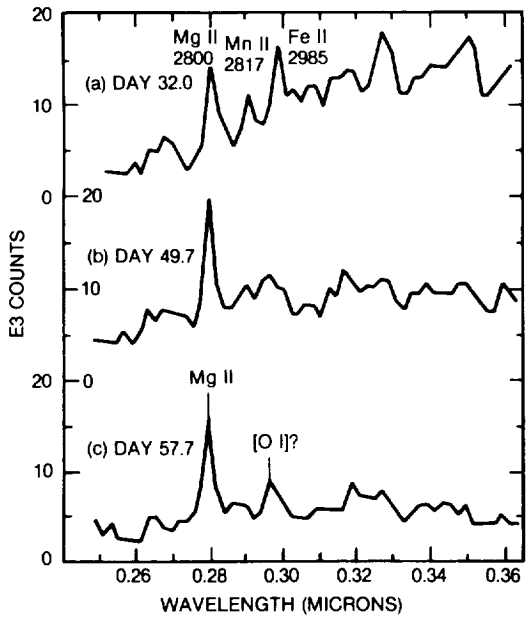

Figure 8-73. Spectral scans of FH Ser made with the spectrometer I on board of OAO-2 after the flare stage showing the increased dominance of Mg II. The data have been corrected for the relative response of the scanner (Gallagher and Code 1974). Additional lines are identified.

to the ultraviolet occurred (the correction for interstellar reddening must be accurate). The increase in IR flux, e.g., the peak in luminosity at wavelengths between 2.2 and 22 μm, which occurred about 100^d after maximum, is explained in terms of the observed trend for more energy radiated at shorter wavelengths, if efficient conversion of far-UV flux in the heating of grains occurs (see Figure 8-74).

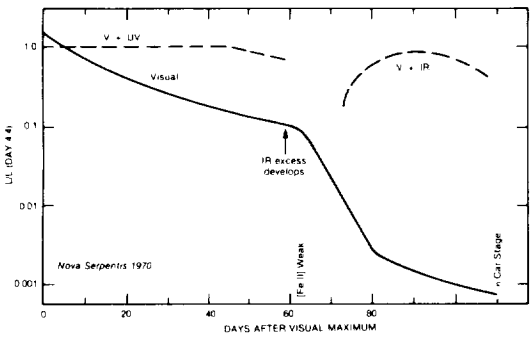

Figure 8-74. Smoothed energy budget for FH Ser as a function of time based on ultraviolet, optical and infrared data. The data show the postmaximum luminosity plateau, and the correlation between optical light curve as well as spectral features and the development of the thermal infrared excess (Gallagher and Starrfield 1978).

A more detailed study, taking into account infrared observations obtained more than 500 days after outburst, shows that from day 60 to 111, the light curve can be explained by rapid grain growth, and from day 111 to 129, by grain destruction. The luminosity appears to remain constant until day 200, after which it fell inversely proportional with t (Mitchell et al., (1985). (See Figures 6-28 and 6-29).

FH Ser is a good example for a nova to be a constant-luminosity system for a period of at least 10^7 sec after visual maximum. The hypothesis that the light curve changes are primarily due to the effective photosphere of the star, which in term is dominated by the mass-ejection rate, can explain the observed features.

From the strength of the IS lines, Huchings et al. estimated a distance of 750 pc, and an interstellar extinction A_v = 1.5; thus, the absolute magnitude of the nova was M_v = -6.5.

VII.G. THE REMNANT

A CCD image of the resolved shell of FH Ser is given by Seitter and Duerbeck (1987). The frame taken in mid-August 1984 shows an oval shell (with some indications of polar condensations at the end of the larger axis with a size of 3.9" x 3.1". The nebular expansion parallax is ambiguous due to the variable radial velocity observed during outburst; a good guess of 550 km/s (also based on emission line widths) leads to a distance of 825 pc. If the fairly strong expansion velocity component with 1100 km/s is used, the distance would not be reconcilable with other distance estimates (see Section VII.F.).

The orbital motion of FH Ser is unknown. Vogt (1981) estimates from the dereddened colors of the nova that the orbital period is of the order of 7.5 hours.

VIII. DQ HER 1934: A SLOW NOVA
(written by Hack)

DQ Her — a typical slow nova — has been observed very extensively, and its history has been reported in great detail by Beer (1974).

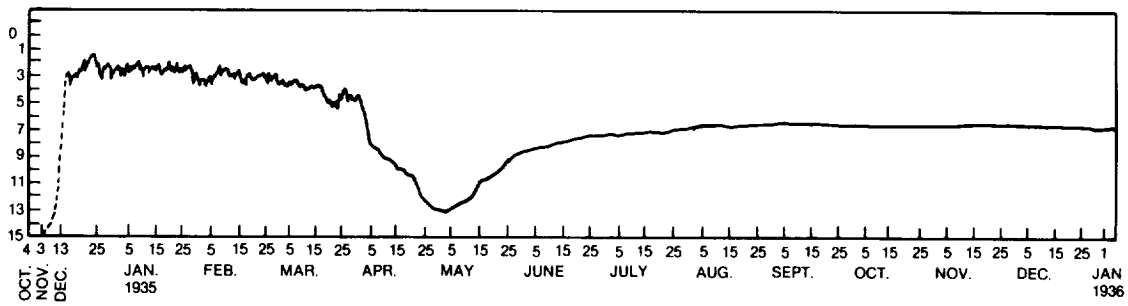

Figure 8-75. The light curve of Nova DQ Her, covering the period 1934-1936. (from Beer, 1935, 1936).

This history is very instructive as a detailed example of the complexity of the spectrum of a nova.

The magnitude before outburst was about 15. It rose to mag 3 on December 13, 1934, and reached maximum brightness 10 days later with mag 1.3. It went back to mag 3 on December 25 and then decreased slowly, with several oscillations, to reach mag 5 at the beginning of April, when the deep minimum, which is a common feature of the light curves of several slow novae, started. At the beginning of May, the magnitude was about 13, then the light increased again, and on June 15, it was about 7.5 and the phase of smooth decline began (Figure 8-75).

VIII.A. SPECTRAL VARIATIONS DURING OUTBURST

The premaximum spectrum (Abs.I and Em.I) changed from type B to type A during the day of discovery. A second shell (Abs.II and Em.II) was seen on December 23, a day after maximum brightness. Then several shells appeared: III and IV with multilple components; shell V, on January 13; shell VI on January 23; shell VIII, on March 23-25; shell IX, in the second half of March; shell X, on March 20-24; shell XI, in January. These shells are identified by the various systems of lines having the same radial velocities and are subject to different interpretations. For instance, McLaughlin, in his study (1937), identified shells II, III = VII, IV, V, VI, VIII, IX, X, and XI, while in his successive interpretation of 1954, he identified just shells II, III with several components, IV and V.

The expansional velocities range between 300 and 1000 km/s. Shortly before the start of the deep light minimum, the emergence of [FeII] emissions was observed. The same phenomenon was observed in other novae having the same type of light curve. It is evident that the expanding envelope has reached a sufficiently low density for the forbidden lines to appear.

It is interesting to recall that Struve in 1947 expressed the idea that the nebulosity where [Fe II] is formed is not purely gaseous but contains also iron-rich dust particles; Stratton (1945) suggested that the deep minimum in the nova light curves is due to an obscuring cloud formed inside the main outer shell. Now infrared observations have shown that these suggestions were fundamentally correct and that a dust shell is actually formed in moderately slow novae, just coinciding with the dip in the light curve.

Before the deep minimum, the emission bands in DQ Her spectrum started to show two maxima (Figure 8-76). During the deep minimum (from the beginning of April to the end of May), the longward components faded and disappeared, suggesting that the increasing opacity of the shell permitted the observation only of that part of the envelope expanding toward us. At the end of the deep minimum, the longward emission reappeared.

Interactions between different shells seem evident from the observational data. These are described in detail by Beer (1974). Let us consider just one significant example, quoting from Beer:

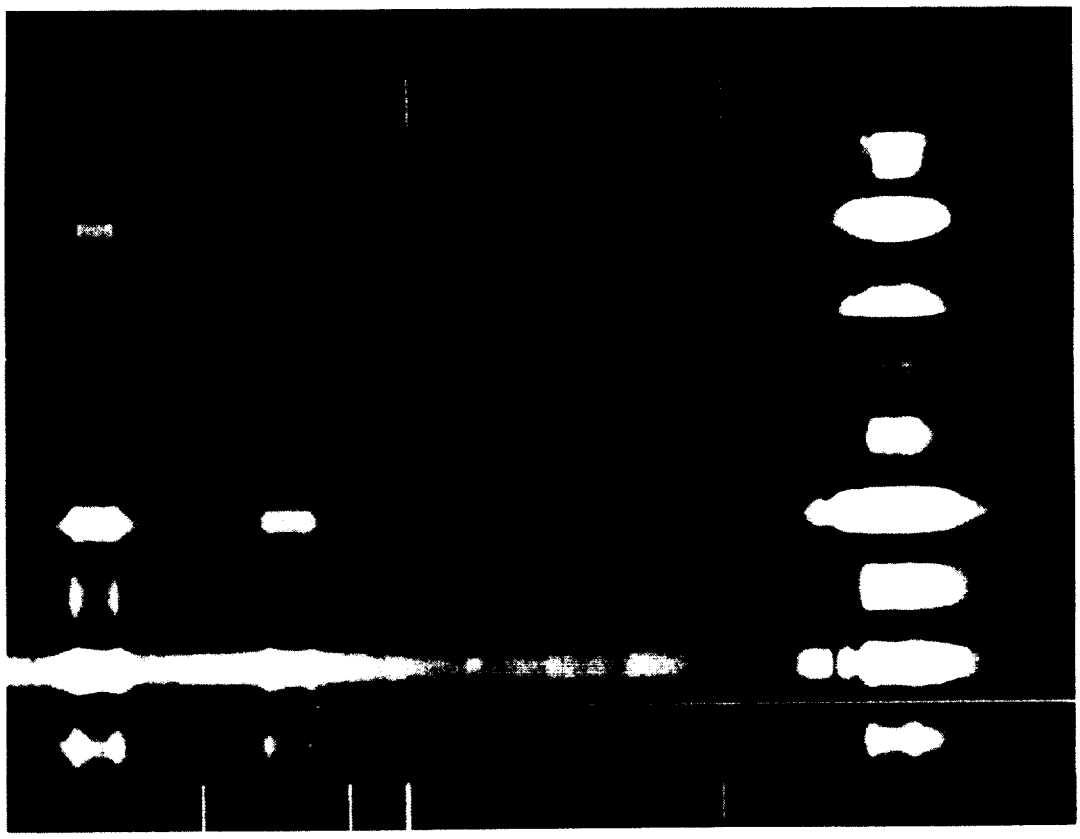

Figure 8-76. DQ Her: the structure of Hα between January 12, 1935 and March 24, 1935 (adapted from Stratton and Manning, 1939).

"With regard to the later shells McLaughlin (1947) pointed out that while the atoms of the shells giving the Orion spectrum were so rarified as to be unlikely to produce any results on the outer shells, the atoms from the diffuse enhanced shells III and IV might overtake the principal shell II before they get too rarified. We might observe an acceleration of the principal shell and possibly the disappearance or a retardation of the later component. McLaughlin (1954, p. 135) has discussed in more detail the problem of shells overtaking each other with special reference to shell III and shell IV overtaking shell II. The view that the particles in the different clouds continue to move outwards at a constant or slightly increasing speed is strongly supported by the presence of separate narrow components in the second half of March...Let us first consider the question on what date shell III should have collided with shell II. McLaughlin gives 1934 December 26 as the date of emergence of shell II. An independent study of early plates (Stratton, 1936, p. 148) suggests December 24. Let us accept December 25. Taking a mean velocity of 317 km/s for 1934 December 25 to 1935, January 15, of 323 km/s for January 15-25, and of 333 km/s for Jamuary 25-29, we find that by January 29 the original particles of shell II would have travelled outwards 9.6 x 10^8 km".

"For shell III McLaughlin gives January 8 as the date of emergence; a study of the Stratton and Manning Atlas (1934) and of the Cambridge plates suggests January 10. Let us accept January 9, the date of a maximum in the light curve. Then with an average velocity of 569 km/s the original atoms of shell III would have travelled 9.7 x 10^8 km by January 29. We may note also that the largest increase of velocity of

shell II occurred between January 26 and 30. It seems reasonable to accept the view that shell III overtook shell II on or a little before January 29. McLaughlin's date for this event is January 23 . In support of January 29 we may add that according to Rottenberg (1952), when an inner shell overtakes an outer shell, the peaks in the emission bands should strengthen relatively to the centres of the bands. Emission maxima in the Fe II bands shortward of H Beta are first detected on January 29 and rapidly strengthen though they are visible in the H and K bands of Ca II a few days earlier, suggestive again of stratification, the Ca II atoms being ahead of the Fe II atoms. We may further note that Absorption III faded out on January 25 and did not reappear until February 3".

"This was probably mainly due to the strengthening of the emission from shell IV: The emission bands widened on both wings during the last few days of January. By this time the leading atoms of shell III and shell IVi were closely intermingled with each other and with shell II. Taking the date of emergence of shell IVi as January 12 and its mean outward velocity as 674 km/s, the date of collision of shells III and IVi becomes January 28. By this date Absorption IVii had become the strongest absorption".

"1935 January 19 (another maximum in the light curve) is McLaughlin's date for the emergence of shell IVii and his mean velocity is 800 km/s. Cambridge plates give January 20 and 779 km/s. Both sets of figures agree in giving February 5 as the date when shell IVii overtakes shell II, by which date absorption IViii had become the strongest component. During the first week of February there was a further increase of velocity of shell II."

"Absorption IViii was measured on Mount Wilson plates as early as January 20, but it was not clearly separated on Cambridge plates until January 28. McLaughlin gives January 24 as the date of emergence and 900 km/s as the mean outward velocity. This gives February 10 as the date on which the initial particles of shell IViii would overtake shell II, a date coinciding with another increase of velocity of shell II. If shell V can be regarded as starting on January 27 with a velocity of 1100 km/s, it would overtake shell II about the same time as shell IViii, thus accentuating the effect on the outward velocity of shell II. By this time, however, the picture is getting very complicated and the conclusions to be drawn from these figures must be regarded with considerable caution".

"Shell VI would not have reached shell II before deep minimum : Absorption VIII was too fitful in appearance and strength to be discussed in connection with collisions; all that can be said is that its shell was outside shell VI late in March, as its absorptions completely wiped out emissions of shell VI. Shell XIi, if it started on February 16, would have overtaken shell II about March 5, and it was in the first week in March that shell II increased again in velocity. Shell XIii which emerged early in March would not have reached shells III and IV by March 18, and its emission might have provided the background for the narrow absorption lines of shells III and IV measured around that date. But this is a hazardous speculation and would require the spectroscopically active region of shell XIii to be close to the star. All that can really be said on the idea of shells overtaking one another is that it is a crude simplification of "what is really a very complicated state of affairs, but that it is not inconsistent with a number of changes during the first three months of the observed history of the nova."

This decription of the spectral evolution of DQ Her gives an idea of how complicated the spectrum of a nova can be and how difficult is its interpretation.

Spectra taken after 1942 show a strong ultraviolet continuum due to the central star and line emission profiles showing double maxima, clearly indicating that they are produced in the expanding optically thin envelope. The double maxima are especially clearly observable for the hydrogen lines and for 4686 He II (Figure 8-77).

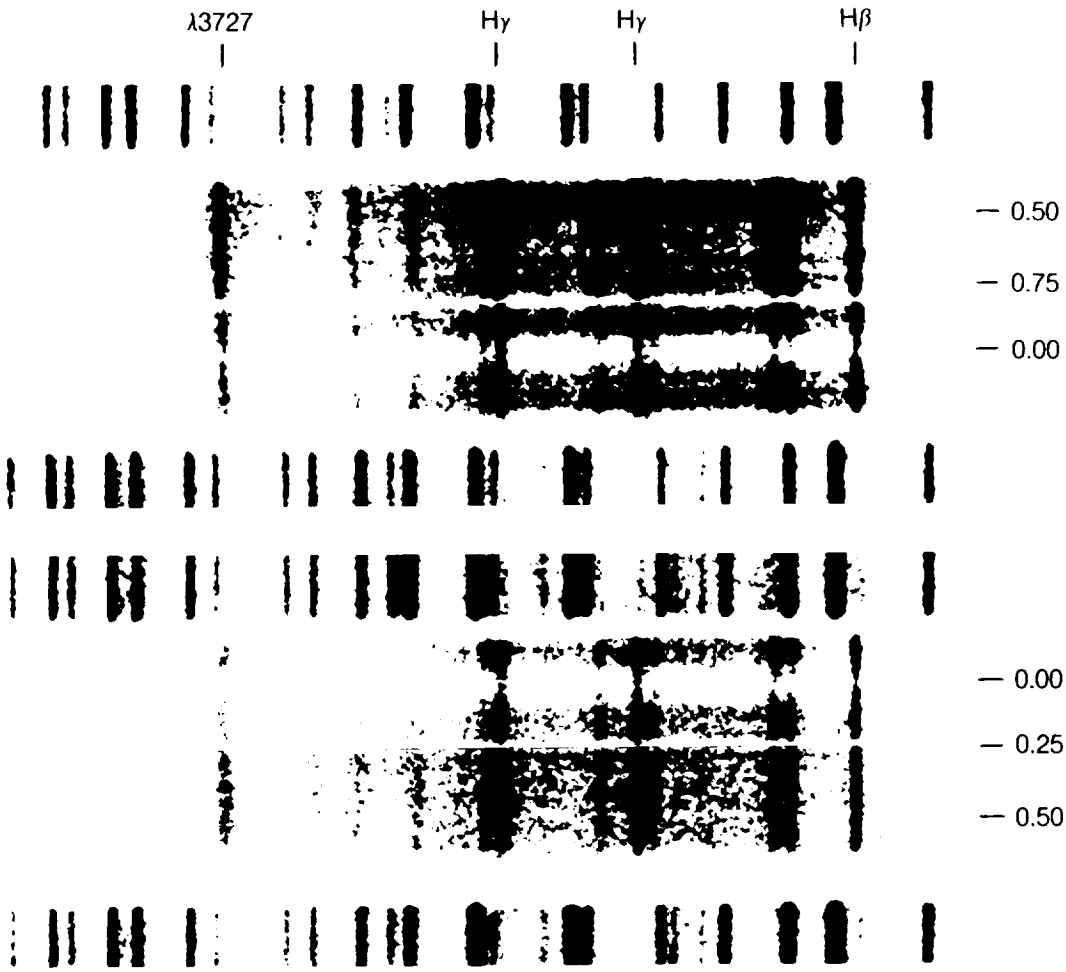

Figure 8-77. The central star of DQ Her in 1955. (from pictures taken by G. Herbig, Lick Observatory).

VIII.B. CHEMICAL COMPOSITION AND EXTENDED ENVELOPE CHARACTERISTICS

Curve of growth analysis of the absorption lines in the pre-maximum spectrum (Abs.I) and in the principal spectrum (Abs.II) were made by Mustel (1956, 1958, 1963), by Mustel and coworkers (1958, 1959, 1965, 1966, 1972), by Gorbatsky (1958, 1962) and by Gorbatsky and Minin (1963). The chemical composition of the absorption-line region at maximum light and at other dates is practically the same and it is compared with the average chemical composition of normal stars. The relative abundance of metals is normal; instead, carbon, nitrogen and oxygen are more than 100 times higher than in normal stars. Although this kind of analysis is very uncertain, because the intensity of the absorption lines may be seriously affected by the presence of the emission components and especially because the pseudophotosphere is very far from the condition of LTE, Pottasch (1967) confirmed this result by measuring the emission forbidden lines of these elements. He gave the average abundances of CNO for five novae including DQ Her, and found an excess by at least a factor of 10.

Direct photographs of DQ Her taken on July 6, 1945, in the light of [OIII] lines of 4959 and 5007 A and in the light of [NII] lines at 6548 and 6584 A, look very different from each other. Both are similar to a planetary nebula, but the image in the light of [OIII] (Figure 8-78) shows an elongated ring surrounding the

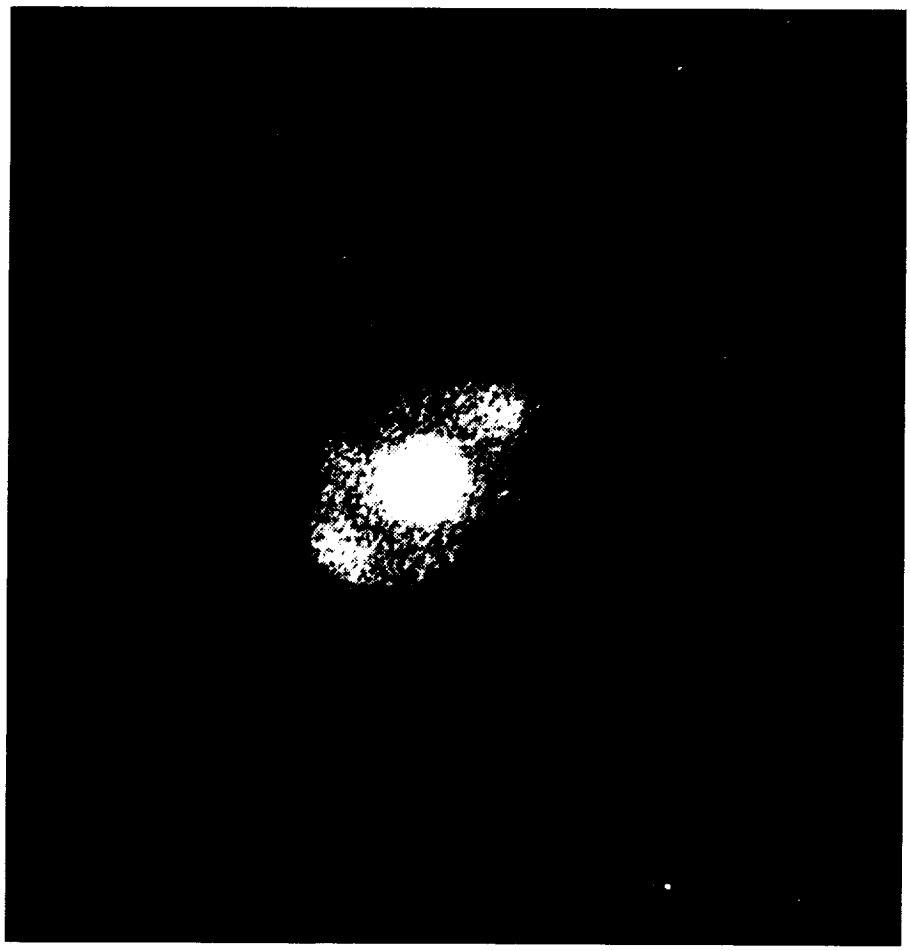

Figure 8-78. The envelope of DQ Her in the light of the [O III] lines at 4959 A and 5007 A, photographed by W. Baade on July 6, 1945 with the M. Wilson 100 inch telescope.

central source, with two slightly stronger blobs in the direction of the major axis; the image in the light of [NII] (Figure 8-79), on the contrary, shows three strong condensations along the minor axis. Spectra taken with different orientations of the slit indicate that each line shows longward and shortward displacements, highest at the center of the slit and least at the two ends of the slit: expansional velocities of the order of 70 km/s and of 300 km/s were found at the border and at the center of the expanding nebula respectively.

Figure 8-80 shows the monochromatic image of the nova shell surrounding DQ Her in the light of H Alpha obtained more than 40 years after outburst. The circles indicate the regions where the spectra given in Figure 8-81 were taken (Williams et al., 1978). These spectra are very similar to those of a typical planetary nebula. However, certain permitted recombination lines of C and N are unusually strong for a typical planetary nebula, while 5007 [OIII] is not present. A strong emission feature at 3646 A is attributed to the Balmer continuum, formed at the very low electron temperature of about 500 K.

Mustel and Boyarchuck (1970) noted that the 4959, 5007 lines of [OIII] weakened already during the 1940s and had practically disappeared by 1950. This weakening was attributed to a drastic decrease of the temperature, as confirmed by the strong Balmer jump observed by Williams et al. (1978) indicating $T_e \simeq 500$ K. The gas in the envelope presented the sharp Balmer jump already in old spectra obtained in 1956-58 (Greenstein and Kraft, 1959). On the other hand, the emissions of C II 4267 and N II 4237 and 4242 indicate an elec-

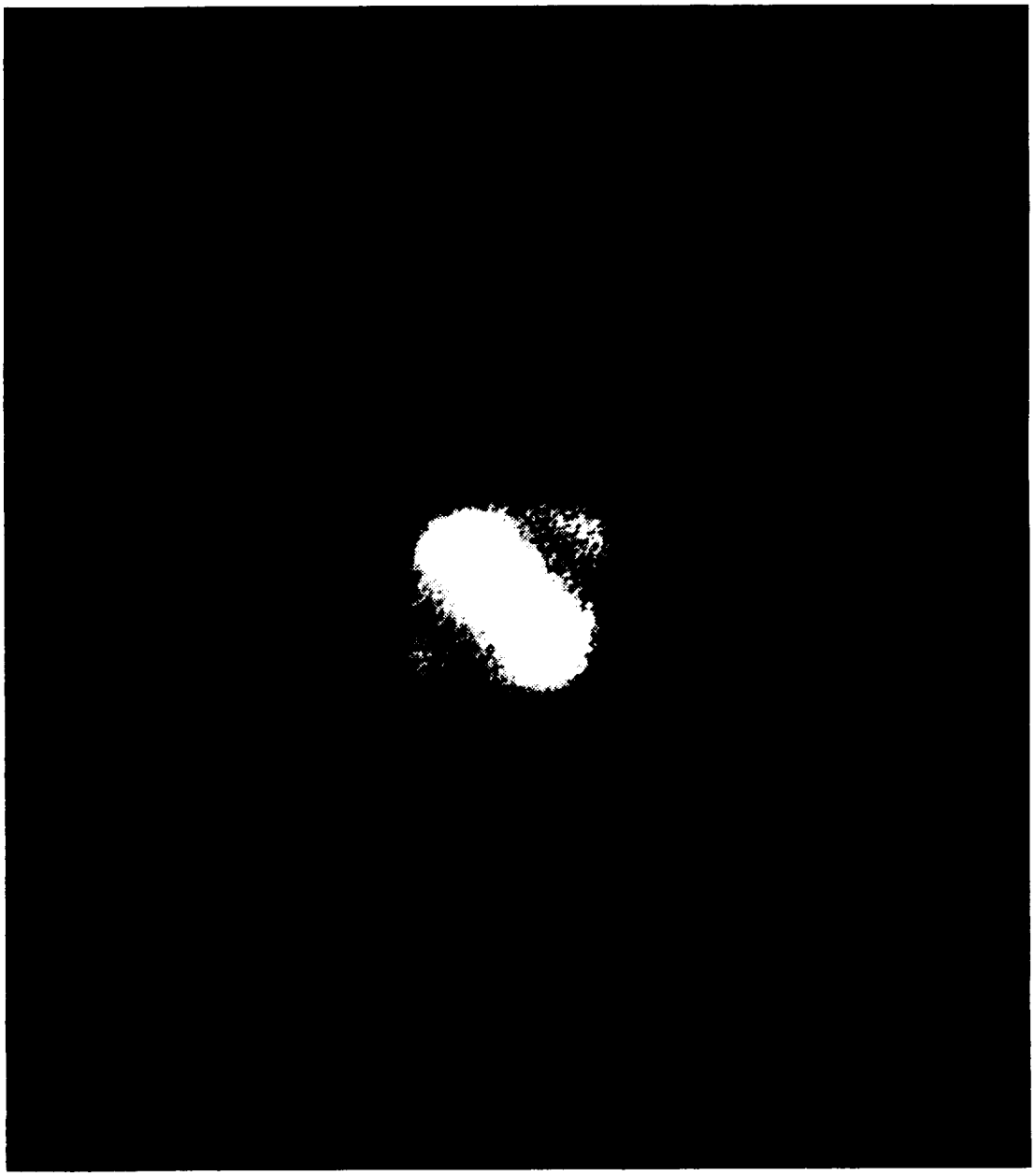

Figure 8-79. Same as Figure 8-78, but in the light of [N II] lines at 6548 and 6584 A.

tron temperature of about 10^4 K, and their strength is about one or two order of magnitude greater than in planetary nebulae.

These data suggest that the shell contains two regions: one that is hot and the other that is cold. The C II and N II permitted lines are pure recombination lines, because they originate in levels high above the ground state (20 eV), which are not directly coupled to the ground state by permitted transitions. Hence, radiative or collisional excitation from the ground line is very unlikely. Since the emission coefficients of the C II and N II lines have about the same temperature and density dependence as the Balmer recombination lines, the relative intensities depend only on the relative abundance of the emitting ions integrated over the emitting region. It is found that $C/H \simeq 10^{-3}$ and $N/H \simeq 10^{-2}$. Hence, C and N appear to be enhanced relatively to H by factors of 20 and 100, respectively, in comparison with the solar values. The He abundance derived by 4471 He I appears to be essentially solar. The determina-

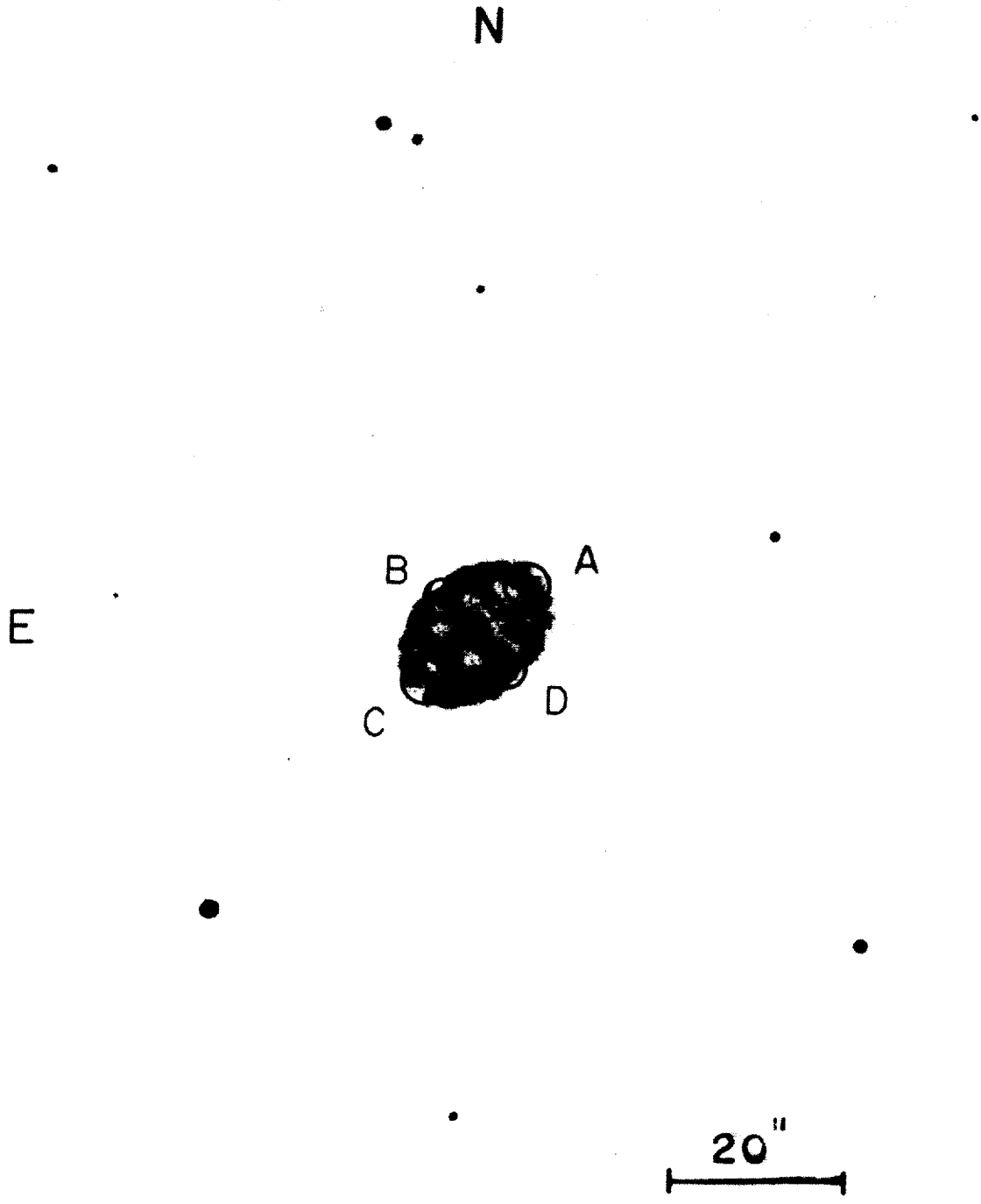

Figure 8-80. Monochromatic photograph of the shell surrounding DQ Her in the light of Hα. The circles indicate the regions where spectra were obtained. (from Williams et al., 1978).

tion of the oxygen abundance is difficult because no recombination lines are observable, but only forbidden lines whose intensity depends strongly on the assumed electron temperature.

Now the problem is to understand why the electron temperature in the shell is so low as indicated by the sharp Balmer jump and by the absence of collisionally excited forbidden lines and why strong (C,N) once-ionized recombina-

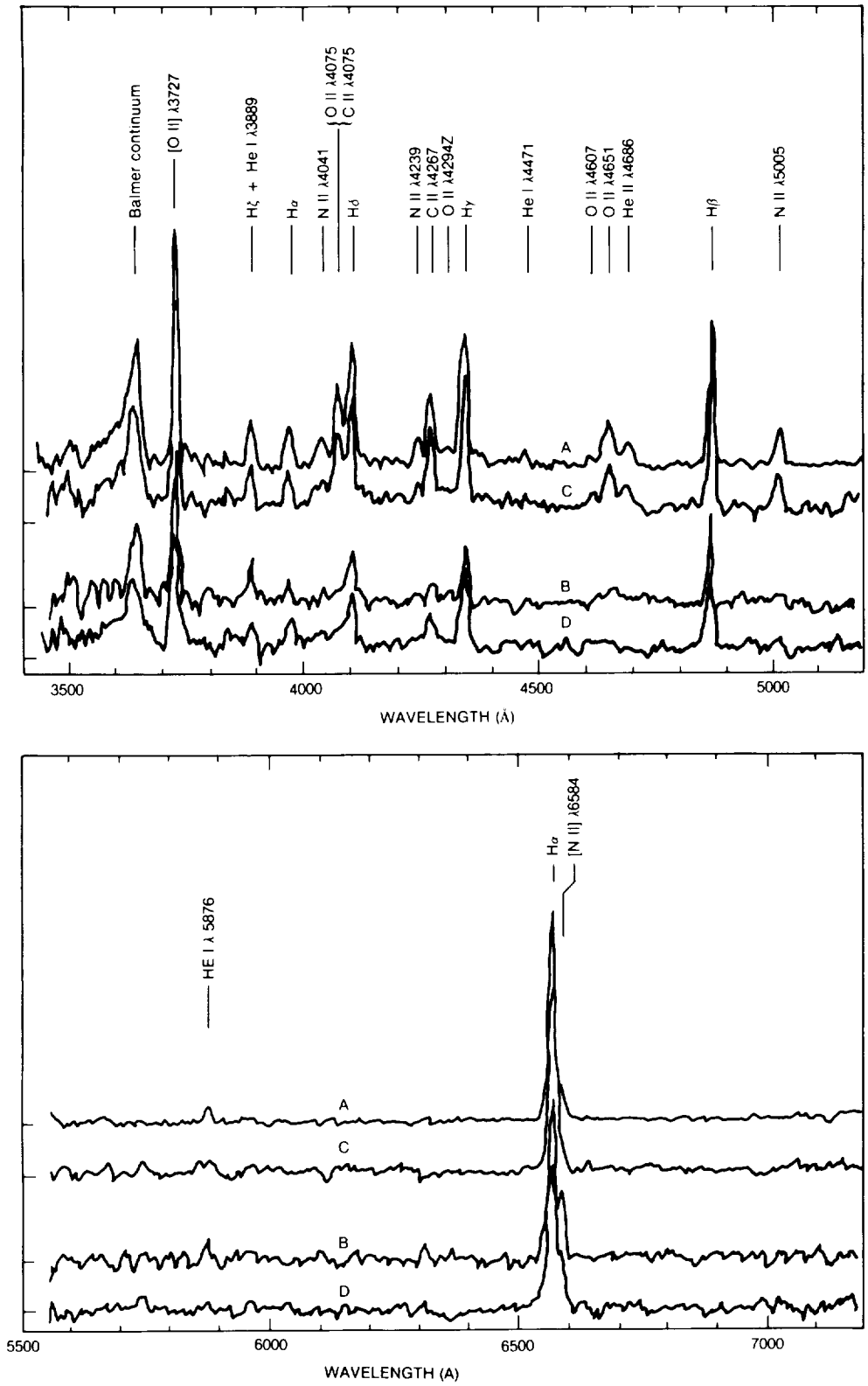

Figure 8-81. a) blue spectral scans of the regions indicated in Figure 8-80; b) red spectral scans of the same four regions. (from Williams et al., 1978).

tion lines are present, which indicate a temperature of at least 10^4.

One can think of various possibilities: the ionization of the gas is a relic of an earlier phase, the gas expands more rapidly then it recombines as suggested by Williams et al. (1978).

Or alternatively, the radiation field emitted by a hot central object (e.g., an X-ray source produced by matter accreting on the white dwarf) ionizes the shell producing very little heating, as suggested by Ferland and Truran (1981). However, both these hypotheses have been discussed by Ferland et al. (1984), who were able to show that both are not acceptable. On the contrary, the large overabundance of heavy elements indicated by the nebular spectrum explains the low temperature and the strength of the recombination lines.

But let us see in more detail the conclusions of this latter work. Ferland et al. have used the infrared, optical, ultraviolet and X-ray observations of the nebula and the central object. The composite spectrum is derived by ground-based observations in the optical and infrared range obtained by Schneider and Greenstein (1979) by ultraviolet observations obtained with IUE and x-ray observations obtained by Cordova et al. (1981b) with EINSTEIN. According to the generally accepted model, the continuum is essentially due to the central object and is shown in Figure 8-82 (corrected for interstellar extinction). The emission line spectrum is due to an accretion disk and to the shell. The UV emissions originating in the shell are spatially resolved on the two-dimensional image obtained through the large aperture of IUE (10" x 20"). The only feature clearly originating in the shell is 1335 C II. The optical emissions and their intensity relative to H Beta are given in Table 2 of Ferland et al. (1984). From these data, the authors show that the recombination time for 4686 He II, which has been always present in the nebula spectrum, is of the order of 20 years (for T_e = 500 K and N_e = 100 cm^{-3}). The low value of T is confirmed also from the ratio of the two lines of C II: I(1335)/ I(4267). For temperatures included

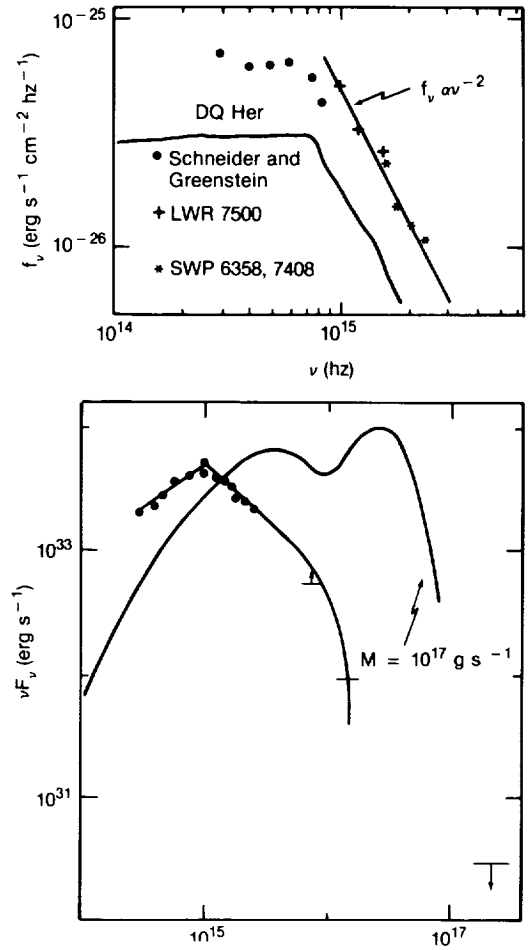

Figure 8-82. a) Composite ultraviolet-infrared continuum. The points are reddening-corrected fluxes and are averages over emission-line free continuum intervals. A line corresponding to a power law with spectral index -2 is drawn for comparison, it fits well the UV continuum. b) The dereddened observed continuum, for E(B-V) = 0.12, corrected for the assumed geometry (a flat disk seen at inclination of 80°) is compared with the theoretical continuum for an accretion disk with mass transfer of 10^{17} g s^{-1}.
(from Ferland et al., 1984).

between 7000 and 15,000 K, this ratio varies only from 56.3 and 59.8 (Storey, 1981; Seaton, 1978b). It becomes much lower for $T<10^3$. Since the observed ratio is 9, the value of $T_e \approx$ 500 K is confirmed. The value of N_e is indicated by the volume of the shell and the H Beta luminosity. The expansion time for the nebula is of the order of 50 years. Hence, the continuous presence of 4686 He II indicates that the gas is being ionized continuously since the epoch of the outburst, contrary to the assumption by Williams et al. (1978).

The observed continuum for the central object (Figure 8-82b) is very different from that expected from an accretion disk and a mass-transfer rate of 10^{17} g s^{-1} (Smak, 1982) and also the following section), and especially the EINSTEIN observations have shown that DQ Her (as well as the other quiescent novae) are not strong X-ray sources. Hence, the model by Ferland and Truran (1981) is not acceptable. Instead, photoionization calculations indicate that for a wide variety of ionizing radiation fields, the nebula will stay at $T < 10^{3}$ K if the heavy elements are overabundant and the density low enough.

Actually Ferland et al. (1984) show that the low density and an enhanced oxygen abundance permit the production of low electron temperature. Infrared fine-structure lines of carbon, nitrogen, and oxygen are very efficient coolants for low-density nebulae. It is shown that at the ionization conditions and chemical composition of the nebula surrounding DQ Her, the IR lines at 88 μm and 52 μm of [O III] can easily cool the gas at 500 K. Table 3 from their paper and Figure 8.83 show the electron temperature which is reached for different oxygen overabundances through these two IR lines. For O/H varying between 10 and 100 times the solar value, the electron temperature varies between 1150 and 180 K. The graph gives the electron temperature versus the density, computed for a given $\dot{M} = 10^{17}$ gs^{-1} and a ratio U of photon density to electron density equal to 10^{-3}. (Here U =Q(H) / $4\pi r^2 Nc$.) Q(H) is the number of ionizing photons emitted by the central object per second, r is the separation between the source and the nebula, (which is of the order of 4×10^{16} cm, as estimated from the angular diameter of the nebula and the distance of the system), and N and c are the density of the gas and the speed of light.

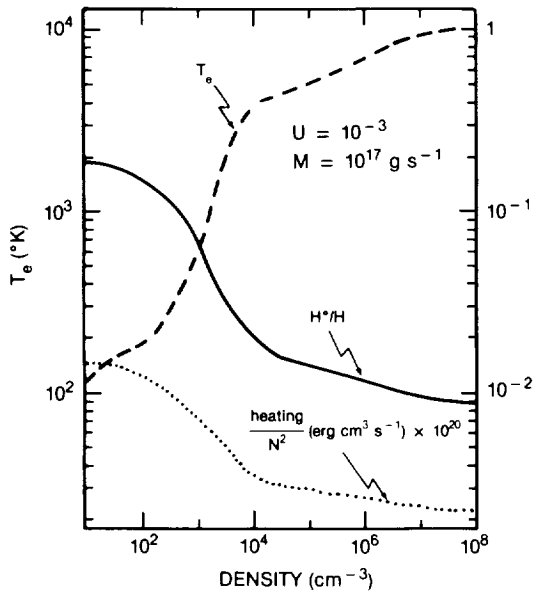

Figure 8-83. Dependence of the electronic temperature on the gas density in the shell. The temperature falls dramatically at N<1000 particles per cc because the infrared fine structure lines become efficient coolants. (adapted from Ferland et al., 1984).

In fact, for a luminosity of the central object of the order of 10^{32} erg/s, and assuming that the ionizing photons correspond to wavelength lower than 3500 A, it follows that L = h v x Q (H), Q (H) = 7×10^{43}, U = 10^{-3}. The observed photoionizing continuum and the observed electron density permit us to predict the intensities of the emission lines and to compare them with the observations (see Tables 2 and 3 of Ferland et al. (1984)). The agreement is satisfactory and gives a positive test of this model. However, the predicted intensities of the 88 μm and 52 μm lines should be revealed by the IRAS observations. Instead, very few of the observed novae show measurable far IR flux.

The hydrogen emission in the envelope has been used by several investigators to derive the mass of the envelope; its value is found to be included between 1.4×10^{28} and 10^{29} g (7×10^{-6} and 5×10^{-5} solar masses). If we estimate the mass fraction of carbon, oxygen, nitrogen, and neon, we find that half of the mass is due to these elements.

VIII.C. DQ HER PARALLAX FROM NEBULAR EXPANSION

Observations of the nebula made by Williams et al. (1978) in 1977 have been used by Ferland (1980) for deriving the distance of the nova from the nebular expansion. The distance derived in 1940, when the size of the nebula was estimated at about 3", gave d = 230 pcs. According to Ferland, this value was probably overestimated, because the value derived about

40 years later was 15", implying a deceleration on the expansion. Such a deceleration due to interaction with the interstellar medium should produce high temperature in the nebula. However, the absence of coronal lines through 1940 rules out high temperatures. Ferland concludes that the size of the nebula was overestimated in 1940. On this assumption, the present size gives a distance of 420 +/- 100pcs, i.e., considerably larger than that previously estimated. This new value of the distance brings the absolute magnitude of DQ Her at maximum light to Mv = -7.1 +/- 0.7 and Mv on the broad plateau at -5.9 +/- 0.7. With this revision of the distance the luminosity at maximum become close to the Eddington limit for one solar mass star.

VIII. D. THE ECLIPSING BINARY DQ HER

In 1954, Walker discovered that the nova is an eclipsing binary of the Algol type with the very short period of 4h39m (Figure 8-84). After this discovery, Ahnert (1960) measured 27 Sonnenberg plates taken in the years 1930-1934 in the field of the prenova, and found that DQ Her was an eclipsing binary with a period of 0.1932084 days, while, according to Walker, after the explosion, the period was 0.19362060. From this value of dP/dt, Ahnert estimates a mass ejection during the eruption of 1.6 x 10^{-3} solar masses, two orders of magnitude larger than that derived by the spectral emissions. However, we remark that if there are both mass loss and mass exchange, as is probably the case, it is impossible to derive them simply from dP/dt. Moreover, Schaefer and Patterson (1983), using the archival plates of Harvard college Observatory, did not confirm the period given by Ahnert for the prenova. The Fourier transform of 50 prenova observations does not have any significant peaks. According to them, this is because there are too few observations with too long exposures to detect the eclipse. The same authors were able to derive the mass of the ejecta for another nova, BT Mon, by comparing its orbital period before (0.3338010 d) and after (0.3338141 d) erup-

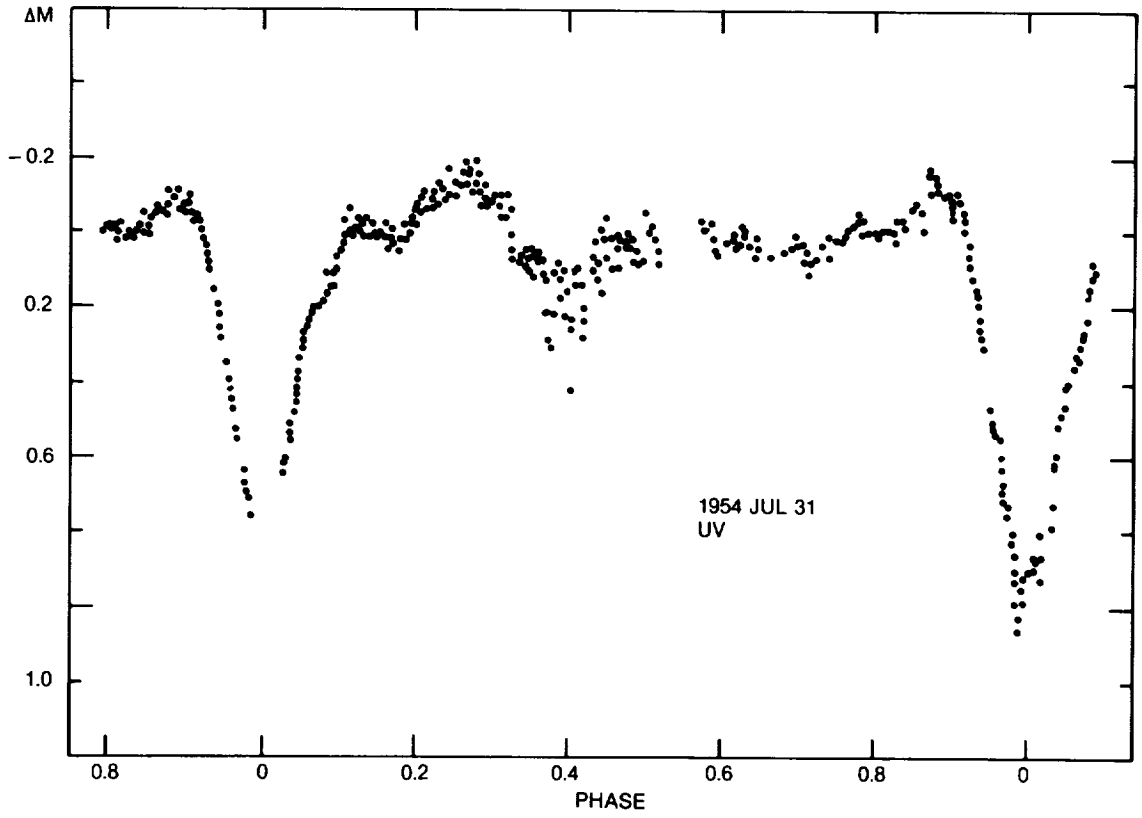

Figure 8-84. Photometric observations of DQ Her (from Walker, 1956).

tion. They found a reasonable value, 3 x 10^{-5} solar masses. However, the variation of the period depends also on the mass lost from the system and not only from mass transfer. Hence, these determinations are not very reliable.

According to the Ritter catalog (1987), the masses of the two components are 0.62 +/- 0.09 for the hot primary and 0.44 +/- 0.02 for the secondary.

Spectra of the old nova obtained by Herbig (see Figure 8.77) in 1955 show that the permitted lines of C II, C III, NII, and He II and the continuum are greatly weakened during primary eclipse, while the Balmer lines H Alpha, H Beta, H Gamma, and the forbidden lines of [OII] and [OIII] do not change in strength and, therefore, are formed in an extended envelope or in an expanding gas unaffected by the eclipse.

The variation of the emission lines H Beta, H Gamma, and 4686 He II during eclipse has been studied by Young and Schneider (1980), who took spectra with an exposure time of 300 seconds at phases included between 0.80 and 0.15 P. The radial velocity curve given by 4686 He II presents the classical rotation disturbance: the velocity jumps to +400 km/s before eclipse, when only part of the eclipsed body (which can be an accretion disk) that is rotating outward from us is not yet eclipsed, and to more than -200 km/s after the eclipse, when the part of the eclipsed body rotating toward us is already out of eclipse. The Balmer lines are eclipsed slightly before the He II lines, and go out of eclipse slightly later, this fact suggesting that they are formed farther out in the disk.

The UV spectrum of DQ Her has been observed with IUE at various phases. In contrast to other old novae, it is flat, $F_{\lambda} \propto \lambda^{0}$.

This flat continuum may indicate that, because of the high inclination of the system (according to Ritter, 1987, i = 70° +/-17°), we are observing the outer and cooler parts of the disk.

The UV line spectrum shows strong emissions of N V and C IV and fainter emissions of He II and Si IV. All these features vary with the orbital phase, being all fainter at phase zero. He II practically disappears during the eclipse.

We recall that a peculiarity of the photometric behavior of DQ Her is the presence of coherent oscillations with a 71-second period. These are low-amplitude sinusoidal variations remaining coherent for several years. The reciprocal of the period variation $(\dot{P})^{-1} = 10^{12}$ suggests that we are dealing with the rotation of a solid body, e.g., the white dwarf. Now a peculiar behavior of these oscillations is shown during the eclipse: at eclipse ingress (phase 0.91), the oscillations begin to come earlier and earlier, until at mid eclipse, they jump from 90° early to 90° late, and then gradually come back to the phase they had originally when the eclipse ends (phase 1.08). Petterson (1979, 1980) proposes the following model to explain this behavior: He suggests that the oscillating light is not coming directly from the white dwarf, but the illuminating beam on the white dwarf surface is reflected by the accretion disk. This is because the phase shift has the same duration of the eclipse itself. Moreover, the variation of the phase shift can be explained by assuming that the reflecting point is located in the backside of the disk. By assuming different inclinations of the orbital plane, the phase shift and the oscillation amplitude vary (see also Chapter 4. Section III.F.2).

IX. THE OLD SLOW NOVA T AUR 1891

(written by Hack)

T Aur is the oldest galactic nova for which a complete record of the outburst is available and which was observed by photographic spectroscopy (see Payne-Gaposchkin, 1957, pp. 93-97, for complete references). The visual magnitude range is $V_{max} = 4.1$ and $V_{min} = 15.8$; the absolute magnitude at maximum-derived from the nebular expansion parallax- is -4.2 or -5.7, if we assume the expansion velocity equal to 500 or to 1000 km/s^{-1} (i.e., velocities included between those oberved for the more recent observed novae; in fact, in 1891 no high-resolution spectra were obtained, permitting us to

measure the expansional radial velocity), and neglecting the interstellar extinction.

T Aur is very similar to DQ Her, concerning both the light curve and the spectroscopic appearance and spectral variations. It was this strict similarity which suggested to Walker (1963) to search whether it was also an eclipsing binary like DQ Her. He was successful in his expectations and found that T Aur is an eclipsing binary with period of 0.2043786 days. The eclipsing light curve is in many ways reminiscent of dwarf nova light curves. Its main characteristics are:

1) short period,

2) Algol type,

3) absence of detectable secondary eclipse,

4) asymmetry of the rising branch of the eclipsing curve,

5) occurrence of a bright shoulder before and somtimes after eclipse,

6) occasional presence of a depression in the light curve at 0.7 P,

7) occurence of intrinsic variations outside of eclipse (Figure 8-85).

Moreover, the colors B-V = +0.28 and U-B = -0.64 place it in the same position as dwarf novae in the two-color diagram and correspond to the colors of a composite object sdO+dK.

The distorted light curve does not permit one to find any geometrical solution of the kind obtained for detached binaries, but only indicates that both components must be small and dense. Differently from DQ Her, T Aur does not show any coherent oscillations, but just rapid flickering.

The spectrum of the nova at minimum was described by Humason (1938) as dominated by weak emission lines of hydrogen and He II and a continuum well extended in the ultraviolet.

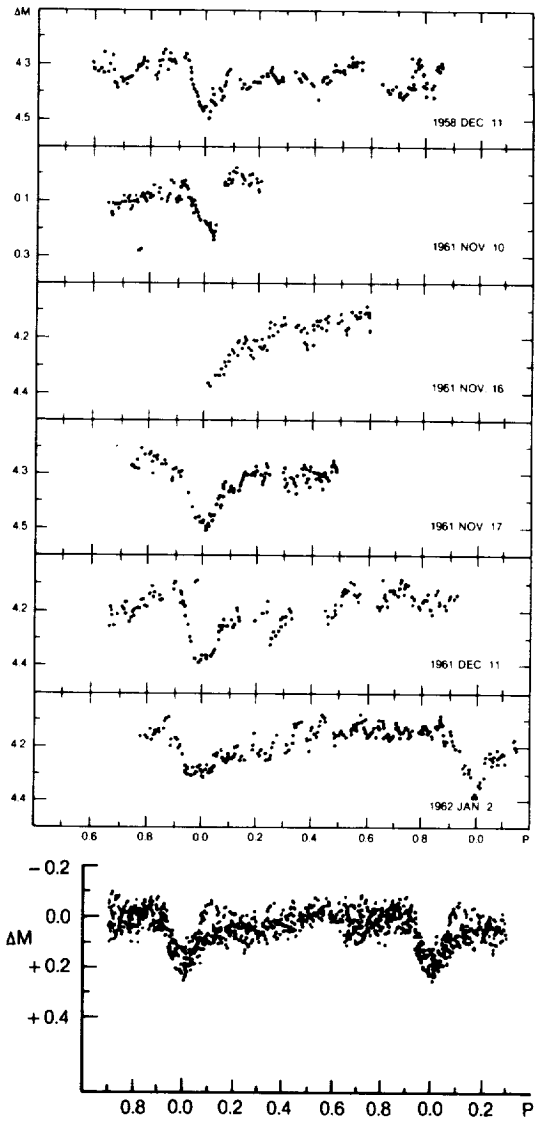

Figure 8-85. a) Light curves of T Aur; b) Composite light curve. Zero point of the magnitude scale is the average brightness of the system outside the eclipse. The phases are computed from the elements derived by Walker (1963).
(from Walker, 1963).

No other detailed spectroscopic observations were made since the recent ones by Bianchini (1980). Study of the variations of the 4686 He profile along the 4h54m period shows that the emission lines reach a maximum at phase 0.85, when the light curve presents, a hump, and a minimum at phase 0.53 (Figures 8-86 a,b). Phases 0.0 is at the epoch of the Algol-type minimum. This behavior indicates the presence of a hot spot observable in its full size at phase 0.85 in the light of He II. A broad absorption

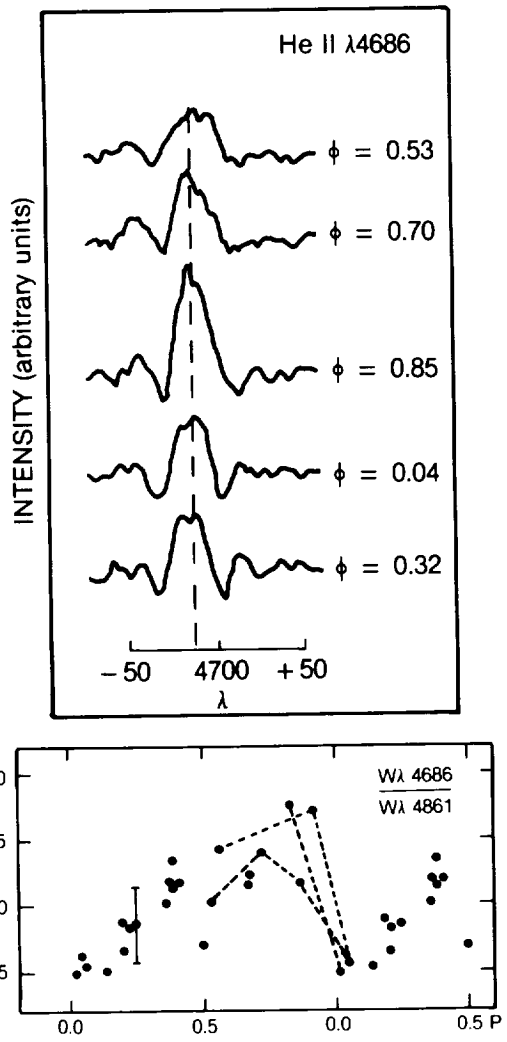

Figure 8-86. a) He II 4686 emission line profiles at selected orbital phases. b) Plot of the ratio W(4686 He II)/W(Hβ) versus the orbital phase. Observations made during the same orbital phase are connected by the dashed lines.
(from Bianchini, 1980).

line is detectable, underlying the emission, and suggests the presence of an optically thick body (stellar atmosphere or accretion disk). This absorption line is more evident around phase 0.00 (Figure 8-86a). Low-resolution (R = 6A) ultraviolet spectra have been obtained with IUE (SWP 21454 and 21456, LWP 2268) and combined together (Figure 8-87). The exposures needed to obtain a measurable signal are too long to detect spectral variations related to the phase.

The S/N is low, but it is evident that the flux increases toward shorter wavelengths, and the energy distribution is very different from the flat spectrum of DQ Her, in spite of the other many similarities of the two objects.

An interesting spectrophotometric study of the faint nebula surrounding T Aur has been made by Gallagher et al . (1980). The nebula is faint and has an ellipsoidal ring-like shape with a major axis of 26" (see Figure 6-68). This nebula is very similar to that produced by DQ Her. In both nebular spectra, recombination lines dominate over forbidden lines: The spectrum of T Aur presents recombination lines of once-ionized helium, twice-ionized nitrogen and oxygen, while forbidden lines are faint (Figure 8-88).

After correction for interstellar extinction, the abundance ratio of helium to hydrogen can be evaluated from the ratio I (5876)/ I(4861) according to the relation

$$\frac{N(He^+)}{N(H^+)} = \frac{\alpha_{H\beta}(T_e)\, h\nu_{4861}\, I(\lambda 5876)}{\alpha_{5876}(T_e)\, h\nu_{5876}\, I(H\beta)}$$

where the α are the effective recombination-line coefficients at electron temperature T_e (Osterbrock, 1974). Helium is found to be overabundant by a factor of 2 or 3, like most slow novae. Also, nitrogen and oxygen are found overabundant by factors of 60 and 25 (by number), respectively, over cosmic abundance.

Like DQ Her, T Aur also shows regions of the nebula where the electron temperature is low, but not so extremely low as in the case of DQ Her. From the ratio 4651 O II/5007 [O III], a value of T_e lower than 3000 K is derived. The nebula surrounding T Aur has a substantially lower content of heavy elements than that around DQ Her, in spite of the great similarity of the two novae, which is reflected not only in their light curve, but also in the manner in which their ejecta have evolved.

The evolution of the nebulae of old novae presents several problems. For instance, T Aur and DQ Her extend their similarities in the outburst to the similarities in how their nebulae

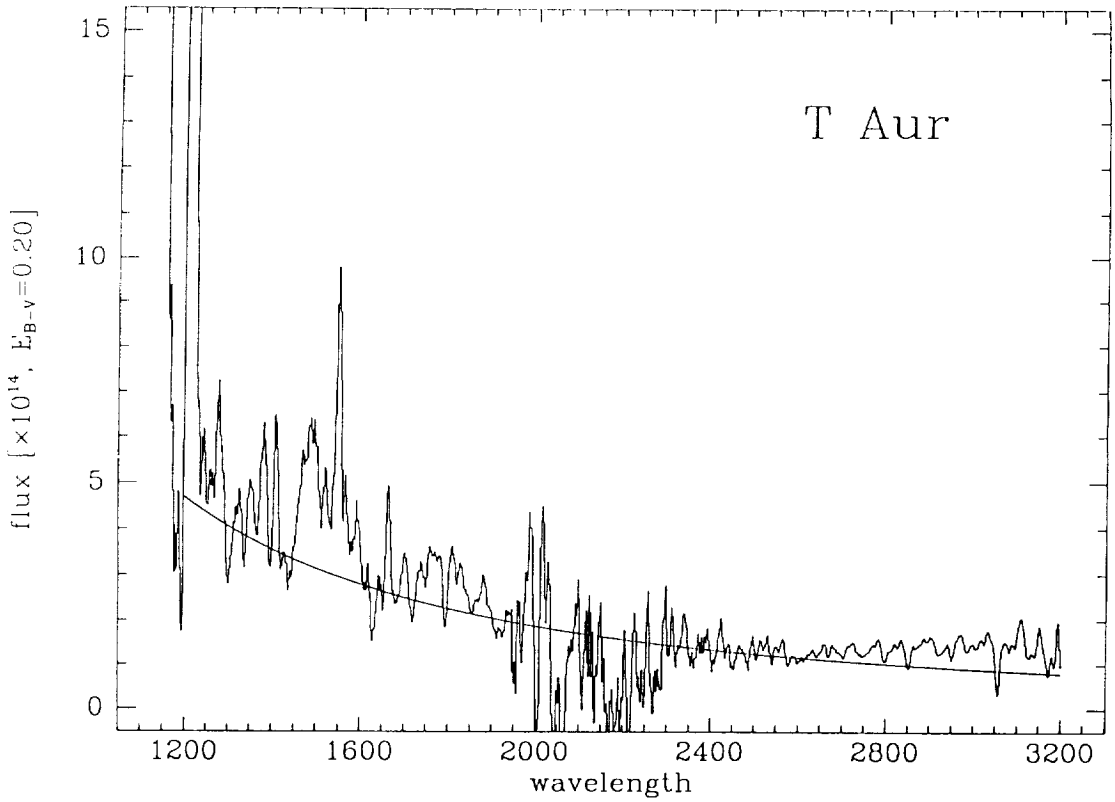

Figure 8-87. The low resolution IUE spectrum of T Aur, obtained combining the short wave spectra SWP 21454 at phase 0.92 and SWP 21456 at phase 0.74 and the long wave spectrum LWP 2268 at phase 0.24. Although the noise is strong, and the region 1950-2500 is completely drowned in the noise, it is evident that the flux increases from 1600 A toward shorter wavelengths.
(from the IUE data bank).

evolved. RR Pic, on the other hand, is an older nebula than DQ Her, but presents higher T_e and high ionization. Therefore, it is very important to follow the development of nebulae of recent well-observed novae.

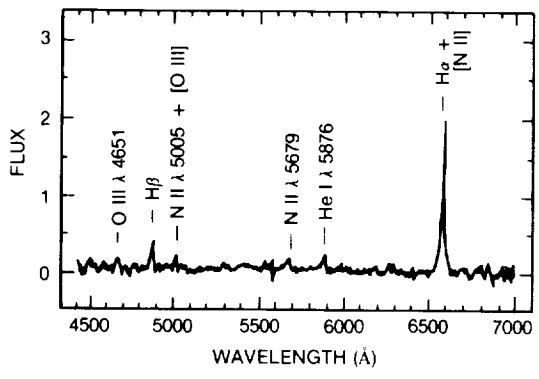

Figure 8-88. The optical spectrum of T Aur obtained by summing several spectral scans. The flux units are 10^{-16} ergs cm^{-2} s^{-1} A^{-1}. (from Gallagher et al., 1980)

X. RR PIC

(written by Selvelli)

X.A. THE HISTORICAL OUTBURST

The outburst of RR Pic was first noticed by R. Watson, on May 25, 1925, when the star reached magnitude 2.4, while the maximum (m= 1.0 - 1.2) was reached on June 9, 1925. The light curve was characteristic of a "slow" nova with t_3 ~ 150 (182) days. The light curve has been studied by several authors: e.g., Spencer Jones (1931), Campbell (1929) and Payne-Gaposchkin (1957). Characteristic were the large oscillations during the early decline, with several maxima of nearly equal magnitude (Figure 8-89). It is notable that the preoutburst magnitude was estimated as 12.8 (12.7, 13.3) and that the present magnitude is 12.3 (12.1). Sixty years after outburst, the star has not yet returned to its preoutburst magnitude. This

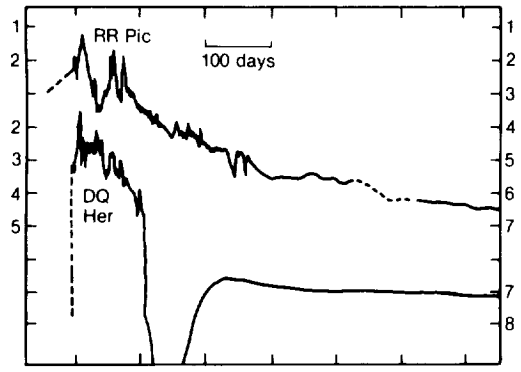

Figure 8-89. The light curve of the slow nova RR Pic, and, for comparison, the light curve of the other slow nova DQ Her. The typical dip in the light curve, characteristics of several slow novae, is missing in RR Pic, as well as in the extremely slow nova HR Del (see next section 8-11).
(from McLaughlin 1960).

behavior seems in contrast with the general conclusion by Robinson (1975) that novae before and after outburst are characterized by the same m_v value.

The spectral type of the nova at the time of the first spectroscopic observations was estimated as F2, while at maximum it was F8. This behavior reflects that of slow novae, which near maximum display a later spectral class than fast novae (F2-F8, instead of A0-A5).

The premaximum and maximum spectra have shown outflow velocities of the order of -100 km s^{-1}, while velocities of up to -400 km s^{-1} have been observed at the end of the evolution of the principal spectrum during the first 10 months after outburst.

The spectral behavior after maximum has shown a very complex behavior and has been

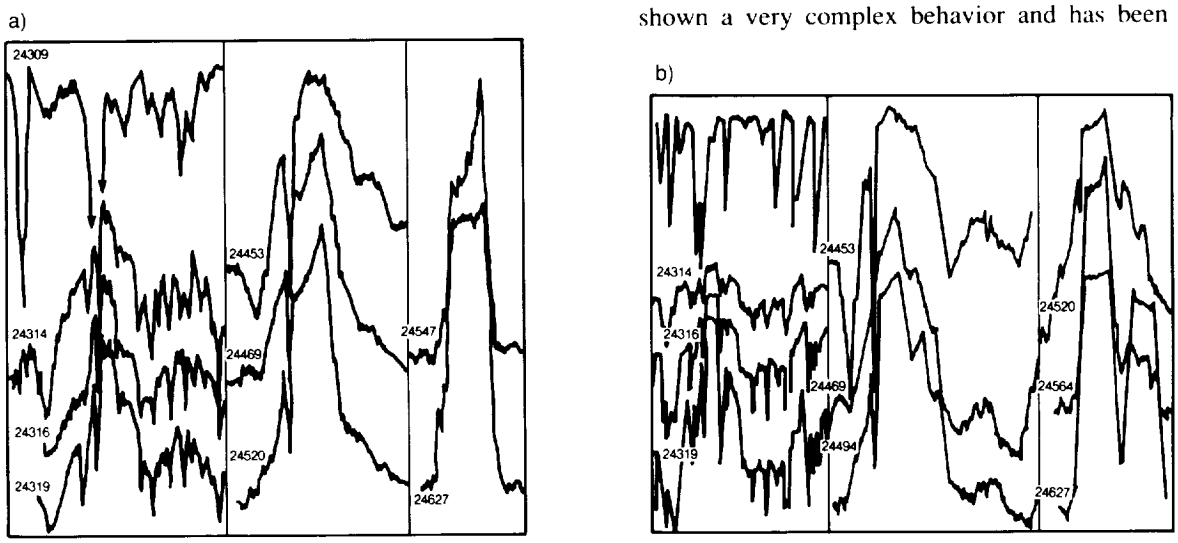

Figure 8-90. a) RR Pictoris, changes in the spectrum near Hd 4101 over about 320 days; tracings from Lick spectra, not reduced to intensities. Left strip, top to bottom: JD 24309 (date of maximum; for clarity the deep center of the hydrogen line is omitted), 24314, 24316, 24319; center strip: JD 24453, 24469, 24520; right strip: JD 24541, 24627. The development is similar to that shown in Figure 4, but the later spectra are less complicated by emissions other than that of hydrogen. Note that all the dates on the two figures are not identical. Violet is to the left.
(from C.P. Gaposchkin in HP 51 / 752) 1958.

b) RR Pictoris, changes in the spectrum near Hg 4340 over about 320 days; tracings from Lick spectra, not reduced to intensities. Left strip, top to bottom: JD 24309 (date of maximum), 24314, 24316, 24319; middlestrip: JD 24453, 24469, 24474; right string JD 24520, 24564, 24627. The first tracing shows only the pre-maximum spectrum. In the subsequent tracings, the principal spectrum emerges and strengthens to the violet of the pre-maximum spectrum, which gradually fades. In the second strip the principal spectrum, and the intense, more highly-displaced spectra of hydrogen dominate the absorptions, and the bright redward edge, associated principally with the highly-displayed spectrum, becomes conspicuous. By JD 24469 the bright line has developed a distinctive structure, with a strong redward edge; the violetward and redward edges of the Fe II line at 14351 have also become prominent. In the third strip, the hydrogen absorptions are diminishing in intensity, the bright lines displacing more structure. On JD 24564 the absorptions are almost gone, and the violetward and redward edges of the [O III] line 14363 are superimposed on those of the Fe II line. On JD 24627, only the lines of hydrogen and [O III] are discernible, each with complex structure. Note that the two last tracings cross. Violet is to the left.

described in great detail by H. Spencer Jones (1931), by W.H. Right (1925), and by C. Payne-Gaposchkin (1957). Outflow velocities were lower than in other novae, and the Orion spectrum showed absorption displacements of up to -1500 km s^{-1}. A peculiarity of RR Pic has been the extreme weakness of the N III λ4100 lines during the Orion stage. These lines are usually associated with the "nitrogen flaring," the secondary fluorescence produced after the excitation of the 3d P° level of O III by He II Lyα.

Another distinction between fast and slow novae during the Orion stage is the presence of numerous [FeII] emissions in slow novae and their weakness or absence in fast novae (McLaughlin, 1960, p.585). It is also remarkable that RR Pic, during the nebular stage, has shown unusually weak lines of [O III] λ4957 and 5007.

The nebula surrounding RR Pic has shown an expansion rate of 0.18 arc sec yr^{-1}. The fact that the nebula of RR Pic was not strictly spherically symmetric was reported by Payne-Gaposchkin (1957). In a direct photography of the remnant, taken by Duerbeck and Seitter (1979) at the prime focus of the ESO 3.6 m. telescope, the ex-nova is surrounded by a structured nebulosity; an equatorial ring(s) and double "polar caps" or "knots" are clearly evident on opposite sides of the remnant, in a structure which somehow resembles that surrounding the slow nova DQ Her (see Figure 6-69).

Williams and Gallagher (1979) have studied the nebula surrounding RR Pic using the Cerro Tololo Vidicon spectrometer. The filaments have spectra very similar to those of high excitation planetary nebulae, and show also prominent [Fe V] emissions. The source of excitation of the nebula is in the UV radiation field of the hot component of the system (Figure 8-91; see also Figure 6-70).

Photoionization models suggest temperatures of the order of 2.5 x 10^5 K and L(Star) ~ 4.4 x 10^{34} erg. s^{-1}. An enhancement of Helium

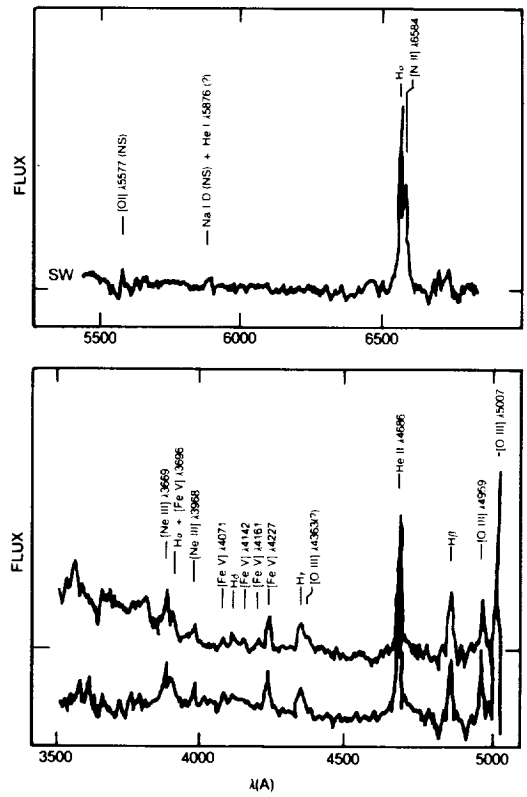

Figure 8-91. Spectral scans of the nebular condensations to the NE and SW of RR Pic. The zero flux levels of the scans are indicated on the ordinate axis. (from Williams and Gallagher, 1979).

by at least a factor of two over the solar abundances is required to explain the He II λ4686 emissions flux.

Moreover, the fact that the low-ionization line [N II] λ6584 Å is seen with moderate strength indicates overabundances of nitrogen by a factor of at least 10, while oxygen is probably underabundant.

The dimensions of the nebula are presently 18" x 23".

X.B. RR PIC IN QUIESCENCE: OF HUMPS AND DIPS IN THE LIGHT CURVE

The first photoelectric observations of RR Pic were made by Van Houten (1966), who found a light curve with a period of approximately 3.5 hours and suggested the presence of an eclipse. This period was confirmed by the observations of Mumford (1971). Vogt (1975)

made an extensive set of observations with the purpose of determining a more accurate period and confirming the presence of eclipse. The determination of the photometric period by Vogt was made difficult by the near absence of features repeating at equal phases. The light curve was characterized by a broad hump with amplitude 0.3 magnitudes that lasted more than half period. The low amplitude and the singular shape of this hump made difficult its use for the determination of the period. Fortunately, the hump was found to always end in a sudden dip, near minimum brightness; this feature was used to determine the period:

JD (MAX) =2 438 815 379 + 0.1450255

φ= 0 corresponds to the main brightness maximum.

The (B-V) and (U-B) curves show that the bluest parts of the curves are reached near phase 0.0, the reddest, near phase = 0.5 (Figure 8-92).

A drop near $\varphi = 0.4$ seems to be always present, also in the V curve. Since this behavior repeated fairly well from cycle to cycle, it was associated by Vogt to orbital motion.

It is remarkable for what follows that in

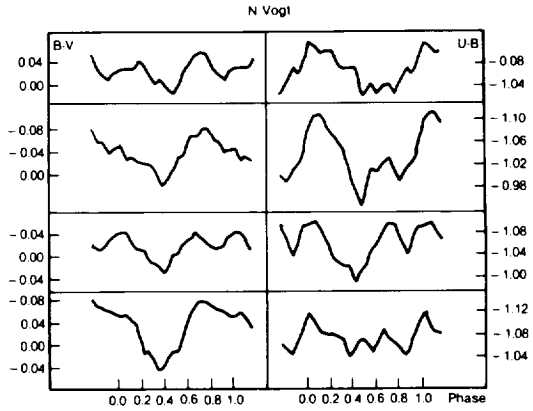

Figure 8-92. Mean colors as a function of phase during December 1972.
(from Vogt, 1975).

Vogt observation, a blue peak, especially pronounced in (B-V), is present near phase 0.75 (Figure 8-93). Vogt also found that, generally, a flickering was superimposed on the light curve with a typical time-scale of 5-15 min and amplitude of 0.05 ÷ 0.10 magnitudes. Also time-resolved observations by Warner (1981) have revealed the presence of occasional multi-periodic rapid oscillations, which were present in about one-quarter of the observing runs. The periodogram analysis showed periods in the range of 20-40 s, with a more persistent one with P = 32 s. Schoembs and Stolz (1981) have

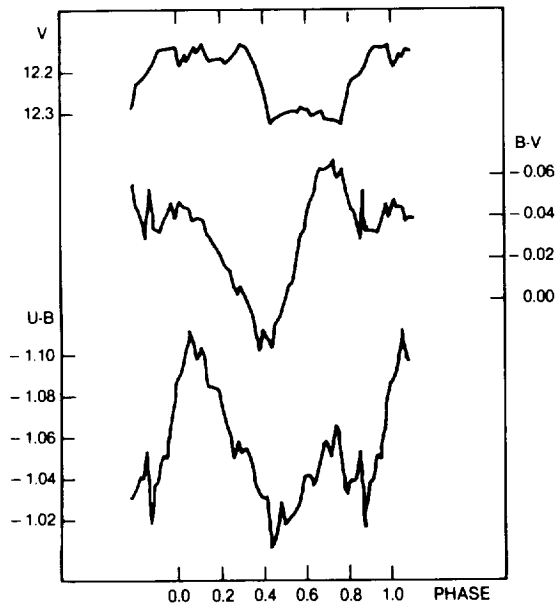

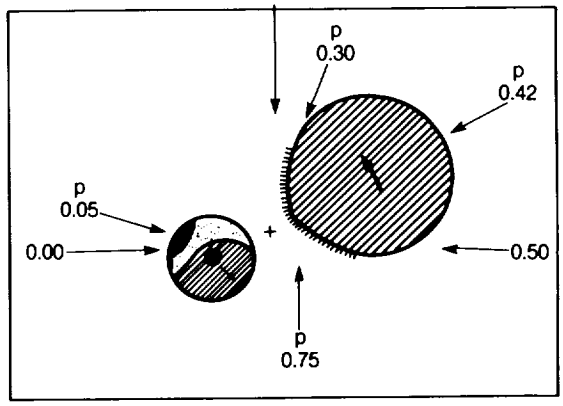

Figure 8-93. Left: Mean light curves and colors versus phase for all observations of Dec. 1972 averaged in 0.02 P intervals. Right: the phases are indicated in this schematic model for RR Pic.
(from Vogt 1975).

confirmed the presence of such rapid oscillation with P=32 s.

New UBV measurements by Haefner and Metz (1982) have confirmed the period of Vogt and have also indicated the high stability of the period, with $\frac{dP}{P} = 1.4 \times 10^{-11}$.

However, they found a quite different behavior in the light curve with a "w" shape as a characteristic feature of *all* light curves (Figure 8-94), and much more pronounced than in Vogt's observations. Different curves behave similarly and show minima near phase 0.43 and phase 0.74 (deeper). This behavior is in contrast with that described by Vogt who reported

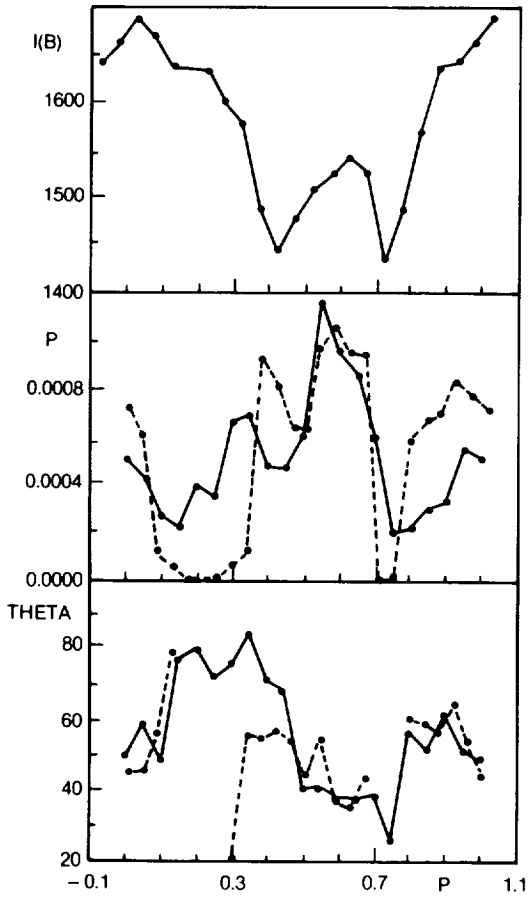

Figure 8-94. Top:B intensity derived by averaging the B light curve within a phase interval of 0.05 and represented by arbitrary count numbers. Middle and bottom: the hot spot polarization percentage and angle, respectively. Solid line: derived from the observations, dashed line: numerical approximation (θ is indefinite for phase 0.0P).
(from Haefner and Metz, 1982).

the presence of a blue peak near φ=0.75. Spectroscopic observations by Wyckhoff and Wehinger (1977) have revealed the presence of radial-velocity variations in the He II λ4686 emission. These variations are nearly sinusoidal with 2K ~120 km s^{-1}. The minimum in this spectroscopic curve is quite close to φ = 0, the principal maximum of Vogt's observations. Combining their photometric results with these radial-velocity observations, Haefner and Metz (1982) have suggested that, since φ = 0.75 corresponds to the orbital condition in which the red component is in front of the white dwarf, the minima they observed near φ= 0.74 were caused by occultations (eclipses) of the hot component (white dwarf, accretion disk).

This suggestion was supported by the fact that optical spectra showed that the Hβ emission was weaker near φ =0.7. (But He II λ4686 remained constant.)

The suggestion reported above is in contrast, however, with the indications of Vogt (1975) who found the presence of a blue peak near φ = 0.75.

New observations by Kubiak (1984) confirmed the shape of the V curve found by Vogt. The U curve, however, suggested the presence of an eclipse beginning near φ = 0.8 and lasting until φ= 0.96. In the V and B bands, the eclipse was less evident. The system appeared bluest at the beginning of the "eclipse."

Kubiak claimed the presence of coherent brightness modulation in all bands with a period of about 15 min. A study by Haefner and Schoembs (1985) of a large amount of photometric data has not confirmed the permanent existence of this period. They suggested that the 15-min period found by Kubiak was attributable to transient phenomena in the disk.

The new observations by Warner (1986a) have not confirmed the periodicity either. Power spectra of its extensive observations have not detected the periodicities found by Kubiak, nor the presence of any other period larger than 1 min (except for the orbital one).

Probably most of the contradictory indications reported above are attributable to real intrinsic changes with time in the photometric behavior. Warner (1986a) has also recently pointed out that in the last years, the variations in the light curve have had a smaller range and that more evident flickering activity has been present (see Figure 6-4). A comparison of these curves clearly indicates that from 1975 to 1984 there has been a reduction both in the amplitude and in the phase interval of the hump. This has coincided with a decline in the mean brightness of the system.

RR Pic is currently at m_v ~12.3 and is still declining in luminosity.

The light curve in recent observations (Warner 1986a) is characterized by repetitive but singular "eclipse-like" features superimposed on a highly variable background.. The minimum near φ~0.42 reported by Haefner and Metz (1982) is now scarcely evident; whereas, that near φ~0.74 is the dominant feature. The interpretation of this complex behavior is not straightforward and unequivocal. The origin of the hump, its progressive decay, the reality of the interpretations of the dips (minima) as eclipses needs further investigations.

X.C. THE UV BEHAVIOR OF RR PIC

UV observations of RR Pic can set some constraints on the physical parameters and the location of the region where the (hot) radiation emitted by the system is produced.

Optical observations by Vogt (1976) showed that the ex-nova had a blue continuum with He II 4686 as the strongest emission line, with W ~ 8Å.

Other (fainter) emissions are the hydrogen Balmer lines, the Pickering series of He II, and the CIII 4650 line. These features are typical signatures of a high-temperature object.

The first UV observations of RR Pic were made by Gallagher and Holm (1974) using the 8-inch photometric telescope of the OAO-2 Wisconsin Experiment Package. Fair data were obtained for RR Pic, which indicated a quite high (color) temperature, in excess of 35,000 K, and a bolometric luminosity of the order of 10 $L_\odot$. Variations of the order of 0.5 mag in two observations separated by about 1.7 hours (~ 0.5 P) seemed also to be present.

Duerbeck et al. (1980a) and Krautter et al. (1981) have reported on the first IUE observations of RR Pic (see Figure 6-36). Krautter et al. estimated UV temperatures of about 28,000 K and suggested the presence of P Cyg profiles (although much weaker than in HR Del) in the NV 1240, CII 1335, and Al III 1860 lines.

He II 1640 and NV 1240 are the strongest emissions in the spectrum, confirming the high-temperature character revealed in the optical emissions.

Krautter et al. (1981) have found temperatures on the order of 28,000 - 40,000 K, or, alternatively, they have made a fitting to the continuum distribution with a power-law λ^{α} , where $\alpha = 1.81 \pm 0.03$.

The UV luminosity was estimated at 4.4 $L_\odot$. Krautter et al. (1981) noticed the presence of two absorption components in the P Cyg profiles with velocities of -2500 km s^{-1} and -4600 km s^{-1}, respectively.

Wargau et al. (1982), using the same spectra, attempted an alternative fit to the continuum distribution and suggested a superposition of two blackbodies, one with T = 14,000 K (originated in the disk) and the other with T = 90,000 K (attributed to the boundary layer).

RR Pic has been also studied by Rosino et al. (1982). The continuum distribution has been interpreted as a combination of two blackbodies with temperatures of 20,000 K and 35,000 K. They detected the presence of (pure) absorption lines of Si II, Si III, Si IV, and S II, but did not confirm the presence of the P Cyg profiles. The width of the emission lines was interpreted in terms of expansion velocity of the shell, and a value of about 1700 km s^{-1} was derived.

RR Pic has been the target of an UV monitor-

ing that covered almost two complete cycles (Selvelli, 1982). A sequence of alternate exposures with the short λ and long λ cameras has made it possible to obtain 12 low-resolution spectra in about 6.5 hours, thus providing a reasonable time-resolution for the detection of φ-related variations. (The typical exposure time was 18 min). After correction for reddening (E (B-V)~ 0.05), the continuum fits quite closely the $\lambda^{-7/3}$ relation, although the index α ranges actually from 1.7 to 2.1 for different spectra. Figure 8-95 shows two fits to the continuum at different phases. Note that the mean time separation between two successive SWP and LWR spectra (which are merged together) is of about 30 min., which corresponds to Δφ~ 0.14.

Having several (6) spectra at disposal for each range, it is easier to detect faint lines (which in a single spectrum could be masked by noise) and to ascertain the reality of doubtful features. A careful examination of the spectra has led to the detection of a wealth of emission lines over the entire range.

The spectrum is characterized by strong permitted transitions of high-ionization species such as N V 1240, Si IV 1400, C IV 1550, He II 1640. Among the low-ionization species, only Mg II is present, while O I 1300, Al II 1670, C II 1335, Si II 1810 and similar species are definitely absent. The intersystem lines are rather weak: O V] 1218, N IV] 1486, O III] 1666, N III] 1750, Al II] 2669, or absent: Si III] 1892, C III] 1909, CII] 2326). [Ne V] 1575. [O II] 2469, and [Mg V] 2784 are probably present although faint.

The lines of the He II Paschen series are clearly present (note that the line of the Pickering series were reported in the optical by Vogt), together with some O III lines, notably 2836, produced in the Bowen fluorescent mechanism originated by He II Lyα.

Some emission features lacking any reasonable identification, such as λ 2575, λ 2405, λ 1446, have been attributed to "coronal lines," although the absence of a few of the strongest coronal lines in the solar spectrum, such as Fe XI 2648.73 and Fe XII 2565.99, poses a serious problem regarding the reality of these proposed identifications.

There is definitely no evidence of P Cyg profiles, neither for the lines proposed by Krautter et al. (1981) nor for any other line. Nor is there evidence of the absorption lines reported by Rosino et al. (1982), except for the feature near λ 1295, attributable to Si III UV 4, which seems to be variable.

C-7

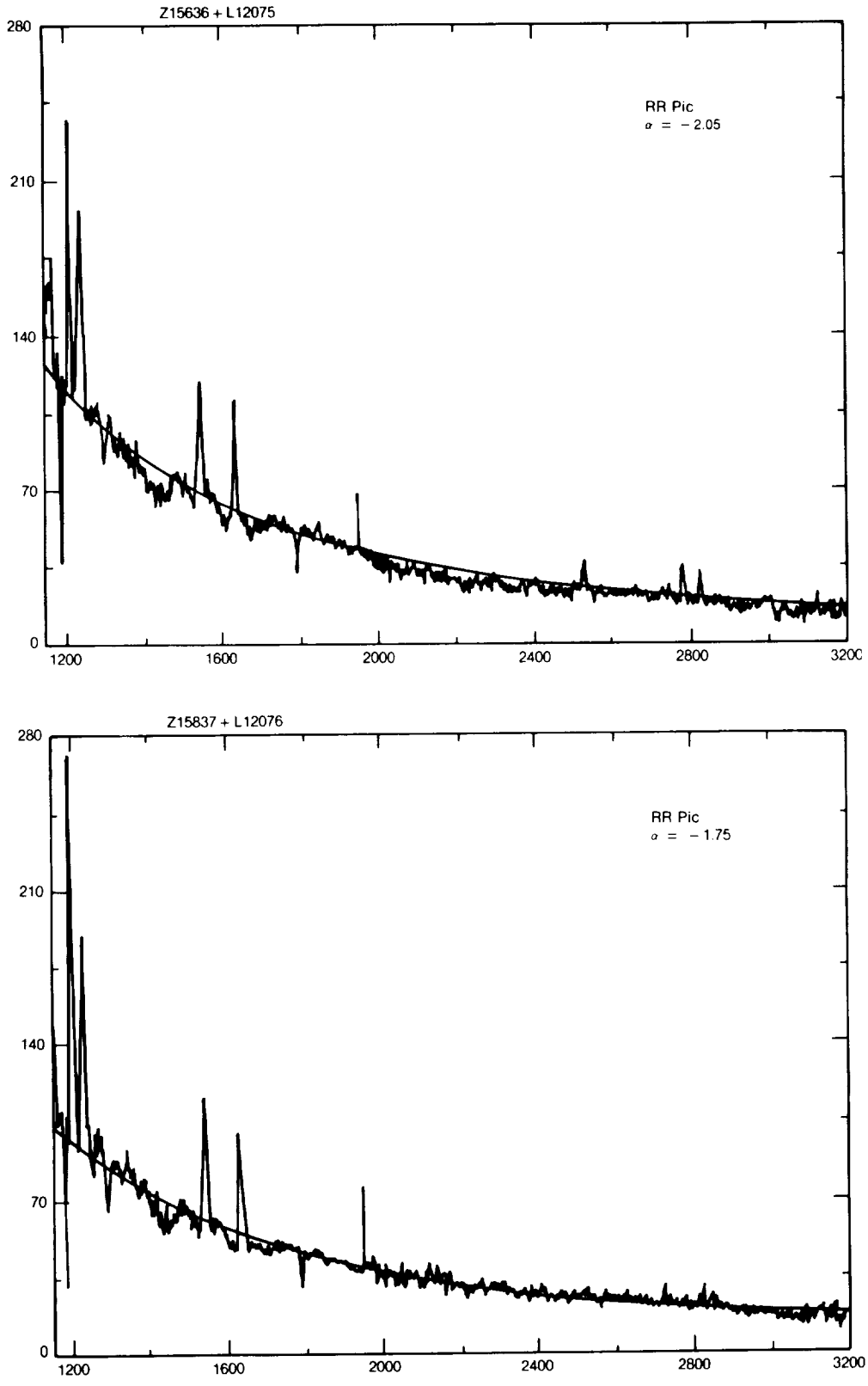

Figure 8-95. Low resolution IUE spectrum of RR Pic and comparison with a power-law spectrum with α = -2.05 *(top) and -1.75 (bottom).*

X.C.1. THE UV SPECTRAL VARIATIONS

The continuum, as well as the emission lines, shows significant variations in the various spectra that have been taken.

As is customary, the various spectral quantities have been ordered as a function of the phase φ, using the ephemeris given by Vogt (1975). The continuum does not vary significantly in shape, and, therefore, only the total flux in the continuum for the SWP asn LWR regions, respectively, has been reported. Variations as large as 1.5 have been found between the weakest and the strongest continua. The line spectrum shows stronger variations, especially in the near UV region, where variations around a factor of 5 have been observed for some lines.

Figure 8-96 reports the phase-related variations of the following quantities: m_v (FES), $\int_{1200}^{2000} F_\lambda^C d\lambda$ and $\int_{2000}^{3200} F_\lambda^C d\lambda$ (in erg cm^{-2} s^{-1}), line-emission intensities (in erg cm^{-2} s^{-1}) for N V, C IV, He II, Mg II, and O III 2836. The phase φ associated with each spectrum is that of mid-exposure. The phase associated with the m(FES) is that of ~ 2 min before the beginning of the exposure. In accordance with Vogt (1975), φ = 0 corresponds to the main maximum in the visible light curve, which has a minimum around φ = 0.42 (center of the eclipse). Schoembs and Stolz (1981) have found minima also around φ = 0.6. Haefner and Metz (1982), on the other hand, give φ = 0.75 for the primary eclipse (in accordance with the He II R.V. curve).

The mean continuum flux in the $\lambda\lambda$1200 - 3000 range is of 6.8 x 10^{-10} erg cm^{-2} s^{-1}. Assuming a distance of 440 pc, the mean UV luminosity results in 1.7 x 10^{34} erg s^{-1} ~ 5$L_\odot$.

From the IUE data, it is easy to see that a maximum common to the above-mentioned quantities falls between φ = 1.6 ÷ 1.9, while a minimum for most quantities occurs around φ = 1.1. ÷ 1.5. These results are in partial agreement with those of Vogt (1975), who found minima around φ ~ 0.4. but the occurrence of maxima centered around φ = 1.75 is in complete contradiction with all previous findings. In addition. the different behavior of the above quantities at about the same phase in two different periods is remarkable. See, for instance, the dramatic changes for Mg II and O III between φ = 0.687 (deep minimum) and φ =1.752.

On the other hand, Kubiak (1984) claims that the "eclipse" occurs between φ = 0.80 and φ = 0.95.

The UV data are in contradiction with conclusions drawn from the behavior in the optical and clearly rule out possible eclipse of the hot component. If the interpretation based on the R.V. curve of the He II λ 4686 line is correct, such eclipses are expected near φ= 0.75 when the companion is in front of the hot component. The UV data, on the other side, indicate that neither the continuum nor the emission lines, which are likely to be formed close to the hot component, become weaker near φ = 0.75. One more indication against a high inclination of the system comes from the considerations of Warner (1986b). Systems with high inclination, seen edge on, are expected to have a flatter UV continuum that RR Pic actually has. Probably, a key to understand both the behavior in the UV and the discrepancies about the phases of the various humps and dips in the light curve at different epochs is the presence of transient phenomena, which are superimposed to the periodic-phase-related changes.

Simultaneous IUE and ground-based observations covering at least two cycles are required.

The x-ray luminosity of RR Pic in the range (0.15 - 4.5 Kev) has been determined by Becker and Marshall (1981) using the Einstein IPC value 2.3 x 10^{31} erg s^{-1}, which is close, although weaker to the mean value of the few old novae detected in the x-ray range.

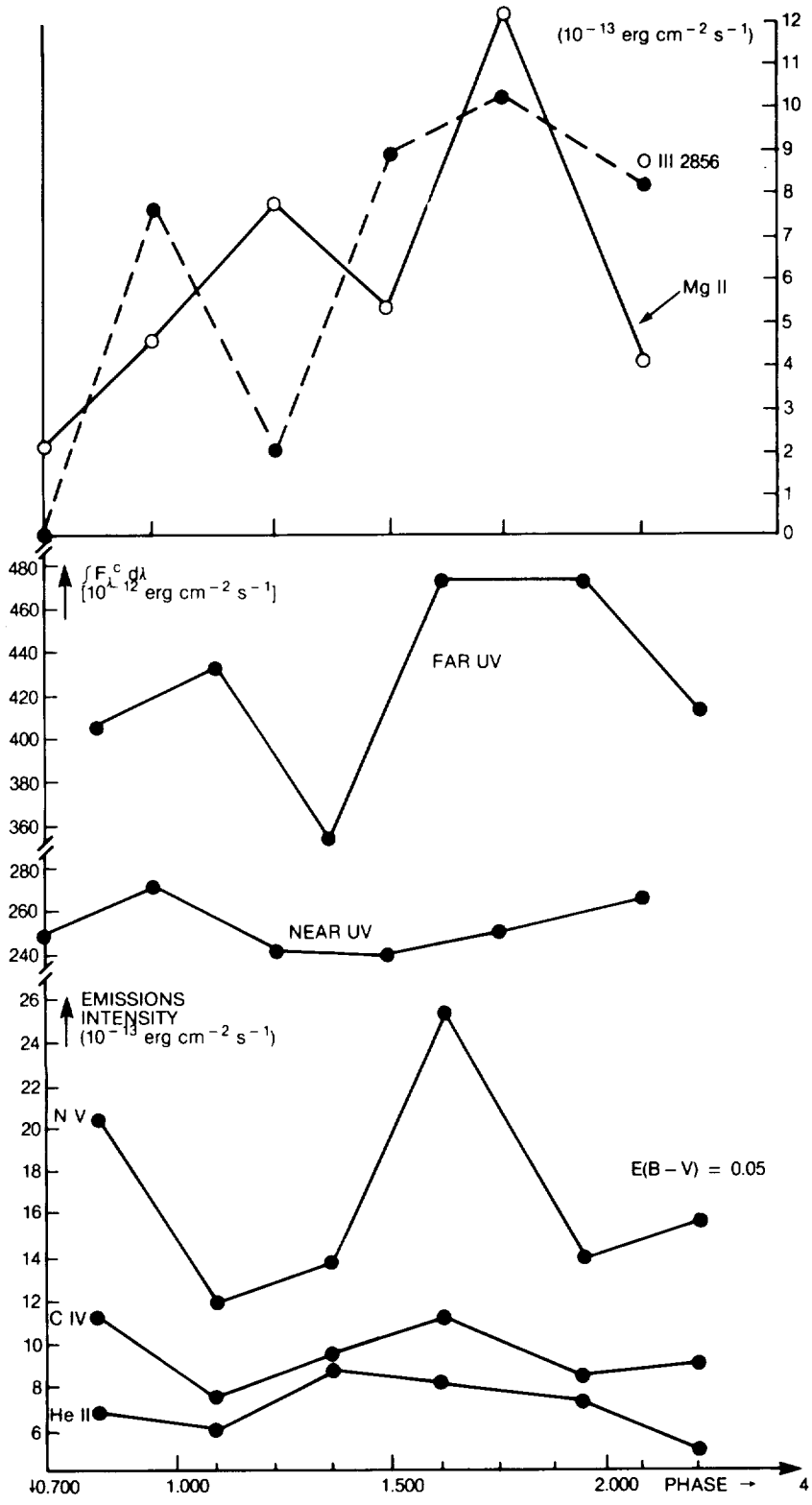

Figure 8-96. Phase variations of the flux in the emission lines of O III 2836, the 2800 resonance doublet of Mg II, the 1240 resonance doublet of N V and the 1550 resonance doublet of C IV, He II 1640, and the integrated continuum flux in the far UV and in the near UV, dereddened for E(B-V)=0.05.

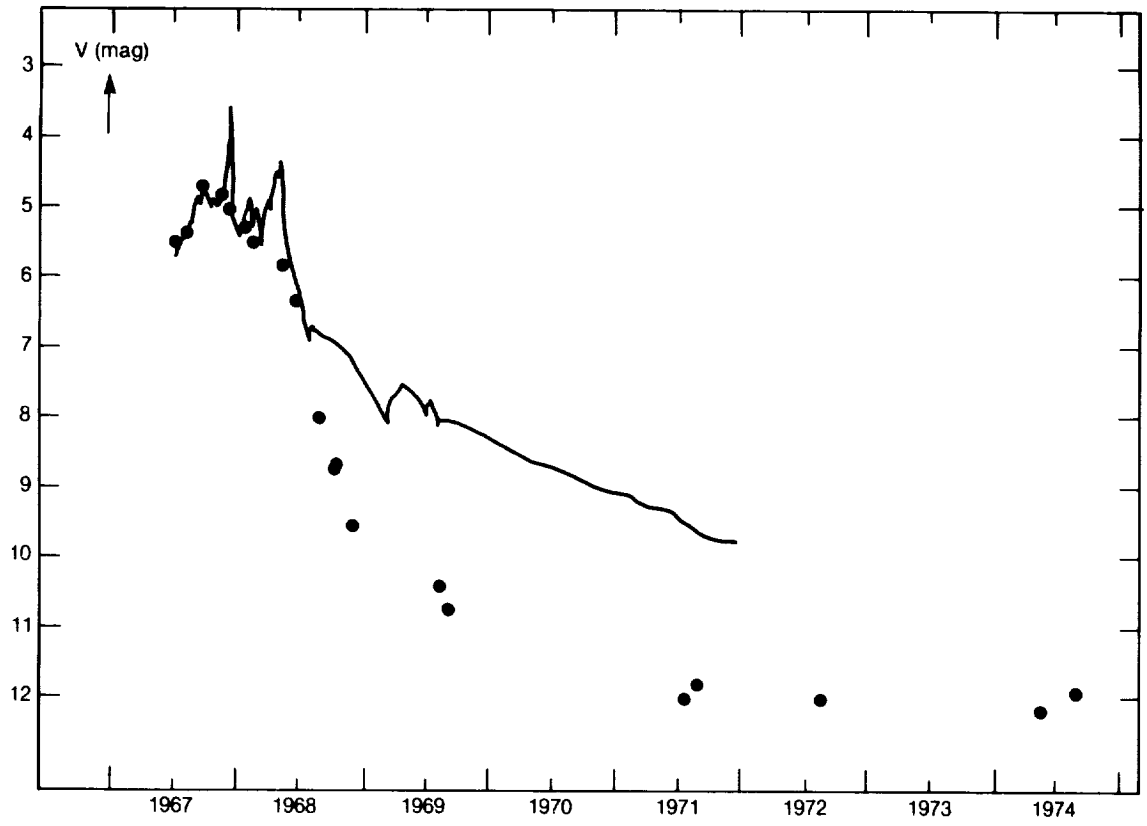

Figure 8-97. The photoelectric and the visual continuum light curve of HR Del (Drechsel et al., 1977).

XI. HR DEL

(written by Duerbeck)

XI.A. THE LIGHT CURVE

The outburst of HR Del (N Del 1967) was discovered by G. Alcock on 1967 July 8. The brightness of the star increased, starting from 1967 June 3, from the prenova magnitude of 12.0 to to a premaximum halt at 5.0; the peak brightness of 3.4 was reached on 1967 December 12. A secondary maximum of 4.3 occured in May 1968, and thereafter, the nova declined gradually. By 1975, it had returned to nearly 12.0 The light curve is well-covered, it shows similarities to that of the slow nova RR Pic, whose early rise however, was, missed.

A visual light curve from the beginning of the outburst to the end of 1971 is given in Drechsel et al. (1977). It shows the broadband V magnitude, which includes continuum + emisssion line light, as well as the continuum magnitude. The continuum magnitude declined much more rapidly, reaching 12.0 in mid-1971 (Figure 8-97).

XI.B. SPECTRAL STUDIES

High-dispersion spectroscopic studies were made by Sobotka and Grygar (1979), by Hutchings (1969), by Yamashita (1968, 1975), by Barlt and Szumiejko (1975), and by various astronomers using coude spectra of the Haute Provence Observatory (Andrillat and Houziaux 1970a, 1970b, 1971, Andrillat, Fehrenbach and Hou-ziaux 1974, Andrillat and Fehrenbach 1981, Friedjung (1977), Malakpur (1973), Antipova, 1977). Medium-dispersion studies were made by Galeotti and Pasinetti (1970), and by Rafanelli and Rosino (1978). Low-dispersion studies were reported by Seitter (1969, 1974) and Woszczyk et al. (1968). Spectrophotometric studies based on objective spectra were published by Drechsel et al. (1977).

XI.C. THE REMNANT

Models of the evolutionary remnant were computed and compared with observations by Tylenda (1977, 1978, 1979).

The nebular remnant was spatially resolved on direct photographs by Kohoutek (1981). Observations in 1981 show an oval shell with a size 3.7" x 2.5". The nebular expansion parallax yields a distance of 850 ± 50 pc.

A kinematical model was developed by Solf (1983) from the study of spatially resolved coude spectra. The main body of the material is found in an equatorial ring and two "polar" rings (rings at higher azimuthal angle). The polar axis is seen at position angle 45° and has an inclination of 38° with respect to the celestial sphere (Figure 8-98).

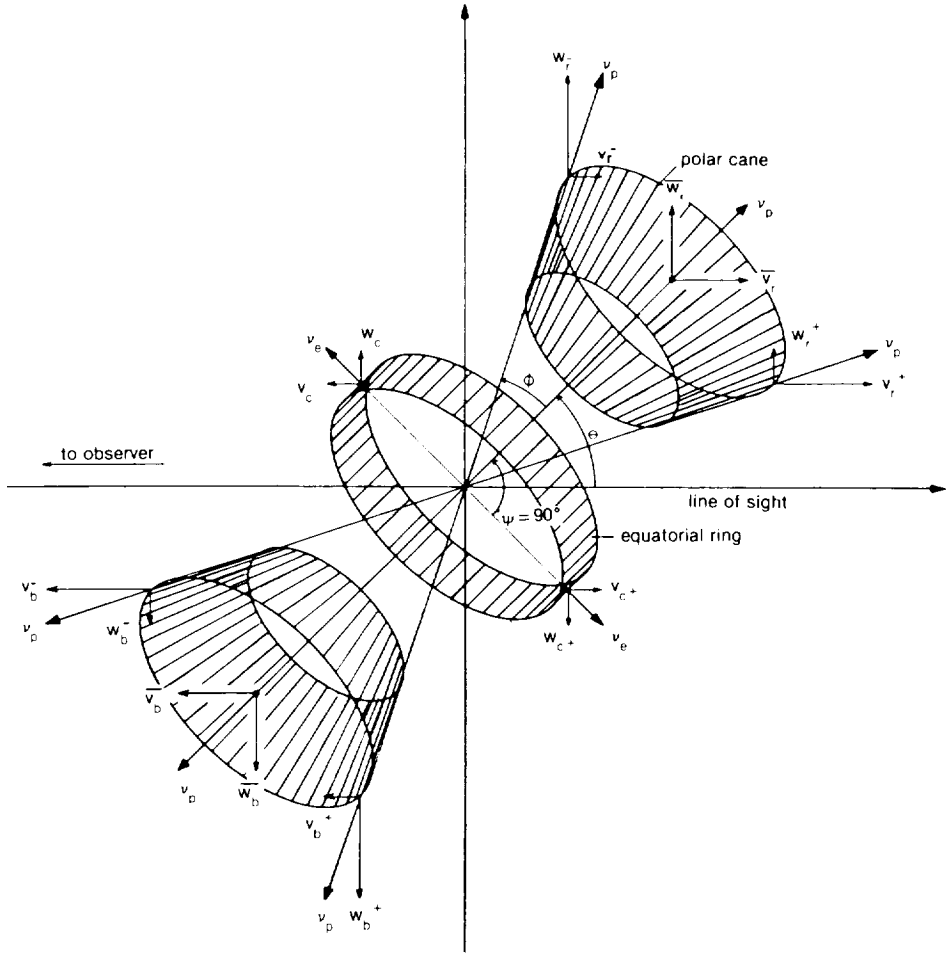

Figure 8-98. A geometrical and kinematical model of the shell of HR Del, consisting of two polar caps (sketched by truncated cones) and an equatorial ring (radial thickness not sketched). Radial (V_h) and tangential (W_h) components of the polar (V_p) and equatorial (V_e) expansion velocities, occurring on the near (−) or the far (+) side of the shell. Also indicated are the velocity components of the bulk motion of the caps (V_r, W_r). The caps and the ring are filled with matter which is heavily clumped (Solf 1983).

XI.D. HR DEL AS A CLOSE BINARY

The most complete study of the binary motion was made by Bruch (1982), using his own and previously published material. The period is unambiguously determined to be 0.2141674 days; the amplitude of radial velocity of the He II 4686 line is 104 km/s, and only 34 km/s for Hβ (Figure 8-99). No trace of the secondary could be detected. The orbital inclination was estimated to be near 41°, which yields for HR Del the most plausible properties of a cataclysmic binary (e.g., mass ratio). This inclination is in good agreement with the results of the study of the nebular shell, assuming that the polar axis of the nebula is perpendicular to the orbital plane. A combination of Kepler's third law, Paczynski's (1971) analytical expression for Roche-lobe geometry, and Lacy's (1977) mass radius relation for low-mass main-sequence stars yields for the late-type component

$$M_2 = 7.7 \cdot 10^{-5} P^{1.142}$$

with P measured in seconds, M_2 in solar masses. In the case of HR Del, $M_2 = 0.58 \pm 0.01\ M_\odot$.

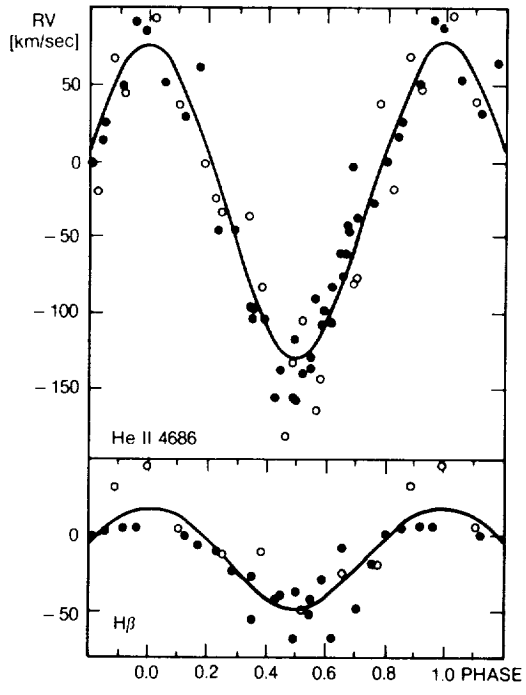

Figure 8-99. Radial velocity curves of HR Del for He II 4686 and Hβ. Filled and open circles are data from various sources (Bruch 1982).

From the observed radial velocity amplitude and the inclination angle, for the compact component, $M_1 = 0.9 \pm 0.1\ M_\odot$.

XI.E. EVOLUTION OF THE OUTBURST

As is typical for slow novae, the spectral evolution was quite complex; the results of radial velocity measurements of absorption lines is shown in Figure 8-100.

Following Hutchings (1969), the outburst is divided into three phases:

Phases I: Pre-maximum.

June - early December, 1967. The light curve is smooth, levelling off at about 5 m, and shows long term (time scale: weeks) fluctuations of 0.5. The spectrum shows lines normal for the early stages of the nova, and smoothly varying line displacements: The strongest lines are those of H, Fe II, Cr II, and Ti II; during the course of evolution, more lines of lower excitation and ionization appeared (Figure 8-101). The shortward displacement of the absorption lines gradually decreased with time; Malakpur (1973c) identifies the broad main absorption, whose radial velocity decreased from 625 to 230 km/s in this time interval, with the premaximum spectrum. Furthermore, a sharp, stationary emission component was visible. The Ca II H and K lines were strong and showed four narrow highly-displaced absorption components in addition to the broad main absorption, which disappeared on December 12, 1967. They are suspected to originate in pre-existing circumstellar material (Figure 8-102).

Phase II. Maximum.

December 1967 - May 1968. The phase begins with a rapid, short—lived brightening up to 3.5 on December 14. The light curve varies rapidly and irregularly by up to 1.2 and as fast as 0.5 within one night. The spectrum shows equally rapid changes, and each line has several sharp absorption components and a strong, variable emission. The strong lines displayed a number of sharp absorption components, which appeared individually and irregularly, fading away during a period of a few weeks. Malakpur (1973c) notes that the princi-

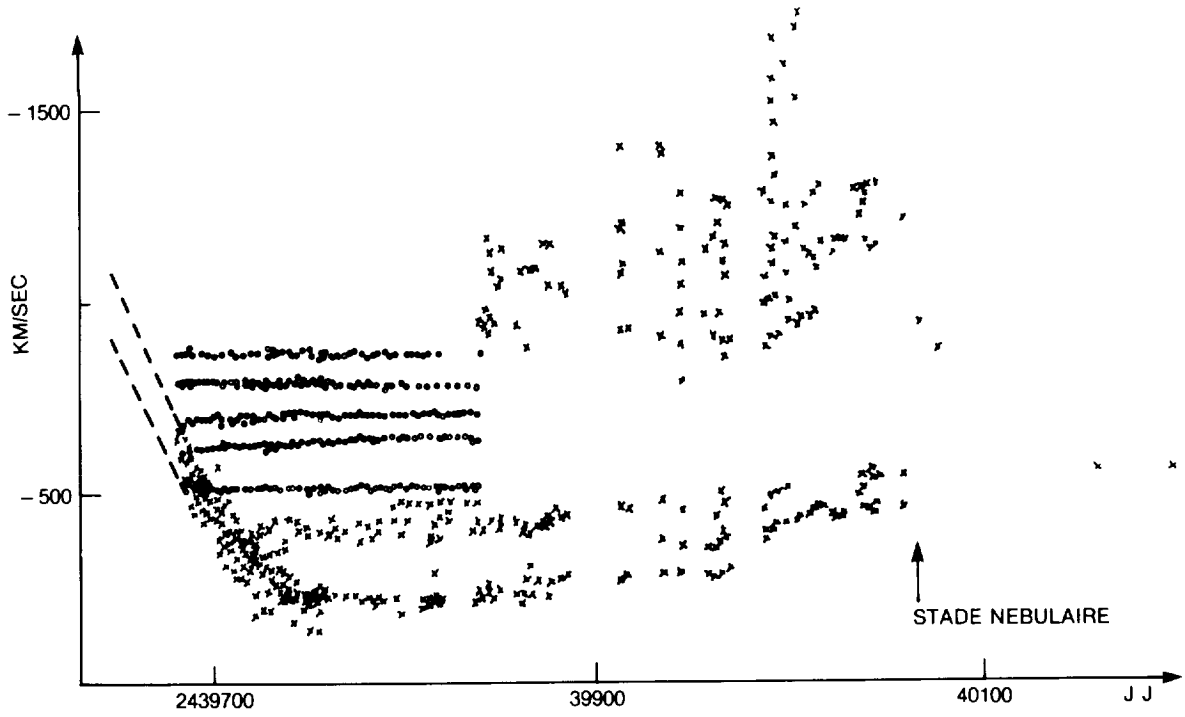

FIGURE 1

Figure 8-100. Radial velocity data of absorption lines in the spectrum of HR Del from the premaximum to the nebular stage (Malakpur 1973c).

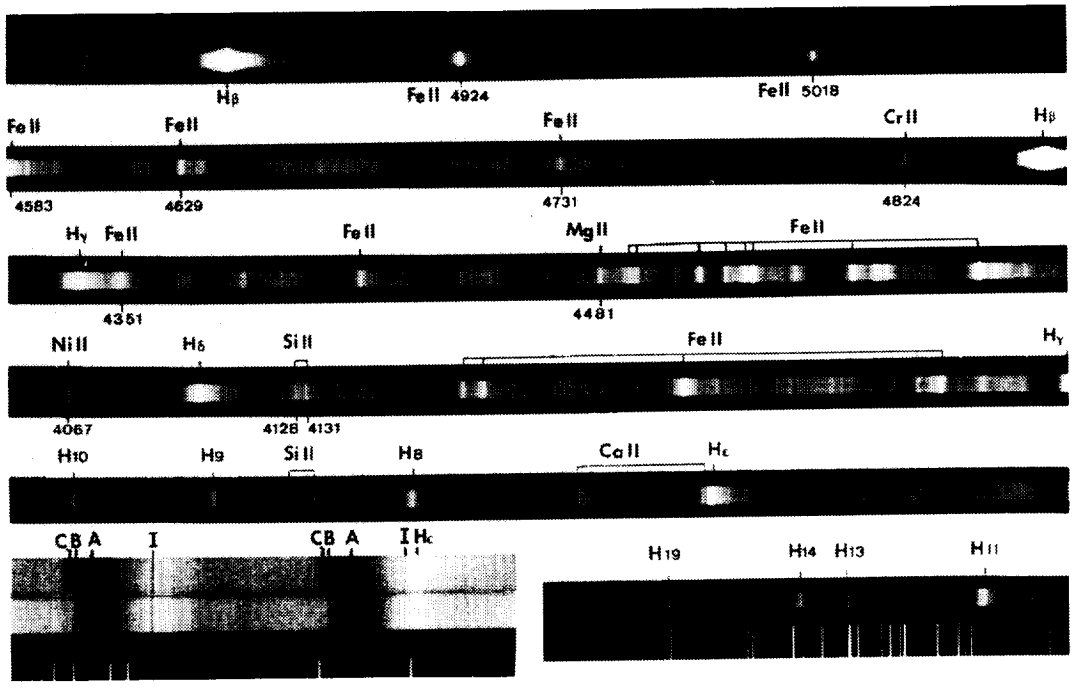

Figure 8-101. The spectrum of HR Del from Hβ to the Balmer limit three days after outburst. On the bottom at left: enlargement of the Ca II H and K region showing the absorption components A, B and C and the interstellar components I. (Courtesy of Ch. Fehrenbach and P. Veron. Observatoire de Haute Provence du Conseil National de la Recherche Scientifique (CNRS)).

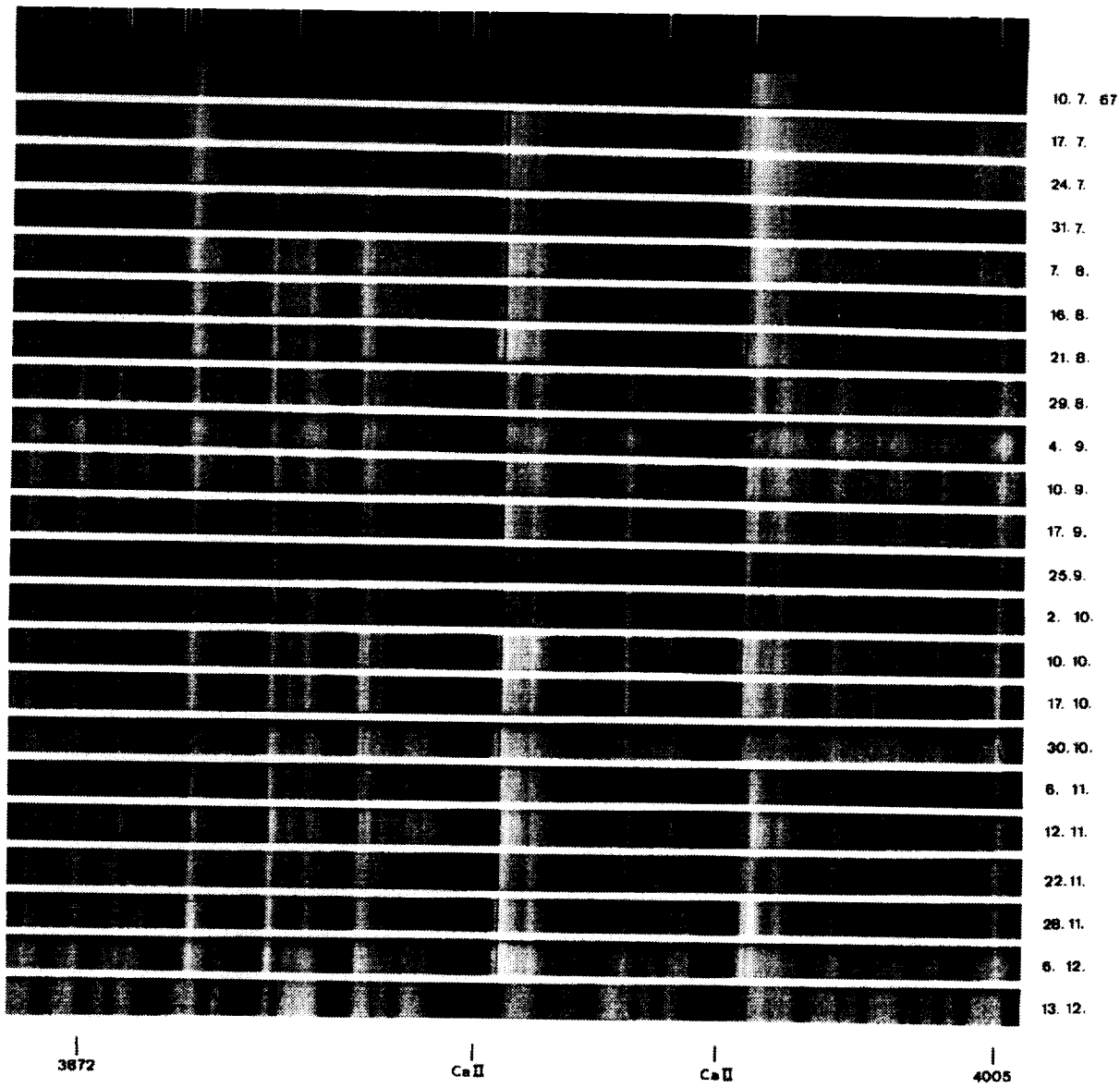

Figure 8-102a. Spectral variations of HR Del from 1967 July 10 to December 13, spectral range λλ 3872-4005. Note the sharp interstellar absorption lines of Ca II, the broad stellar absorption components showing expansion velocities decreasing from -660 to -300 km/s from early July to September, and increasing again to -400 km/s in December. Note also the sharp absorption components which are violet-shifted with respect to the broad absorption line. The emission components, formed in an outer extended envelope, are stationary. For details, see Fehrenbach and Petit (1969). (Courtesy of Ch. Fehrenbach and P. Veron. Observatoire de Haute Provence du Conseil National de la Recherche Scientifique (CNRS)).

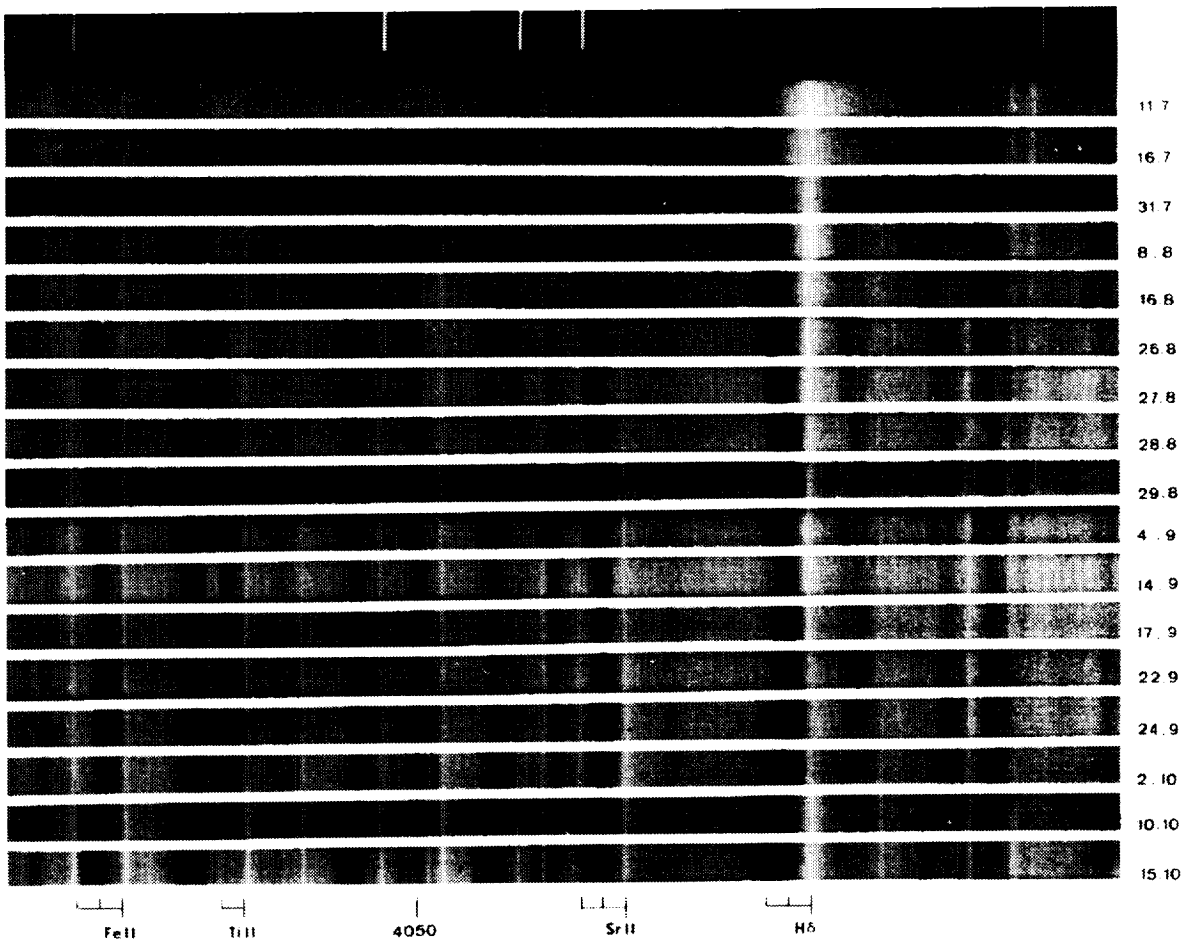

Figure 8-102b. See Figure 8-102b spectral range λλ 4000 - 4150. Note the very remarkable increase in intensity of the emission and absorption lines of Ti II and Sr II and the presence of three absorption components on 1967 August 28 and 29. For details, see Fehrenbach et al. (1968a), and Fehrenbach et al, (1968b). (Courtesy of Ch. Fehrenbach and P. Veron. Observatoire de Haute Provence du Conseil National de la Recherche Scientifique (CNRS)).

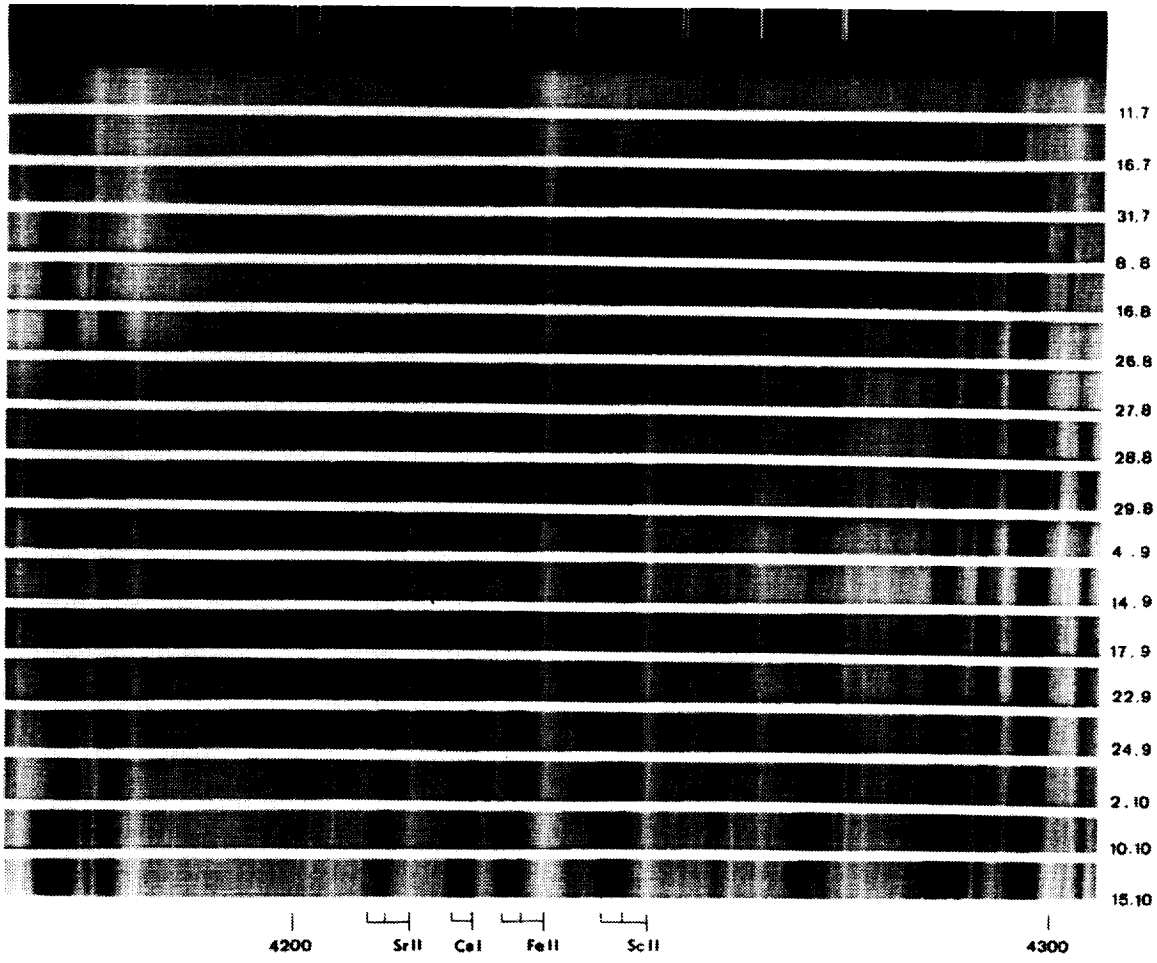

Figure 8-102c. See Figure 8-102a spectral range λλ 4140 - 4300. (Courtesy of Ch. Fehrenbach and P. Veron. Observatoire de Haute Provence du Conseil National de la Recherche Scientifique (CNRS)).

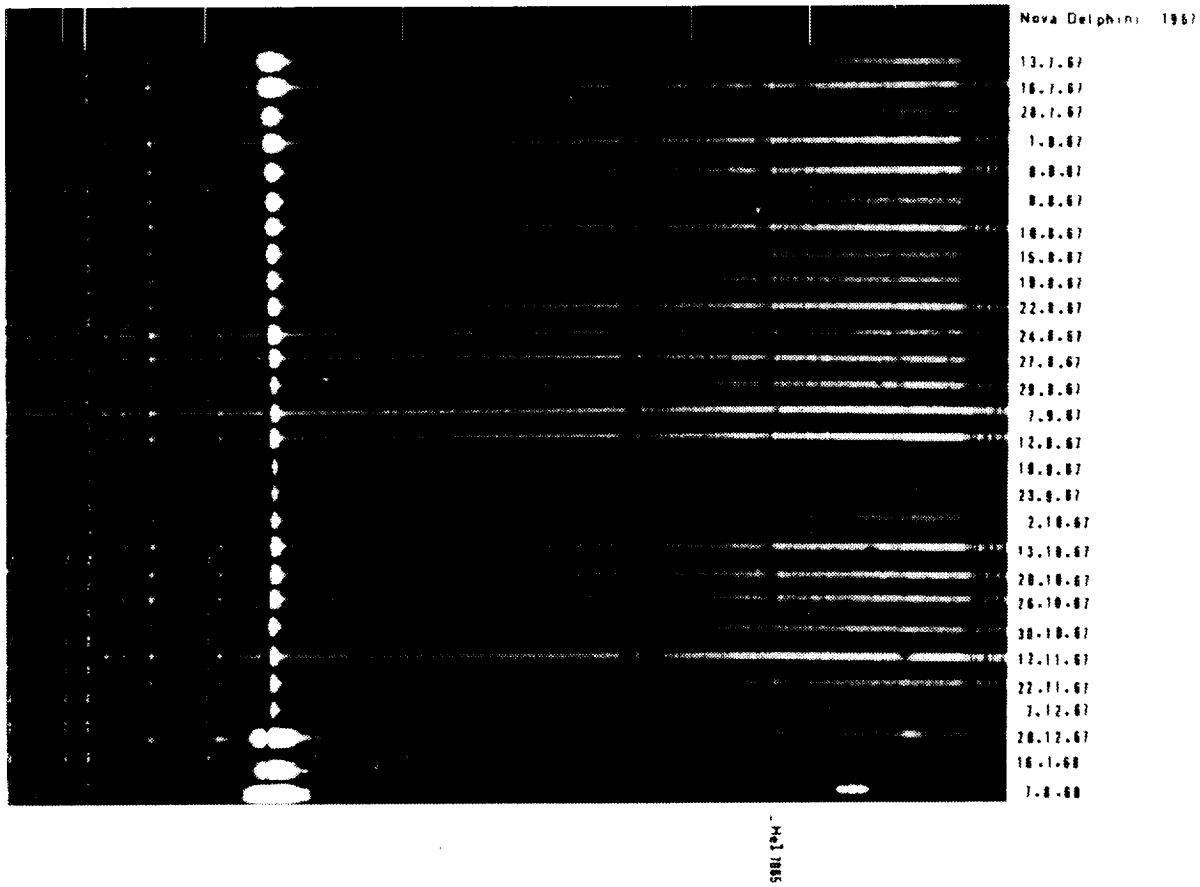

Figure 8-102d. The red spectrum of HR Del: Hα to λ 7400. (Courtesy of Ch. Fehrenbach and P. Veron. Observatoire de Haute Provence du Conseil National de la Recherche Scientifique (CNRS)).

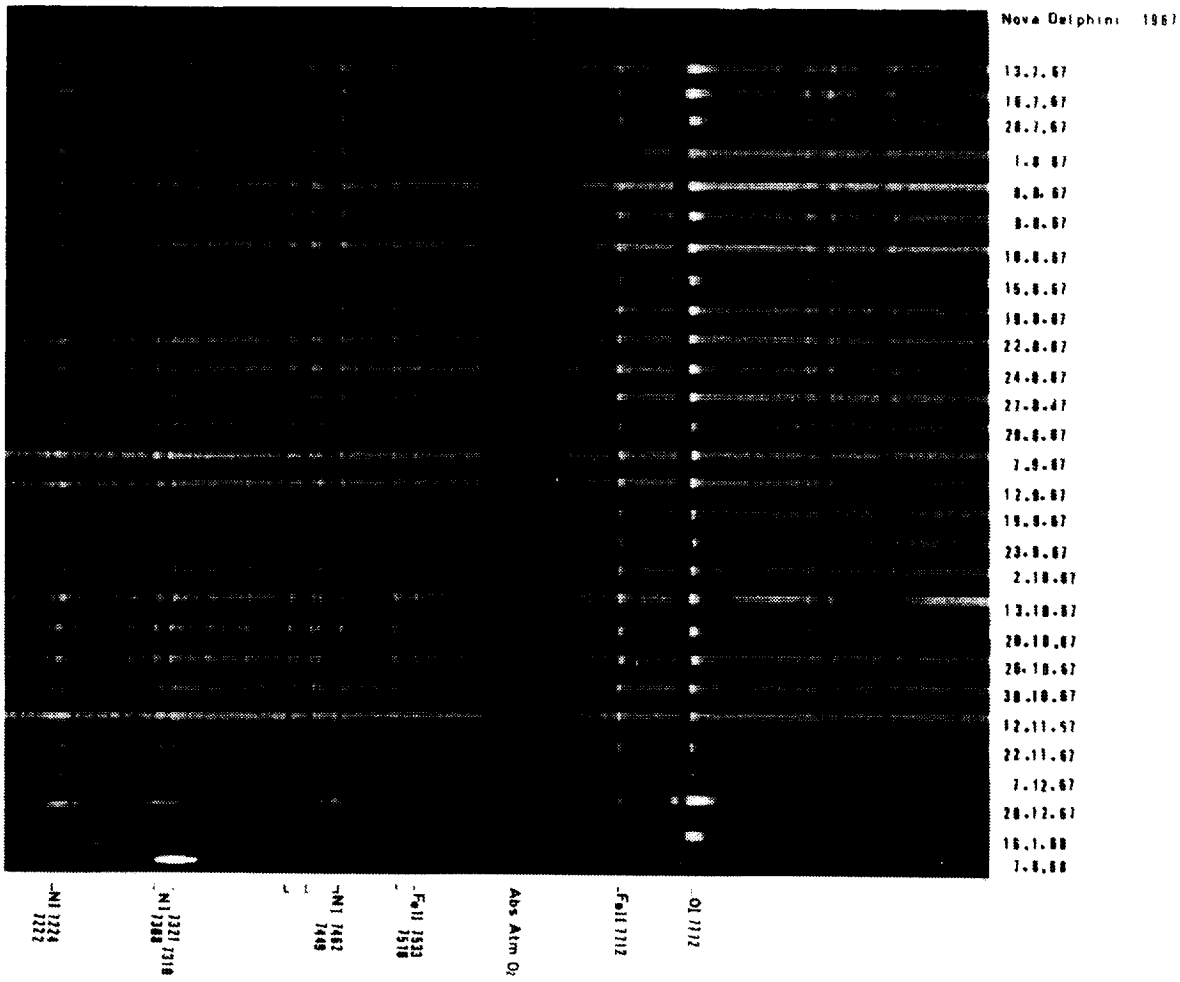

Figure 8-102e. The infrared spectrum of HR Del: λλ 7200 - 8000. (Courtesy of Ch. Fehrenbach and P. Veron. Observatoire de Haute Provence du Conseil National de la Recherche Scientifique (CNRS)).

pal spectrum, visible since August 27, 1967, experienced a sudden increase in velocity on April 21, 1968, (Figure 8-103), when the diffuse-enhanced system, visible since December 17, 1967, merged with it. The emission components were much stronger than during Phase I, and appeared to be a blend of several contributing emissions, each of which was intially sharp and narrow but which gradually spread in wavelength while diminishing in central intensity, again over a period of several weeks. The velocities of some components are in excess of 1700 km/s. The correlation between luminosity and spectrum changes is not clear.

The composition of the spectrum in Phase II is similar to that at the beginning of Phase I. It appears to arise from a number of successive shells each with slightly different temperature, and possibly composition. While the excitation state of lines during Phase I corresponded to excitation potentials of 1 to 5 eV, the excitation state here appears to cover the potentials of 2 to 3 eV in the high-velocity shell (up to 1000 km/s), and of 0.5 to 3 eV in the low-velocity shells.

Malakpur (1973c) notes that the Orion system had its first appearance on May 11, 1968 (Figure 8-104).

Phase III. Transition and nebular stage.

Phase III begins in June, 1968, with the cessation of irregular activity. The light curve falls smoothly to m = 8, and the spectrum changes rapidly through the Orion to the nebular stage, where is characterized by strong, multiple-peaked emissions. Malakpur (1973c) determined the beginning of the nebular stage to be around July 28, 1968. No shells were ejected after May, the spectrum began to change rapidly, going through stages of increasing excitation and dilution, to the final nebular stage, in about 10 weeks. The continuum became very blue and then faded, while the emission line strength increased. The emission lines split into three components, and the relative intensities differed between allowed and forbidden lines.

During August, the continuous spectrum continued to fade. Starting from that date, until 1972, various coronal lines could be seen in the spectrum: [A X], [Fe X], [Fe XI], [Fe XIV], [Fe XV], [Ni XII], and [Ni XV] (Andrillat and Houziaux, 1970a; Rafanelli and Rosino, 1978).

The radio light curve is well covered in the later stages. A Hubble flow model yields a good fit to the observations at several frequencies (Seaquist et al., 1979) (see Figure 6-76).

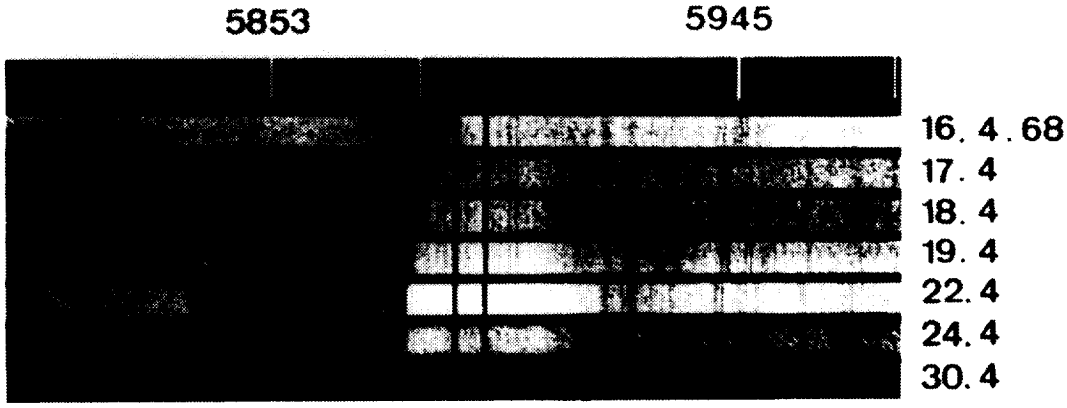

Figure 8-103. Spectral variations of HR Del in 1968 April in the region λλ 5800 - 5950. Note the strong interstellar D lines of Na I and the violet shifted stellar D lines. (Courtesy of Ch. Fehrenbach and P. Veron. Observatoire de Haute Provence du Conseil National de la Recherche Scientifique (CNRS)).

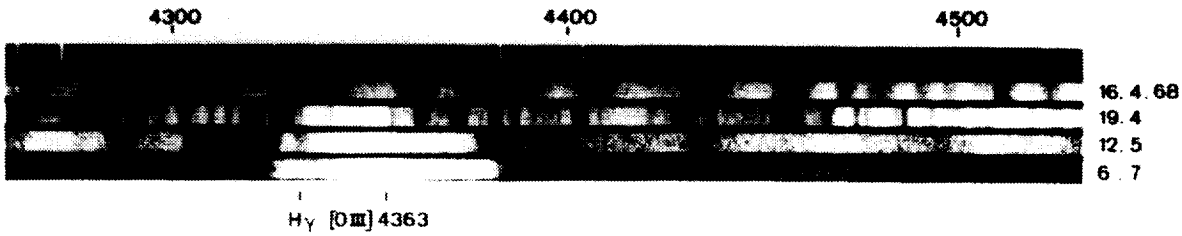

Figure 8-104. The spectral variations of HR Del from 1968 April to 1968 July (Courtesy of Ch. Fehrenbach and P. Veron. Observatoire de Haute Provence du Conseil National de la Recherche Scientifique (CNRS)).

XI.F. CHEMICAL COMPOSITION

Table 8-5 shows the results of various determinations of the chemical composition of HR Del.

The abundance dererminations of Antipova (1977) Raikova (1977), and of Ruusalepp and Luud (1971) are derived from the curve of growth method applied to the absorption lines of the principal spectrum (August - December 1967), and using the usual equations by Boltzmann and Saha, i.e., by assuming that the pseudophotosphere of the nova is in LTE, a condition very far from its real state. The determinations by Tylenda (1979) are more reliable because they are based on the emission lines of the envelope during the nebular stage (1971-72 and August 1975), using two different models (A and B). Tylenda (1978) shows that the observed line intensities of the envelope in the nebular stage cannot be fitted by models that assume that the central source of the ionizing photons radiates as a single star with blackbody spectrum (Tylenda 1978). The theoretical line intensities are 4 to 100 times fainter than the observed ones. Instead, a good fit with the observations is obtained by assuming that the central source of ionizing photons consists of two components. An ionizing radiation, being the sum of two blackbody distributions with almost equal luminosities and temperatures of about 4×10^4 K and 2.5×10^5 K, is adopted. The input parameters of the two source models A and B and the comparison with the observations are given in Tables 3 and 4 of Tylenda (1978).

In spite of the different models and assumptions, all determinations agree in obtaining a CNO excess. Tylenda (1978) gives C(HR Del)/C(Sun) = 25, N(HR Del)/N(Sun) = 630, O(HR Del) O (Sun) = 125, Ne (HR Del)/N(Sun) =37. These values are in good agreement with the average values found for novae (Collin-Souffrin, 1977).

Table 8.5 — The table shows the results of various determinations of the chemical composition of HR Del

element	Antipova	Raikova	Ruusaleep	Tylenda (A)	(B)	Sun
H	24.64		25.49	26.40	25.77	25.0
He				25.83	25.20	23.8
C	22.98	22.42	23.56	23.00	23.00	21.6
N	23.14	22.53	22.80	23.94	23.50	20.9
O	23.59	23.87		24.08	23.70	21.8
Ne				22.78	22.37	21.0
Mg	20.34	20.71	20.28			20.6
Al	19.34					19.5
Si	21.02	20.92	21.52			20.7
Ca	19.02	20.48				19.3
Sc	15.90	16.64	16.83			16.1
Ti	17.72	18.26	18.73			18.1
V	16.60	17.18	17.51			17.0
Cr	18.37	18.22	19.57			18.3
Mn	17.61	18.97				18.0
Fe	20.83	20.83	19.98			20.5
Sr	15.85	16.67	15.36			15.9
Y	15.56	15.97				15.1
Zr	15.37	16.22				15.7
Ba	14.85	15.62				15.1
La	14.64					14.4